International Journal of Dentistry

Materials and Bioactive Factors in Dental Restoration and Periodontal Therapy

Guest Editors: Vesna Miletic, Tihana Divnic-Resnik, Natasa Nikolic Jakoba, Andrija Petar Bosnjak, and Paulo Henrique Perlatti D'Alpino

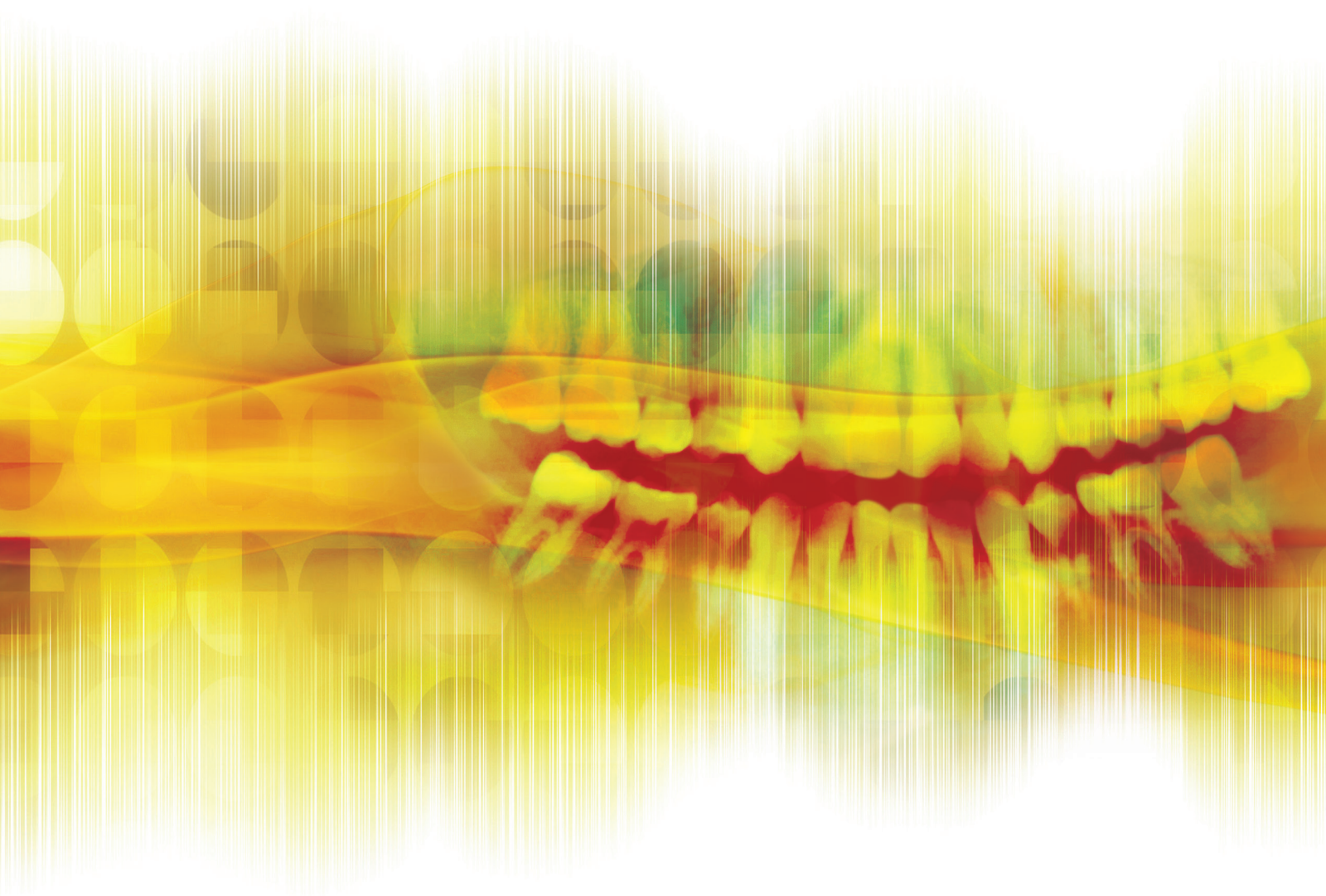

Materials and Bioactive Factors in Dental Restoration and Periodontal Therapy

International Journal of Dentistry

Materials and Bioactive Factors in Dental Restoration and Periodontal Therapy

Guest Editors: Vesna Miletic, Tihana Divnic-Resnik, Natasa Nikolic Jakoba, Andrija Petar Bosnjak, and Paulo Henrique Perlatti D'Alpino

Editorial Board

Contents

Hindawi Publishing Corporation
International Journal of Dentistry
Volume 2016, Article ID 4809051, 2 pages
http://dx.doi.org/10.1155/2016/4809051

Editorial

Materials and Bioactive Factors in Dental Restoration and Periodontal Therapy

Vesna Miletic,[1] Tihana Divnic-Resnik,[2] Natasa Nikolic Jakoba,[3] Andrija Petar Bosnjak,[4,5] and Paulo Henrique Perlatti D'Alpino[6]

[1]*DentalNet Research Group, School of Dental Medicine, University of Belgrade, 11000 Belgrade, Serbia*
[2]*Discipline of Periodontics, Faculty of Dentistry, The University of Sydney, Sydney, NSW 2010, Australia*
[3]*Department of Periodontology and Oral Medicine, School of Dental Medicine, University of Belgrade, 11000 Belgrade, Serbia*
[4]*School of Medicine, University Josip Juraj Strossmayer, 31000 Osijek, Croatia*
[5]*School of Medicine, University of Rijeka, 51000 Rijeka, Croatia*
[6]*School of Dentistry, Biomaterials Research Group, Universidade Anhanguera de São Paulo, 05145-200 São Paulo, SP, Brazil*

Correspondence should be addressed to Vesna Miletic; vesna.miletic@stomf.bg.ac.rs

Received 13 January 2016; Accepted 13 January 2016

Dental restoration and periodontal therapy have undergone tremendous expansion over the past few decades. Improvements have been made in basic and applied material science but also in clinical considerations of functional, esthetic, reparative, and regenerative aspects of materials and bioactive factors. This special issue offers a wide range of topics, broadening knowledge of researchers, dental specialists, and general dental practitioners.

Dentin-adhesive bond remains a challenge in modern adhesive dentistry due to the complex composition and morphology of dentin. Different treatment modalities have been proposed to improve the dentin-adhesive bond and increase its longevity. Among these, conditioning dentin with ethylenediaminetetraacetic acid (EDTA) along with carbodiimide pretreatment have shown potential in preserving bond strength to dentin of self-etch adhesives over time.

Impression materials should withstand tear and tensile forces and be able to recover fully for an ideal impression of intricate details of dental and oral structures. A number of hydrophilic elastomeric impression materials are available on the market. In vitro testing of tensile properties of heavy-body, medium-body, and light-body polyvinylsiloxane, polyether, and vinylpolyether silicone commercial products offers scientific data for clinical selection of impression materials for specific applications.

Platelet-rich fibrin membranes seem to improve the healing process in periodontal regenerative treatments. Leukocyte- and platelet-rich fibrin (L-PRF) is considered a second-generation platelet concentrate, able to form strong fibrin matrices. Early L-PRF membranes have shown stronger mechanical properties, namely, tensile strength, modulus of elasticity, and toughness, than membranes obtained using platelet rich in growth factors (PRGF)/Endoret® technology, indicating potential clinical advantages.

Titanium and titanium alloys are nowadays considered the material of choice for dental implant applications in the replacement of missing teeth. Numerous studies focus on the mechanisms of interaction between the surface of titanium or titanium alloys and host tissues. Recently, the role of titanium oxide surface layer in osteoblast differentiation has been studied in terms of alkaline phosphatase (ALP) activity. Increased ALP activity suggests that titanium oxide acts as a bioactive factor involved in osteoblast differentiation and subsequent osseointegration.

Finite element analysis (FEA) has been used in assessment of stress distribution induced by occlusal loading in diverse dental tissues, restorations, implants, and surrounding alveolar bone (cancellous and cortical). FEA may be particularly useful in designing dental implants. Extensive numerical simulation reveals complex stress distribution in

and around dental implants with different thread designs and abutment angulations restored with porcelain crowns and subjected to a number of occlusal loading conditions.

Vesna Miletic
Tihana Divnic-Resnik
Natasa Nikolic Jakoba
Andrija Petar Bosnjak
Paulo Henrique Perlatti D'Alpino

Hindawi Publishing Corporation
International Journal of Dentistry
Volume 2016, Article ID 4867402, 9 pages
http://dx.doi.org/10.1155/2016/4867402

Research Article

A Three-Dimensional Finite Element Study on the Biomechanical Simulation of Various Structured Dental Implants and Their Surrounding Bone Tissues

Gong Zhang,[1] Hai Yuan,[1] Xianshuai Chen,[1] Weijun Wang,[1] Jianyu Chen,[2] Jimin Liang,[1] and Peng Zhang[3]

[1]*Guangzhou Institute of Advanced Technology, Chinese Academy of Sciences, Guangzhou 511458, China*
[2]*Hospital of Stomatology, Sun Yat-sen University Hospital, Guangzhou 510000, China*
[3]*Foshan Stomatology Hospital, Foshan 528000, China*

Correspondence should be addressed to Gong Zhang; gong.zhang@giat.ac.cn

Received 5 August 2015; Revised 20 November 2015; Accepted 15 December 2015

Academic Editor: Natasa N. Jakoba

Background/Purpose. This three-dimensional finite element study observed the stress distribution characteristics of 12 types of dental implants and their surrounding bone tissues with various structured abutments, implant threads, and healing methods under different amounts of concentrated loading. *Materials and Methods*. A three-dimensional geometrical model of a dental implant and its surrounding bone tissue was created; the model simulated a screw applied with a preload of 200 N or a torque of 0.2 N·m and a prosthetic crown applied with a vertical or an inclined force of 100 N. The Von Mises stress was evaluated on the 12 types of dental implants and their surrounding bone tissues. *Results*. Under the same loading force, the stress influence on the implant threads was not significant; however, the stress influence on the cancellous bone was obvious. The stress applied to the abutment, cortical bone, and cancellous bone by the inclined force applied to the crown was larger than the stress applied by the vertical force to the crown, and the abutment stress of the nonsubmerged healing implant system was higher than that of the submerged healing implant system. *Conclusion*. A dental implant system characterised by a straight abutment, rectangle tooth, and nonsubmerged healing may provide minimum value for the implant-bone interface.

1. Introduction

Since osseointegrated dental implants are introduced for the rehabilitation of the edentulous patient in the late 1960s, a tremendous awareness and subsequent demand have been arising in the field [1–3]. Recently, dental implants have been increasingly applied in oral rehabilitation and orthopedics used as replacements after the natural teeth are lost or partially damaged, which could restore human mastication functions [4]. Previous studies showed that dental implantation could have a high success rate: retention rate is in excess of 95% over a 5-year period if dental implants were correctly designed, manufactured, and inserted [5–7].

However, dental implant treatments are still failing frequently. One of the major causes of failure is that an artificial implant may never function as perfectly as the living tissues it replaces.

As a matter of fact, the success of dental implant is strongly affected by a number of biomechanical factors, including the type of loading, material properties of implant and prosthesis, implant geometry, surface structure, quality and quantity of surrounding bone, nature of implant-bone interface, and surgical procedures [8]. As far as implant shape is concerned, main design parameters affecting load transfer mechanisms include implant diameter and length of implant-bone interface [9], as well as thread pitch, shape, and depth in the case of threaded implants [10, 11]. In consideration of increasing surfaces appointed for osseous integration, threaded implants are generally preferred to smooth cylindrical ones [12].

The use of screw-type implants increases contact area and improves implant stability [13]. Other designs, such as the stepped implant and the tapered body of threaded implant, have also been proposed to mimic the root anatomy and to enhance the bony support in spongy bone, thereby creating a favorable load distribution [14, 15]. In addition, the thread size, thread profile, and surface roughness may affect the stress pattern in the surrounding bone [16–18].

Otherwise, occlusal loading may often be applied to an implant within 48 h after implant placement [19]. Nevertheless, the effectiveness of an immediately loaded implant is less predictable than that of the delay-loaded implant [20]. The main concern is the occurrence of fibrous encapsulation instead of osseointegration around implants [21].

The objective of this research is to compare the biomechanical effects of the immediately loaded dental implants and the surrounding bone tissue with various abutments (straight and angled), implant threads (trapezia tooth, rectangle tooth, and saw tooth), and healing methods (submerged and nonsubmerged) using a three-dimensional finite element analysis, accounting for the interaction between the dental implants and the supporting bone tissues. Three contact models and four types of loading conditions are used to simulate different integration qualities at the implant-bone interface during the osseointegration process. Extensive numerical simulation results show the influences of compositional profile, occlusal force orientations, and preload types on the static and dynamic behavior of the implant/bone system.

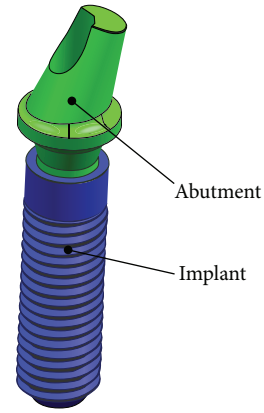

Figure 1: Dental implant system.

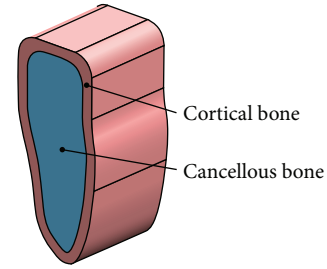

Figure 2: Surrounding bone tissues.

2. Materials and Methods

2.1. CAD Modeling. The three-dimensional geometrical model of the dental implant (Figure 1) and surrounding bone system (shown in Figure 2) was created using the CAD software Unigraphics NX 4.0 (Siemens PLM Software Inc., Germany). The geometry of the adult mandible took the shape created from CT database through image segmentation and spline reconstruction with STP format [24].

The dental implant/supporting bone system comprised abutment, an implant, an internal screw connecting the abutment and implant, and prosthetic crown duplicated from the molar, surrounding cortical bone and cancellous bone in the mandibular section (Figure 3).

As shown in Figure 4, the abutments were divided into straight abutment (shorted for "St") and angled abutment (shorted for "An"), respectively. The maximum diameter was 5.1 mm, wearing gingiva length was 5 mm, and the inclined angle of angled abutment was 15° (Straumann Product Catalog 2012, Straumann AG, Switzerland).

In dentistry, platform switching was a method used to preserve alveolar bone levels around dental implants. A narrower abutment diameter for a given implant platform diameter was used [25].

The diameter and length of the implant were 4.1 mm and 14 mm, respectively (Straumann Product Catalog 2012, Straumann AG, Switzerland). Figure 5 illustrated external thread of the implant comprising trapezia tooth shorted for "Tr" (pitch P was 0.6 mm, thread depth was 0.5P, and thread angle was 30°), rectangle tooth shorted for "Re" (pitch P was 0.6 mm, thread depth is 0.5P, and thread angle was 0°), and saw tooth shorted for "Sa" (pitch P is 0.6 mm, thread depth was 0.75P, face flank angle was 3°, and nonface flank angle was 30°).

In the connection of the implant and the abutment, we adopted internal hexagon and Morse taper. Figure 6 depicted two healing methods of submerged one shorted for "Su" (smooth neck height was 1.2 mm) and nonsubmerged one shorted for "Ns" (smooth neck height was 1.2 mm, the inclination angle was 15°, and total height was 2.0 mm) (Straumann Product Catalog 2012, Straumann AG, Switzerland).

According to the various structured abutments, implant threads, and healing methods, 12 combinations of the dental implant systems were exhibited (Figure 7 and Table 1).

2.2. Finite Element Modeling. All 12 models described above were combined using Boolean operations, and the parasolid format of the solid model was then imported into ANSYS Workbench 14.0 (ANSYS, Inc., USA) to generate the FE model (Figure 8) using 10-node tetrahedral *h*-elements (ANSYS SOLID187 elements).

The convergence of the FEM analysis depended largely on the mesh grid. A standard convergence study was conducted by FEM analysis for mesh grids with different mesh refinement levels. A refined mesh was used in the threaded areas and the surrounding bone. For mesh grid, the relative errors for the maximum Von Mises stress in the implant system and the surrounding bone were computed as the

Table 1: 12 combinations of the dental implant systems.

Category	Abutment	Implant	Healing	Nodes
1#	"St"	"Tr"	"Su"	124,128
2#	"St"	"Re"	"Su"	123,676
3#	"St"	"Sa"	"Su"	123,684
4#	"St"	"Tr"	"Ns"	123,060
5#	"St"	"Re"	"Ns"	123,294
6#	"St"	"Sa"	"Ns"	124,433
7#	"St"	"Tr"	"Su"	129,202
8#	"An"	"Re"	"Su"	128,994
9#	"An"	"Sa"	"Su"	129,578
10#	"An"	"Tr"	"Ns"	127,706
11#	"An"	"Re"	"Ns"	128,938
12#	"An"	"Sa"	"Ns"	128,721

St: straight; An: angled; Tr: trapezia; Re: rectangle; Sa: saw; Su: submerged; Ns: nonsubmerged.

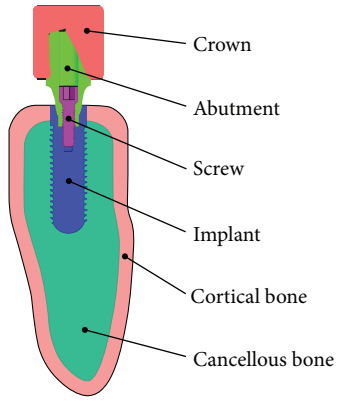

Figure 3: Dental implant/bone system.

percent differences between the current stress values and their counterparts predicted by the previous trial run. The calculation was considered to be convergent and the mesh grid was accepted when the relative errors were less than 1%. Number of total nodes is listed in Table 1, respectively.

2.3. Materials and Load Conditions. The abutment, implant, screw, cortical bone, and cancellous bone were treated as isotropic homogeneous linear elastic materials. Table 2 listed Young's modulus (E), Poisson's ratio (υ), and Tensile Strength (Ts) of the materials used in the numerical examples. Because the elements were quite small, the material properties were assumed to be constant within each element.

The bottom of the mandible was treated as fixed boundaries, and both side planes were frictionless, which was normal constraint (Figure 9). Two different contact models ("bonded" and "frictional") are used to simulate different integration qualities at the implant and the supporting bone tissues during the osseointegration process. Using contact type of frictional to describe the integration quality among the abutment, implant, and screw interface and among implant, cortical bone, and cancellous bone interface (Table 3), the friction coefficient was 0.5 and 0.4, respectively [26]. Frictional contact implied that a gap between the implant and the peri-implant part might exist under an occlusal force. The rest of the contact surfaces were Bonded contact (Table 3). The "bonded" type simulated perfect osseointegration in which the implant and the surrounding parts were fully integrated so that neither sliding nor separation in the implant-bone interface was possible.

Based on oral physiology, four types of loading conditions (Figure 6) were simulated:

(1) A vertical occlusal force of 100 N ($\theta = 0$) applied on the crown top surface [4], a preload of 200 N applied to the screw [27].

(2) A vertical occlusal force of 100 N ($\theta = 0$) applied on the crown top surface [4], a torque of 0.2 N·m applied to the screw [27].

(3) An inclined occlusal force of 100 N ($\theta = 15^\circ$) applied on the crown top surface [4], a preload of 200 N applied to the screw [27].

(4) An inclined occlusal force of 100 N ($\theta = 15^\circ$) applied on the crown top surface [4], a torque of 0.2 N·m applied to the screw [27].

3. Results

Figure 7 gave the Von Mises stress distributions of the typical dental implants and the surrounding bone tissues under loading condition (1), (2), (3), or (4), respectively.

As shown in Figure 10, the stress was mainly concentrated at the inner hexagon positioning junction because the force was just applied only on the contact surface. Application of the preload or torque applied to the screw resulted in the stress concentration on the screw, and fatigue failure would occur in the process of long-term use. The stresses in the cortical bone and cancellous bone, which were conjoint with implant, were relatively small due to the design concept of platform switching, which could reduce the stresses gradually at junction between the implant and the surrounding bone tissues, thus avoiding bone level being decreased in the long-term use.

Then we compared the maximum Von Mises stress distributions of 12 types of the dental implants and surrounding bone tissues (Figure 11).

Figure 11(a) exhibited the stress distribution of the abutment. When vertical force was applied on the crown, the abutment stress of the torque applied to the screw was larger than that of the preload condition while in the inclined force the abutment stress of the preload applied to the screw was larger than that of the torque condition. Both in the preload and in torque condition, the abutment stress of the inclined force was significantly higher than that in the vertical force of the crown. Taken together, the abutment maximum stresses of 1#, 2#, 3#, 7#, 8#, and 9# were rather small.

Figure 11(b) presented stress distribution of the implant. In the preloaded screw application, the stress difference was small in both the vertical force and the inclined force conditions. In the torque condition, the implant stress in

Table 2: Material properties used in this study.

Material	Region	E (MPa)	υ	Ts (MPa)	Reference
Titanium	Implant, abutment, screw	102,000	0.35	485	[22]
Porcelain	Crown	68,900	0.28	835	[22]
Cortical bone	Mandible	13,000	0.30	133.9	[23]
Cancellous bone	Mandible	690	0.30	56	[23]

Table 3: Contact methods.

	Abutment	Screw	Implant	Cortical bone	Cancellous bone
Crown	Bonded	—	—	—	—
Abutment	—	Frictional	Frictional	—	—
Screw	—	—	Frictional	—	—
Implant	—	—	—	Frictional	Frictional
Cortical bone	—	—	—	—	Bonded

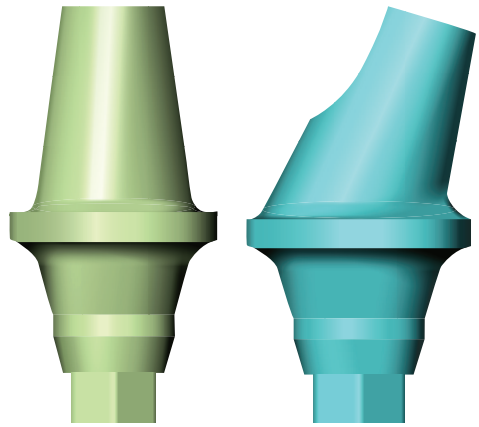

(a) Straight abutment (b) Angled abutment

Figure 4: Abutment category.

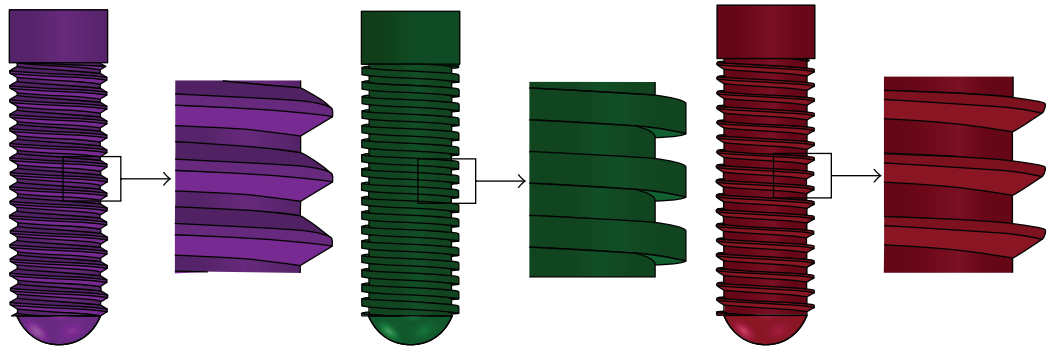

(a) Trapezia tooth (b) Rectangle tooth (c) Saw tooth

Figure 5: Thread category of the implant.

the inclined force was larger than that in the vertical force. Both in the vertical and the inclined force, the preloaded application had great effect on the implant stress. Taken together, the implant maximum stresses of 3#, 4#, 5#, 10#, and 11# were rather small.

Figure 11(c) depicted the stress distribution of the screw. Whether in the preloaded or in torque application, the vertical and inclined force of the crown application had little effect on screw stress. However, under same loading conditions, the screw stress of the preloaded screw had greater effect than the

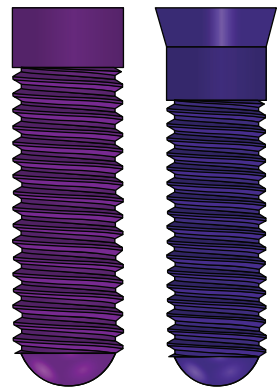

Figure 6: Healing method.

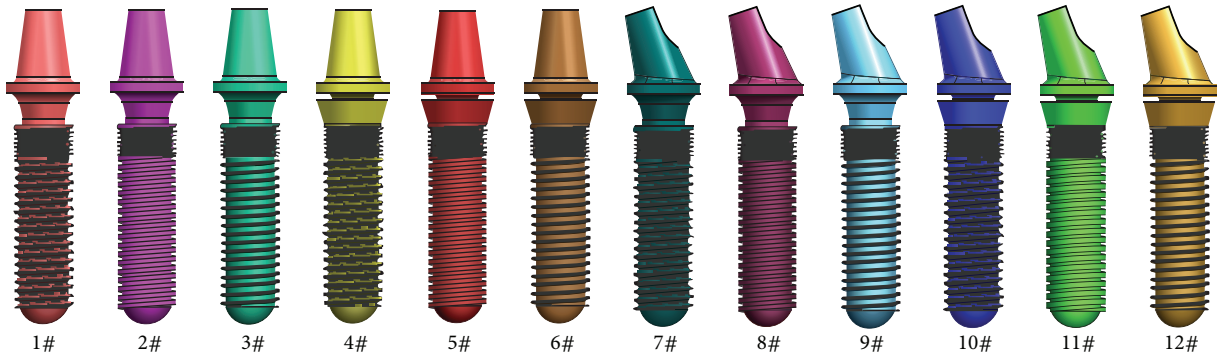

Figure 7: 3D model of 12 dental implant systems.

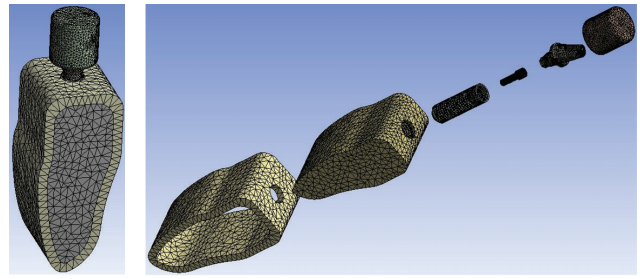

Figure 8: Finite element mesh view.

torque one. Taken together, the screw maximum stresses of 1#, 3#, 5#, 7#, 9#, and 11# were rather small.

Figure 11(d) represented the stress distribution of the cortical bone. The cortical bone stress was relatively small. Whether in the preload or in torque application of the screw, the cortical bone stress of the inclined force was larger than the vertical force while in the vertical force the torqued screw application had greater effect on screw stress than the preloaded one. However, in the inclined force application, the torqued screw had smaller effect on screw stress than the preload condition. Taken together, the cortical bone maximum stresses of 4#, 5#, 6#, 10#, 11#, and 12# were rather small.

Figure 11(e) showed the stress distribution of the cancellous bone. The cancellous bone stress was relatively small. Whether in the preload or in torque application of the screw, the cancellous bone stress of the inclined force was larger than that of the vertical force. However, under same load conditions, the preloaded screw had greater effect on screw stress than the torque condition. Taken together, the cancellous bone maximum stresses of 4#, 5#, 6#, 9#, 10#, and 11# were rather small.

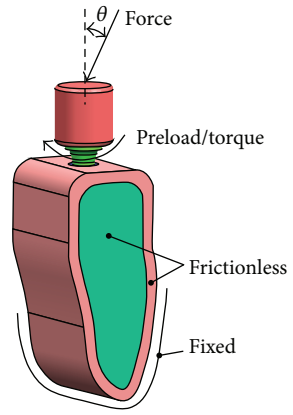

Figure 9: Load conditions of dental implant-bone tissue.

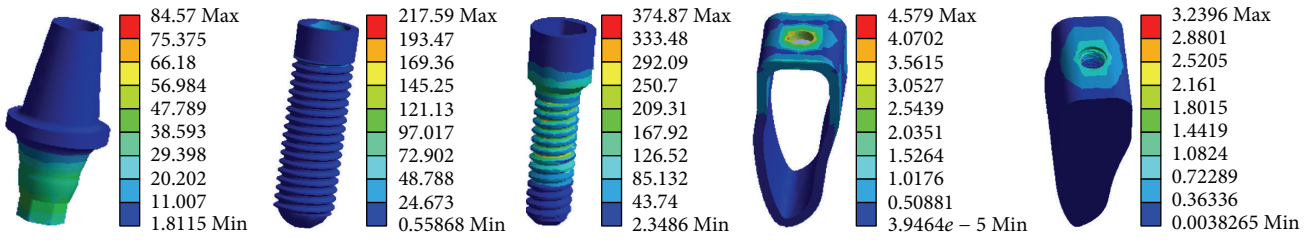

(a) Straight abutment, trapezia tooth, and submerged healing under loading condition (1)

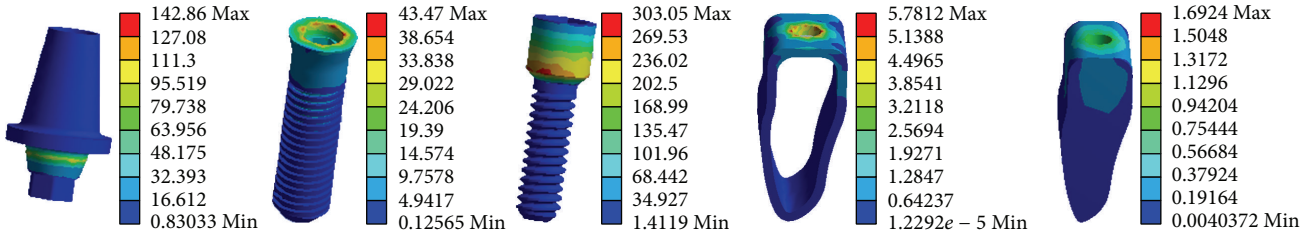

(b) Straight abutment, rectangular tooth, and nonsubmerged healing loading condition (2)

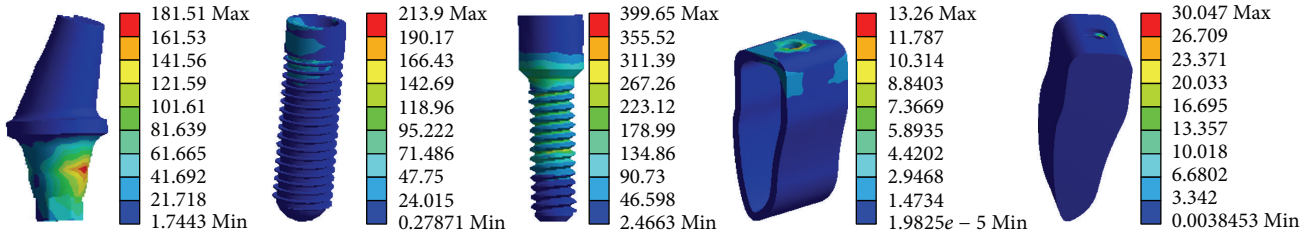

(c) Angled abutment, saw tooth, and submerged healing under loading condition (3)

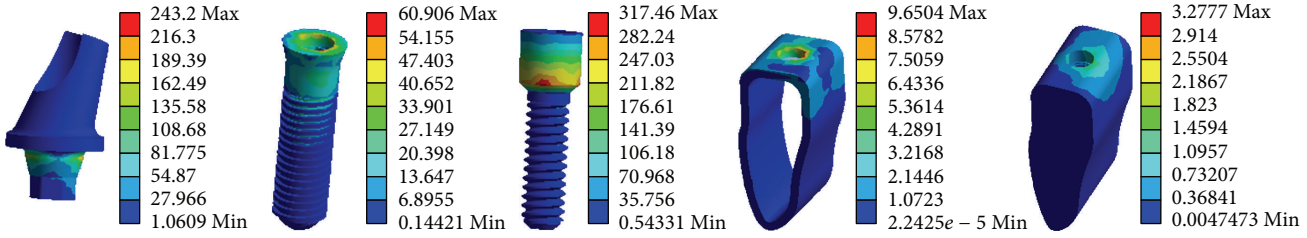

(d) Angled abutment, rectangular tooth, and nonsubmerged healing under loading condition (4)

Figure 10: Stress distributions in the typical dental implants and the surrounding bone tissues.

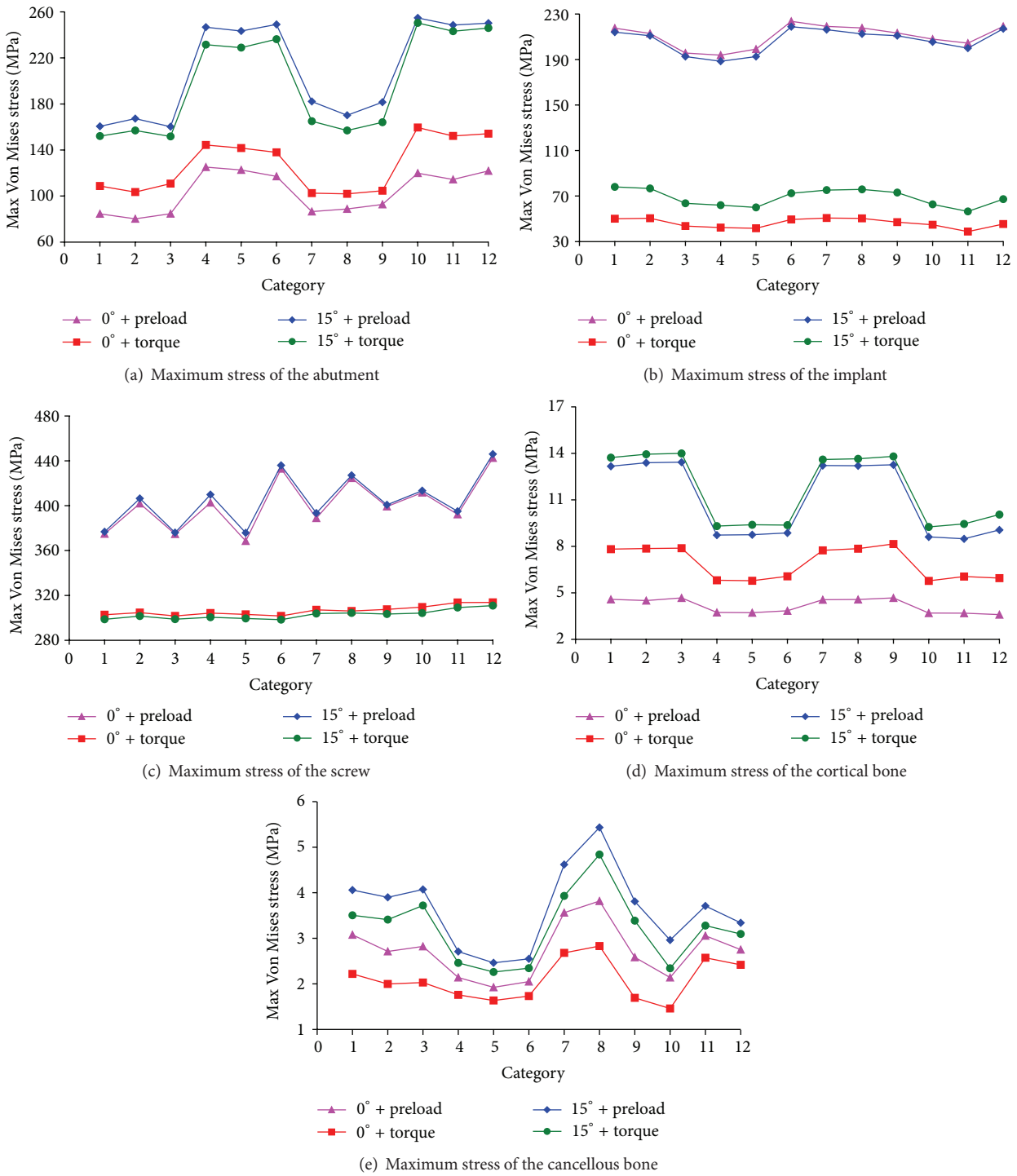

FIGURE 11: Maximum stress distributions of the dental implants and surrounding bone tissues.

4. Discussion

Stress fields around endosteal implants and the supporting bone tissues were closely related to the type of loading and implant geometry [4]. In order to realistically simulate the stress state of the implant/bone system, four types of loading conditions (Figure 9) were studied.

Our results showed that the stress was mainly concentrated at the inner hexagon positioning junction because of the force just applied on the contact surface. The application of the preloaded or torqued screw resulted in stress concentration on the screw. However, the stresses in the cortical bone and cancellous bone which were conjoint with implant were relatively small.

Table 4: Stress comparisons of 12 implants-bone tissues.

		Dental implant-bone system					
		Abutment	Implant	Screw	Cortical bone	Cancellous bone	Frequency
Implant combinations	1#	+		+			2
	2#	+					1
	3#	+	+	+			3
	4#		+		+	+	3
	5#		+	+	+	+	4
	6#				+	+	2
	7#	+		+			2
	8#	+					1
	9#	+		+			2
	10#				+	+	2
	11#		+	+	+		3
	12#				+	+	2

The symbol of "+" meant the unit with minimum stress of the implant-bone tissues.

Under same loading direction of the crown, the stress influence on the torqued screw was greater than that of the preload condition in the abutment and cortical bone while the stress influence of the preloaded screw was greater than that of the torqued condition for the implant, screw, and cancellous bone. The reason was mainly that the torque acted on the upper inner surface of the hexagonal hole of the screw while the preload was applied to the lower outer surface of the screw.

Meanwhile, under same loading mode of the screw, the stress distributions of the abutment, cortical bone, and cancellous bone in the inclined force on the crown were larger than those in the vertical force, up to 2 to 3 times. However, as for the implant and screw, the stress influence with different loading direction applied on the crown was not large. It was mainly due to the fact that the vertical force made stress distribution of the surrounding bone uniform through the cross section and the thread of implant. While the inclined force generated shear force and bending moment on the implant, thus the stress concentration at the implant's neck and bone contact area has taken place.

In addition, the abutment stress of nonsubmerged implant was larger than that of the submerged one under same load conditions. However, the implant, cortical bone, and cancellous bone stresses of nonsubmerged implant were smaller than those of submerged one indicating that if an overload condition occurred during chewing, the abutment of nonsubmerged system and the implant of submerged system would be susceptible to be broken, which could affect the long-term retention rate of the implant system. Therefore, doctors and patients need to take certain protective measures in use.

Table 4 listed stress distributions of 12 combinations of the dental implants and surrounding bone tissues (The symbol of "+" meant the unit with minimum stress of the implant-bone tissues). It was seen from Table 4 that 5# was the best option, which was the straight abutments, rectangular tooth, and nonsubmerged dental implant system. Meanwhile, 3#, 4#, and 11# were also provided with a certain application value.

5. Conclusion

Under same loading conditions, the thread had no significant effect on the implant stress but a greater impact on the cancellous bone stress. The stress distributions of the abutment, cortical bone, and cancellous bone in the inclined force of the crown were larger than that in the vertical force. The abutment stress of nonsubmerged healing implant system was larger than that of the submerged healing one. However, the implant, cortical bone, and cancellous bone stresses of nonsubmerged implant system were smaller than those of submerged one.

In conclusion, a dental implant system characterised by a straight abutment, rectangular tooth, and nonsubmerged healing method is the optimal design.

Conflict of Interests

The authors declare that there is no conflict of interests regarding the publication of this paper.

Acknowledgments

Financial support from the National Natural Science Foundation of China (51307170), the Cooperation Project of Chinese Academy of Sciences and Foshan City Government of China (2014HT10008), the Guangzhou City Key Laboratory project (15180003), and the Guangzhou Nansha District High-Tech Industrialization Project of China (201202005) is gratefully acknowledged.

References

[1] H. İplikçioğlu and K. Akça, "Comparative evaluation of the effect of diameter, length and number of implants supporting three-unit fixed partial prostheses on stress distribution in the bone," *Journal of Dentistry*, vol. 30, no. 1, pp. 41–46, 2002.

[2] R. Adell, B. Eriksson, U. Lekholm, P. I. Brånemark, and T. Jemt, "Long-term follow-up study of osseointegrated implants in the

treatment of totally edentulous jaws," *The International Journal of Oral & Maxillofacial Implants*, vol. 5, no. 4, pp. 347–359, 1990.

[3] R. Adell, U. Lekholm, B. Rockler, and P. I. Branemark, "A 15-year study of osseointegrated implants in the treatment of the edentulous jaw," *International Journal of Oral Surgery*, vol. 10, no. 6, pp. 387–416, 1981.

[4] J. Yang and H.-J. Xiang, "A three-dimensional finite element study on the biomechanical behavior of an FGBM dental implant in surrounding bone," *Journal of Biomechanics*, vol. 40, no. 11, pp. 2377–2385, 2007.

[5] R. Calandriello and M. Tomatis, "Immediate occlusal loading of single lower molars using br anemark system(R) wide platform TiUnite implants: a 5-year follow-up report of a prospective clinical multicenter study," *Clinical Implant Dentistry and Related Research*, vol. 19, pp. 381–396, 2009.

[6] G. O. Gallucci, C. B. Doughtie, J. W. Hwang, J. P. Fiorellini, and H.-P. Weber, "Five-year results of fixed implant-supported rehabilitations with distal cantilevers for the edentulous mandible," *Clinical Oral Implants Research*, vol. 20, no. 6, pp. 601–607, 2009.

[7] F. E. Lambert, H.-P. Weber, S. M. Susarla, U. C. Belserand, and G. O. Gallucci, "Descriptive analysis of implant and prosthodontic survival rates with fixed implant-supported rehabilitations in the edentulous maxilla," *Journal of Periodontology*, vol. 80, no. 8, pp. 1220–1230, 2009.

[8] J. B. Brunski, "Biomechanics of dental implants," in *Implants in Dentistry*, M. Block, J. N. Kent, and L. R. Guerra, Eds., no. 2, pp. 63–71, W.B. Saunders, Philadelphia, Pa, USA, 1997.

[9] T. Li, K. Hu, L. Cheng et al., "Optimum selection of the dental implant diameter and length in the posterior mandible with poor bone quality—A 3D finite element analysis," *Applied Mathematical Modelling*, vol. 35, no. 1, pp. 446–456, 2011.

[10] C.-C. Lee, S.-C. Lin, M.-J. Kang, S.-W. Wu, and P.-Y. Fu, "Effects of implant threads on the contact area and stress distribution of marginal bone," *Journal of Dental Sciences*, vol. 5, no. 3, pp. 156–165, 2010.

[11] H.-L. Huang, C.-H. Chang, J.-T. Hsu, A. M. Fallgatter, and C.-C. Ko, "Comparison of implant body designs and threaded designs of dental implants: a 3-dimensional finite element analysis," *International Journal of Oral and Maxillofacial Implants*, vol. 22, no. 4, pp. 551–562, 2007.

[12] C. E. Misch and M. W. Bidez, "A scientific rationale for dental implant design," in *Contemporary Implant Dentistry*, C. E. Misch, Ed., pp. 329–343, Mosby, St. Louis, Mo, USA, 2nd edition, 1999.

[13] N. Sykaras, A. M. Iacopino, V. A. Marker, R. G. Triplett, and R. D. Woody, "Implant materials, designs, and surface topographies: their effect on osseointegration. A literature review," *International Journal of Oral and Maxillofacial Implants*, vol. 15, no. 5, pp. 675–690, 2000.

[14] C. Maiorana and F. Santoro, "Maxillary and mandibular bone reconstruction with hip grafts and implants using Frialit-2 implants," *International Journal of Periodontics and Restorative Dentistry*, vol. 22, no. 3, pp. 221–229, 2002.

[15] G. H. Nentwig, "Ankylos implant system: concept and clinical application," *Journal of Oral Implantology*, vol. 30, no. 3, pp. 171–177, 2004.

[16] S. Hansson and M. Werke, "The implant thread as a retention element in cortical bone: the effect of thread size and thread profile: A finite element study," *Journal of Biomechanics*, vol. 36, no. 9, pp. 1247–1258, 2003.

[17] L. Kong, K. Hu, D. Li et al., "Evaluation of the cylinder implant thread height and width: a 3-dimensional finite element analysis," *International Journal of Oral and Maxillofacial Implants*, vol. 23, no. 1, pp. 65–74, 2008.

[18] H.-L. Huang, J.-T. Hsu, L.-J. Fuh, D.-J. Lin, and M. Y. C. Chen, "Biomechanical simulation of various surface roughnesses and geometric designs on an immediately loaded dental implant," *Computers in Biology and Medicine*, vol. 40, no. 5, pp. 525–532, 2010.

[19] D. L. Cochran, D. Morton, and H.-P. Weber, "Consensus statements and recommended clinical procedures regarding loading protocols for endosseous dental implants," *International Journal of Oral and Maxillofacial Implants*, vol. 19, no. 5, pp. 109–113, 2004.

[20] C. E. Misch, H.-L. Wang, C. M. Misch, M. Sharawy, J. Lemons, and K. W. M. Judy, "Rationale for the application of immediate load in implant dentistry: part I," *Implant Dentistry*, vol. 13, no. 3, pp. 207–217, 2004.

[21] R. Gapski, H.-L. Wang, P. Mascarenhas, and N. P. Lang, "Critical review of immediate implant loading," *Clinical Oral Implants Research*, vol. 14, no. 5, pp. 515–527, 2003.

[22] J. Chen, X. Lu, N. Paydar, H. U. Akay, and W. E. Roberts, "Mechanical simulation of the human mandible with and without an endosseous implant," *Medical Engineering and Physics*, vol. 16, no. 1, pp. 53–61, 1994.

[23] J. Y. Rho, R. B. Ashman, and H. Turner, "Young's modulus of trabecular and cortical bone material: ultrasonic and microtensile measurements," *Journal of Biomechanics*, vol. 26, no. 2, pp. 111–119, 1993.

[24] A. N. Natali, P. G. Pavan, and A. L. Ruggero, "Analysis of bone-implant interaction phenomena by using a numerical approach," *Clinical Oral Implants Research*, vol. 17, no. 1, pp. 67–74, 2006.

[25] Y. Maeda, J. Miura, I. Taki, and M. Sogo, "Biomechanical analysis on platform switching: is there any biomechanical rationale?" *Clinical Oral Implants Research*, vol. 18, no. 5, pp. 581–584, 2007.

[26] Z. Enwei and G. Fei, "Analysis of static force and fatigue between thread structure of dental implant and contact surface," *Journal of Clinical Rehabilitative Tissue Engineering*, vol. 14, no. 30, pp. 5531–5534, 2010.

[27] C. Luo, "Effects of different shape of occlusal screws on stability for single implant-supported crowns," *Chinese Journal of Oral Implantology*, vol. 14, no. 2, pp. 44–47, 2009.

Hindawi Publishing Corporation
International Journal of Dentistry
Volume 2016, Article ID 1849207, 7 pages
http://dx.doi.org/10.1155/2016/1849207

Research Article

Comparison of the Mechanical Properties of Early Leukocyte- and Platelet-Rich Fibrin versus PRGF/Endoret Membranes

Hooman Khorshidi,[1] Saeed Raoofi,[1] Rafat Bagheri,[2] and Hodasadat Banihashemi[3]

[1]*Department of Periodontology, School of Dentistry, Shiraz University of Medical Sciences, Shiraz, Iran*
[2]*Department of Dental Materials, School of Dentistry, Shiraz University of Medical Sciences, Shiraz, Iran*
[3]*Periodontology Department, Faculty of Dentistry, Shahid Sadoughi University of Medical Sciences, Yazd, Iran*

Correspondence should be addressed to Hodasadat Banihashemi; hoda.banihashemi@gmail.com

Received 19 July 2015; Revised 10 December 2015; Accepted 16 December 2015

Academic Editor: Andrija Bosnjak

Objectives. The mechanical properties of membranes are important factors in the success of treatment and clinical handling. The goal of this study was to compare the mechanical properties of early leukocyte- and platelet-rich fibrin (L-PRF) versus PRGF/Endoret membrane. *Materials and Methods*. In this experimental study, membranes were obtained from 10 healthy male volunteers. After obtaining 20 cc venous blood from each volunteer, 10 cc was used to prepare early L-PRF (group 1) and the rest was used to get a membrane by PRGF-Endoret system (group 2). Tensile loads were applied to specimens using universal testing machine. Tensile strength, stiffness, and toughness of the two groups of membranes were calculated and compared by paired t-test. *Results*. The mean tensile strength and toughness were higher in group 1 with a significant difference ($P < 0.05$). The mean stiffness in group 1 was also higher but not statistically significant ($P > 0.05$). *Conclusions*. The results showed that early L-PRF membranes had stronger mechanical properties than membranes produced by PRGF-Endoret system. Early L-PRF membranes might have easier clinical handling and could be a more proper scaffold in periodontal regenerative procedures. The real results of the current L-PRF should be in fact much higher than what is reported here.

1. Introduction

Periodontal reconstruction is the ideal goal of periodontal treatment and since 1970, many researches led to developing various methods to achieve it. Among these methods, guided tissue regeneration (GTR) and guided bone regeneration (GBR) use barrier membranes to separate the periodontal ligament and bone from the epithelium and connective tissue which allow the former to regenerate the defects [1]. Recently, various growth factors have been studied in periodontal regeneration [2] and it is indicated that they might strongly alter the healing process [3]. A new method in this field is using concentrated platelet products which are the source of autologous platelet derived growth factors and transforming growth factors [4].

Among various concentrated platelet products, preparation rich in growth factor (PRGF) is an autologous platelet-rich plasma product which accelerates local release of growth factors and bioactive proteins following its activation. With various formulations, this product can be used in form of liquid or in form of clot as a membrane which is a biocompatible, dense, and elastic membrane [5]. The new form of concentrated platelet is platelet-rich fibrin (PRF) that can be used directly as a clot or as a strong membrane after compression [6, 7]. PRF as a membrane has shown slow release of growth factors such as vascular endothelial growth factor (VEGF), transforming growth factor (TGF-β), and platelet derived growth factor (PDGF) for at least 7 days in vitro [8]. Leukocyte- and platelet-rich fibrin (L-PRF) can be considered as a second-generation platelet concentrate. It forms a

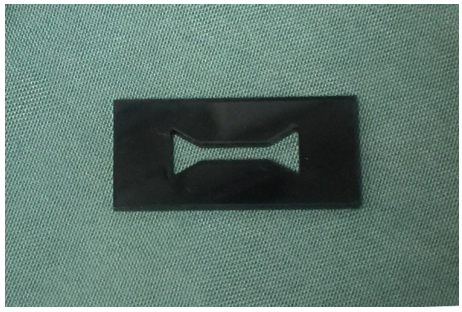

Figure 1: The dog-bone-shape plexiglass mold.

strong fibrin matrix with a complex three-dimensional architecture, in which most of the platelets and leucocytes from the harvested blood are concentrated [9]. Platelet-rich fibrin membranes can be used in various regenerative treatments [10, 11] to accelerate healing, to progress the regeneration process, and also as a scaffold in tissue engineering.

Besides scientific evidences about efficacy, for selection of an appropriate membrane, there are other important parameters including mechanical properties and clinical handling [12, 13]. Mechanical characteristics of the membrane may affect the final results of GBR [14]. Tensile strength of a material when sutured may affect the clinical result of following healing [15]. Moreover strong mechanical characteristics of a scaffold provide a more suitable support for regeneration [16].

It is reported that increasing fibrinogen concentrates and adding calcium chloride increase the adhesion and tensile strength of fibrin clot [17]. It is also indicated that increasing thrombin and fibrinogen may increase the stiffness of fibrin matrix [18].

To the best of authors' knowledge, a comparison of mechanical characteristics of PRF and PRGF membranes is missing in previous studies. The goal of this study was to compare the mechanical properties of early L-PRF and the PRGF membranes. The null hypothesis was that there is no difference between mechanical properties of early L-PRF and PRGF membranes.

2. Materials and Methods

In this experimental study, 20 cc venous blood was obtained from 10 healthy volunteer males with age range of 25 to 35 years. The exclusion criteria were suffering from a known systemic disease, history of taking any anticoagulant medication, smoking, and history of taking any medicine in the past 3 months.

2.1. Preparing a Mold. A specially designed plexiglass mold was fabricated to make the fibrin specimens identical in size, volume, and figure, following a modification of the dog-bone-shape mold in Alston's study [17]. The thickness of the mold was 2 mm and the width was 2 mm in the narrow middle part and 6 mm in the larger ends. The total volume of the mold was 104 mm^3. The narrow neck provided the weakest point where the specimen would break (Figure 1).

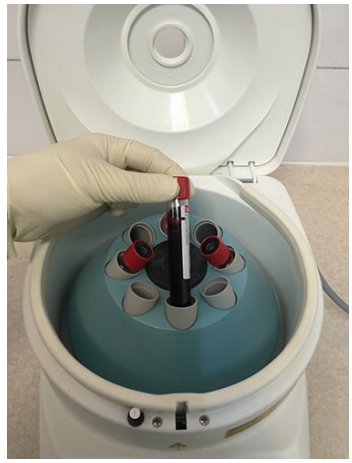

Figure 2: Tube containing blood in the centrifuge machine.

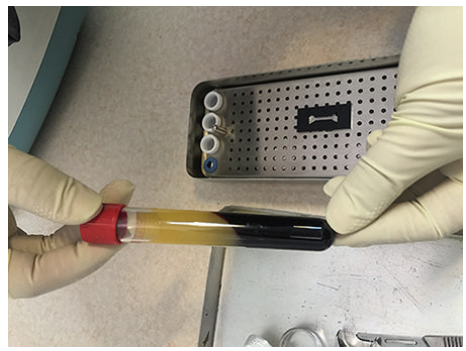

Figure 3: Tube containing early L-PRF after centrifuge.

2.2. Blood Collection. After obtaining informed consent approved by the ethical committee of Shiraz University of Medical Science (Grant number 92-01-03-6162) from all donors, 20 cc venous blood was collected by sterile syringe. 10 cc was placed in a dry sterile tube specific for PC-02 machine and the rest was divided into two 5 cc blood samples placed in two tubes containing 0.5 cc 3.8% concentrate of sodium citrate as anticoagulant specific for PRGF-Endoret system.

2.3. Preparing the Membranes. Platelet-rich membranes were obtained by two different protocols:

The first one was producing early L-PRF [7] by PC-02 machine (Process Ltd., Nice, France) in which the tube that contained blood was centrifuged immediately after blood collection in speed of 400 gr for 10 min [19] (Figure 2). The outcome was a fibrin clot containing platelets in the middle of the tube, between acellular plasma at the top and the red blood cell layer at the bottom (Figure 3). This clot was removed from the tube (Figure 4) and the attached red blood cells were scraped off and discarded. The early L-PRF clot was then placed in the mold (Figure 5) which was placed on the grid in the PRF Box [20] (Process

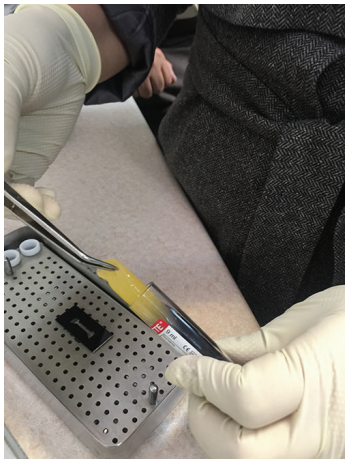

Figure 4: Removing the early L-PRF from the tube.

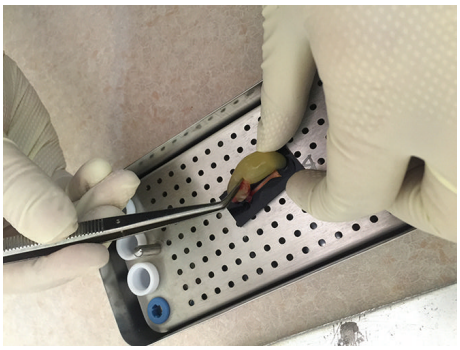

Figure 5: Placing the early L-PRF clot into the mold.

Ltd., Nice, France) (Figure 6) and covered with the compressor and lid. After 10 min the formed early L-PRF membrane was prepared (Figure 7).

The second protocol was performed using PRGF-Endoret system (BTI, Spain) (Figure 8). The two 5 cc tubes were centrifuged in speed of 400 gr for 8 min with BTI centrifuge machine (BTI, Spain) (Figure 9). Then each tube contained red blood cell at the bottom and plasma at the top with a thin layer of WBC in the middle (Figure 10). The inferior half of the plasma which was rich in platelets and growth factors was removed by plasma transfer device 2 (PTD2) (BTI, Spain) and placed in another tube. As the manufacturer instructions, 0.05 mL PRGF-Endoret activator per 1 mL plasma was added and then placed on incubator at 37°C for 30 min to obtain the clot (Figure 11). The clot was placed in the mold and after 10 min the formed membrane was obtained (Figure 12).

2.4. Tensile Test. Tensile test was performed using universal testing machine (Zwick/Roll Z020, Zwick GmbH & Co., Germany) (Figure 13). The larger ends of the dog-bone shape specimen were held with the clips of the machine without any

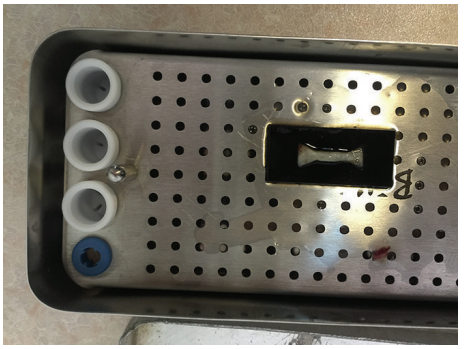

Figure 6: A fibrin specimen in the mold.

Figure 7: A formed specimen.

Figure 8: A BTI kit.

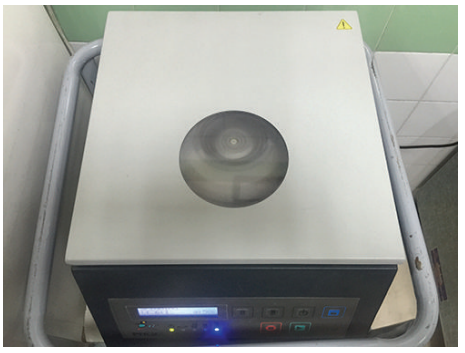

Figure 9: BTI centrifuging machine.

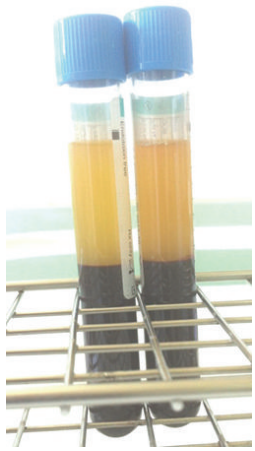

Figure 10: Tubes containing PRGF after centrifuge.

Figure 11: Mixture of the platelet-rich plasma and the activator on the incubator.

tension. Tensile loading was applied at a cross head speed of 2 mm/min; the maximum load at specimen failure was recorded and tensile strength was calculated using following formula: $S = F/A$, where F is maximum force (N) and A is unit area (m^2).

Stress-strain curve was recorded with test Xpert II software simultaneously. Stiffness of the specimen (modulus of elasticity) was obtained by stress/strain and the total area under the curve designated as toughness of the specimens.

2.5. Data Analysis. Data were collected and analyzed using SPSS version 16; Student t-test was used to compare the groups: the early L-PRF as group 1 and the PRGF-Endoret system as group 2.

3. Results

The results of all tests for two groups are summarized in Table 1.

Figure 12: A formed specimen.

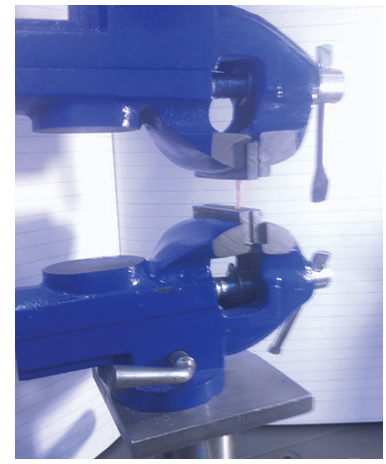

Figure 13: The universal testing machine.

Table 1: Mean values and standard deviation (±SD) for all tested properties in the two groups.

Measured values	Group	Mean ± SD	P value
Tensile strength (MPa)	1	0.20 ± 0.06	0.049
	2	0.14 ± 0.07	
Modulus of elasticity (MPa)	1	0.13 ± 0.07	0.69
	2	0.11 ± 0.09	
Toughness (Joule/m^3)	1	1.87 ± 0.61	0.001
	2	0.81 ± 0.53	

Tensile strength of early L-PRF group with mean value of 0.20 ± 0.06 MPa was significantly higher than PRGF group with mean value of 0.14 ± 0.07 MPa ($P = 0.049$). Early L-PRF group was slightly stiffer than PRGF group but was not statistically significant ($P = 0.69$). Toughness of early L-PRF group was significantly higher than PRGF group ($P = 0.001$).

4. Discussion

This study experienced that the mechanical properties of early L-PRF membranes are stronger than the PRGF-Endoret membranes.

Platelet-rich fibrin membrane releases various growth factors such as PDGF, TGF-β, and VEGF slowly [21] and its supportive fibrin matrix plays an important role in its

therapeutic effects [6]. The potential of platelet-rich membrane in accelerating regeneration has led to its application in various regenerative treatments like sinus floor elevation, ridge augmentation, socket preservation, root coverage, intrabony defects, and furcation defects [22–31]. It has been shown that fibrin membranes could be better scaffolds for proliferation of periosteal and osseous cells than collagen membranes in vitro [32, 33]. The membranes that are used in regenerative procedures should have strong mechanical properties to protect blood clot and healing process [13]. As a scaffold, they provide better support against forces from infiltrating cells and adjacent tissues [16, 34].

The specimens of this study were selected from healthy male individuals with the age range of 25–35 to prevent possible bias from varieties in blood components of different sexes, ages, and systemic conditions. These issues were not considered together in the previous studies on fibrin clots [17, 35, 36]. The dog-bone-shape mold was used to make the specimens identical in size, volume, and shape. It was a modification of Alston's method [17], since the volume of clot we could obtain and consequently the volume of our specimen were lesser than Alston's study. Mechanical measurements were performed by universal testing machine as some other studies [17, 35–38].

According to the results of our study, the tensile strength, stiffness, and toughness of early L-PRF membranes were higher than the PRGF-Endoret membranes though the stiffness difference was not significant. This result may be due to their structural differences which may be affected by some factors like their differences in polymerization. The mode of polymerization has significant effects on mechanical properties of fibrin matrix [39]. This is consistent with the studies that evaluated their polymerization and internal structure [9, 39]. The last stage of clotting, in which fibrinogen is converted to fibrin, can be accelerated by adding calcium chloride [40]. In PRGF-Endoret system, calcium chloride is used to initiate the last coagulation stage; then sudden fibrin polymerization occurs [39]. Therefore the fibrin matrix is immature and most of the fibrils are thin [9]. On the other hand, a slow and natural polymerization occurs during the centrifuge process in L-PRF producing method. The fibrin fibrillae can be assembled in 2 different biochemical architectures during gelling process: condensed tetramolecular or bilateral junctions and connected trimolecular or equilateral junctions [39]. PRGF mostly have the bilateral junctions which are weaker than the equilateral junctions [9] that are mostly found in L-PRF. This provides a flexible and elastic fibrin network [39]. L-PRF has thick fibers and strong matrix [9].

The density of the final fibrin matrix is another important factor that has an influence on the mechanical properties [41] and fibrinogen concentration affects this parameter. Fibrinogen mostly originates from the α-granules of the platelet in PRGF so the final fibrin has low density, while the circulating fibrinogen present in L-PRF strengthens the final fibrin matrix [9]. Alston et al. (2007) and Duong et al. (2009) indicated that increase in fibrinogen concentration makes the final fibrin matrix stronger [17, 18].

Another difference of these two membranes is the presence of large quantities of leukocytes in L-PRF and lack of them in PRGF. Some studies indicated that leukocytes have a key role in immune regulation, anti-infection properties [42–45], and angiogenesis [46] in platelet-rich concentrates. On the other hand, some authors claim that leukocytes may destroy the extracellular matrix of fibrin by the anti-inflammatory effects of proteases and hydrolase; therefore they suggest removing the leukocytes from platelet-rich concentrates to prevent their negative effects on autologous fibrin formation [5, 47]. The interaction of platelets and leukocytes in platelet-rich concentrates is not completely analyzed; they may also show synergistic effect [9]. Therefore the negative effects of leukocytes on fibrin matrix are controversial yet and our results suggest that these effects are not significant.

In producing the early L-PRF, no anticoagulant is employed but, in PRGF, sodium citrate is used. This difference of these two methods may affect the fibrin matrix. Kingston showed that high concentration of sodium citrate in blood samples decreases the ionized calcium of plasma leading to decrease in platelet accumulation and fibrinogen binding [48]. However, it is not obvious that 0.5 cc 3.8% concentration of sodium citrate can have such an effect on PRGF matrix and controlled studies are needed to confirm this issue.

The room temperature during the process and the speed of centrifuge were the same in both groups but the duration was less in PRGF. Perez et al. showed that longer duration of centrifuge increases the platelet recovery [49] so this may affect the plasma components and final fibrin matrix properties.

Parameters such as manufacturing property of the blood collecting tubes and the pressure applied during the process do not affect the biomaterial structure [8].

It should be noted that we used the early protocol (3000 rpm, 10 minutes) to produce L-PRF, while since years the 2700 rpm/12 minutes protocol is mostly used that gives much better polymerized L-PRF and therefore stronger membranes than the 3000 rpm/10 min protocol. The real results of the current L-PRF should be in fact much higher than what is reported here. However the material we used is adequate for the production of a good quality original L-PRF (early protocol). The original L-PRF system now exists only in one CE/FDA cleared form that is termed Intra-Spin L-PRF (Intra-lock, Boca Raton, FL, USA), and, legally, it is the only kit/system allowed in Western countries (CE/FDA).

5. Conclusion

Considering the limitations, this study showed that early L-PRF membranes have stronger mechanical properties than platelet-rich membranes obtained by PRGF-Endoret system. Probably, they have easier clinical application and handling, and they may also be stronger during suturing and provide more supportive scaffold in periodontal regeneration. The real results of the current L-PRF should be in fact much higher than what is reported here.

Conflict of Interests

The authors declare that there is no conflict of interests regarding the publication of this paper.

Acknowledgments

The authors thank the Vice-Chancellory of Research Shiraz University of Medical Science for supporting this research (Grant no. 92-01-03-6162). This paper is based on the thesis by Dr. Hodasadat Banihashemi. The authors also thank Dr. Mehrdad Vosooghi of the Dental Research Development Center, of the School of Dentistry, for the statistical analysis and Dr. Shahram Hamedani for his suggestions and editorial assistance in the paper.

References

[1] M. G. Newman, H. Takei, P. R. Klokkevold, and F. A. Carranza, *Carranza's Clinical Periodontology*, Elsevier Health Sciences, 2011.

[2] P. J. Boyne, R. E. Marx, M. Nevins et al., "A feasibility study evaluating rhBMP-2/absorbable collagen sponge for maxillary sinus floor augmentation," *The International Journal of Periodontics & Restorative Dentistry*, vol. 17, no. 1, pp. 11–25, 1997.

[3] Z. Schwartz, D. L. Carnes Jr., R. Pulliam et al., "Porcine fetal enamel matrix derivative stimulates proliferation but not differentiation of pre-osteoblastic 2T9 cells, inhibits proliferation and stimulates differentiation of osteoblast-like MG63 cells, and increases proliferation and differentiation of normal human osteoblast NHOst cells," *Journal of Periodontology*, vol. 71, no. 8, pp. 1287–1296, 2000.

[4] R. E. Marx, E. R. Carlson, R. M. Eichstaedt, S. R. Schimmele, J. E. Strauss, and K. R. Georgeff, "Platelet-rich plasma: growth factor enhancement for bone grafts," *Oral Surgery, Oral Medicine, Oral Pathology, Oral Radiology, and Endodontics*, vol. 85, no. 6, pp. 638–646, 1998.

[5] E. Anitua, M. Sánchez, G. Orive, and I. Andia, "Delivering growth factors for therapeutics," *Trends in Pharmacological Sciences*, vol. 29, no. 1, pp. 37–41, 2008.

[6] M. Toffler, N. Toscano, D. Holtzclaw, M. Corso, and D. D. Ehrenfest, "Introducing Choukroun's platelet rich fibrin (PRF) to the reconstructive surgery milieu," *The Journal of Implant & Advanced Clinical Dentistry*, vol. 1, no. 6, pp. 21–32, 2009.

[7] D. M. Dohan, J. Choukroun, A. Diss et al., "Platelet-rich fibrin (PRF): a second-generation platelet concentrate. Part I: technological concepts and evolution," *Oral Surgery, Oral Medicine, Oral Pathology, Oral Radiology and Endodontology*, vol. 101, no. 3, pp. E37–E44, 2006.

[8] D. M. Dohan Ehrenfest, G. M. de Peppo, P. Doglioli, and G. Sammartino, "Slow release of growth factors and thrombospondin-1 in Choukroun's platelet-rich fibrin (PRF): a gold standard to achieve for all surgical platelet concentrates technologies," *Growth Factors*, vol. 27, no. 1, pp. 63–69, 2009.

[9] D. M. D. Ehrenfest, L. Rasmusson, and T. Albrektsson, "Classification of platelet concentrates: from pure platelet-rich plasma (P-PRP) to leucocyte- and platelet-rich fibrin (L-PRF)," *Trends in Biotechnology*, vol. 27, no. 3, pp. 158–167, 2009.

[10] M. Del Corso, A. Vervelle, A. Simonpieri et al., "Current knowledge and perspectives for the use of Platelet-Rich Plasma (PRP) and Platelet-Rich Fibrin (PRF) in oral and maxillofacial surgery part 1: periodontal and dentoalveolar surgery," *Current Pharmaceutical Biotechnology*, vol. 13, no. 7, pp. 1207–1230, 2012.

[11] A. Simonpieri, M. Del Corso, A. Vervelle et al., "Current knowledge and perspectives for the use of platelet-rich plasma (PRP) and platelet-rich fibrin (PRF) in oral and maxillofacial surgery part 2: bone graft, implant and reconstructive surgery," *Current Pharmaceutical Biotechnology*, vol. 13, no. 7, pp. 1231–1256, 2012.

[12] J. Lindhe, T. Karring, and N. Lang, *Clinical Periodontology and Implant Dentistry*, Blackwell Munksgaard Blackwell Publishing, Oxford, UK, 5th edition, 2008.

[13] Y. Zhang, X. Zhang, B. Shi, and R. Miron, "Membranes for guided tissue and bone regeneration," *Annals of Oral & Maxillofacial Surgery*, vol. 1, no. 1, article 10, 2013.

[14] S.-B. Lee, J.-S. Kwon, Y.-K. Lee, K.-M. Kim, and K.-N. Kim, "Bioactivity and mechanical properties of collagen composite membranes reinforced by chitosan and β-tricalcium phosphate," *Journal of Biomedical Materials Research Part B: Applied Biomaterials*, vol. 100, no. 7, pp. 1935–1942, 2012.

[15] J. B. Herrmann, "Changes in tensile strength and knot security of surgical sutures in vivo," *Archives of Surgery*, vol. 106, no. 5, pp. 707–710, 1973.

[16] S. E. Lynch, *Tissue Engineering: Applications in Oral and Maxillofacial Surgery and Periodontics*, Quintessence Publishing Company, 2008.

[17] S. M. Alston, K. A. Solen, A. H. Broderick, S. Sukavaneshvar, and S. F. Mohammad, "New method to prepare autologous fibrin glue on demand," *Translational Research*, vol. 149, no. 4, pp. 187–195, 2007.

[18] H. Duong, B. Wu, and B. Tawil, "Modulation of 3D fibrin matrix stiffness by intrinsic fibrinogen-thrombin compositions and by extrinsic cellular activity," *Tissue Engineering—Part A*, vol. 15, no. 7, pp. 1865–1876, 2009.

[19] D. M. D. Ehrenfest, M. Del Corso, A. Diss, J. Mouhyi, and J.-B. Charrier, "Three-dimensional architecture and cell composition of a Choukroun's platelet-rich fibrin clot and membrane," *Journal of Periodontology*, vol. 81, no. 4, pp. 546–555, 2010.

[20] D. M. D. Ehrenfest, "How to optimize the preparation of leukocyte- and platelet-rich fibrin (L-PRF, Choukroun's technique) clots and membranes: introducing the PRF Box," *Oral Surgery, Oral Medicine, Oral Pathology, Oral Radiology and Endodontology*, vol. 110, no. 3, pp. 275–278, 2010.

[21] J. Gottlow, S. Nyman, T. Karring, and J. Lindhe, "New attachment formation as the result of controlled tissue regeneration," *Journal of Clinical Periodontology*, vol. 11, no. 8, pp. 494–503, 1984.

[22] J. Choukroun, A. Diss, A. Simonpieri et al., "Platelet-rich fibrin (PRF): a second-generation platelet concentrate. Part V: histologic evaluations of PRF effects on bone allograft maturation in sinus lift," *Oral Surgery, Oral Medicine, Oral Pathology, Oral Radiology and Endodontology*, vol. 101, no. 3, pp. 299–303, 2006.

[23] Z. Mazor, R. A. Horowitz, M. Del Corso, H. S. Prasad, M. D. Rohrer, and D. M. D. Ehrenfest, "Sinus floor augmentation with simultaneous implant placement using Choukroun's platelet-rich fibrin as the sole grafting material: a radiologic and histologic study at 6 months," *Journal of Periodontology*, vol. 80, no. 12, pp. 2056–2064, 2009.

[24] F. Inchingolo, M. Tatullo, M. Marrelli et al., "Trial with platelet-rich fibrin and Bio-Oss used as grafting materials in the treatment of the severe maxillar bone atrophy: clinical and radiological evaluations," *European Review for Medical and Pharmacological Sciences*, vol. 14, no. 12, pp. 1075–1084, 2010.

[25] M. Del Corso, M. Toffler, and D. Dohan Ehrenfest, "Use of an autologous leukocyte and platelet-rich fibrin (L-PRF) membrane in post-avulsion sites: an overview of Choukroun's PRF," *The Journal of Implant & Advanced Clinical Dentistry*, vol. 1, no. 9, pp. 27–35, 2010.

[26] J.-H. Zhao, C.-H. Tsai, and Y.-C. Chang, "Clinical and histologic evaluations of healing in an extraction socket filled with platelet-rich fibrin," *Journal of Dental Sciences*, vol. 6, no. 2, pp. 116–122, 2011.

[27] B. I. Simon, P. Gupta, and S. Tajbakhsh, "Quantitative evaluation of extraction socket healing following the use of autologous platelet-rich fibrin matrix in humans," *The International Journal of Periodontics & Restorative Dentistry*, vol. 31, no. 3, pp. 285–295, 2011.

[28] K. Anilkumar, A. Geetha, Umasudhakar, T. Ramakrishnan, R. Vijayalakshmi, and E. Pameela, "Platelet-rich-fibrin: a novel root coverage approach," *Journal of Indian Society of Periodontology*, vol. 13, no. 1, pp. 50–54, 2009.

[29] S. Aroca, T. Keglevich, B. Barbieri, I. Gera, and D. Etienne, "Clinical evaluation of a modified coronally advanced flap alone or in combination with a platelet-rich fibrin membrane for the treatment of adjacent multiple gingival recessions: a 6-month study," *Journal of Periodontology*, vol. 80, no. 2, pp. 244–252, 2009.

[30] Y.-C. Chang and J.-H. Zhao, "Effects of platelet-rich fibrin on human periodontal ligament fibroblasts and application for periodontal infrabony defects," *Australian Dental Journal*, vol. 56, no. 4, pp. 365–371, 2011.

[31] A. Sharma and A. R. Pradeep, "Autologous platelet-rich fibrin in the treatment of mandibular degree II furcation defects: a randomized clinical trial," *Journal of Periodontology*, vol. 82, no. 10, pp. 1396–1403, 2011.

[32] V. Gassling, T. Douglas, P. H. Warnke, Y. Açil, J. Wiltfang, and S. T. Becker, "Platelet-rich fibrin membranes as scaffolds for periosteal tissue engineering," *Clinical Oral Implants Research*, vol. 21, no. 5, pp. 543–549, 2010.

[33] V. Gassling, J. Hedderich, Y. Açil, N. Purcz, J. Wiltfang, and T. Douglas, "Comparison of platelet rich fibrin and collagen as osteoblast–seeded scaffolds for bone tissue engineering applications," *Clinical Oral Implants Research*, vol. 24, no. 3, pp. 320–328, 2013.

[34] T. E. Orr, P. A. Villars, S. L. Mitchell, H.-P. Hsu, and M. Spector, "Compressive properties of cancellous bone defects in a rabbit model treated with particles of natural bone mineral and synthetic hydroxyapatite," *Biomaterials*, vol. 22, no. 14, pp. 1953–1959, 2001.

[35] E. Lucarelli, R. Beretta, B. Dozza et al., "A recently developed bifacial platelet-rich fibrin matrix," *European Cells and Materials*, vol. 20, pp. 13–23, 2010.

[36] J. L. Velada, D. A. Hollingsbee, A. R. Menzies, R. Cornwell, and R. A. Dodd, "Reproducibility of the mechanical properties of Vivostat system patient-derived fibrin sealant," *Biomaterials*, vol. 23, no. 10, pp. 2249–2254, 2002.

[37] S. L. Rowe, S. Lee, and J. P. Stegemann, "Influence of thrombin concentration on the mechanical and morphological properties of cell-seeded fibrin hydrogels," *Acta Biomaterialia*, vol. 3, no. 1, pp. 59–67, 2007.

[38] B. Blombäck and N. Bark, "Fibrinopeptides and fibrin gel structure," *Biophysical Chemistry*, vol. 112, no. 2-3, pp. 147–151, 2004.

[39] R. V. Kumar and N. Shubhashini, "Platelet rich fibrin: a new paradigm in periodontal regeneration," *Cell and Tissue Banking*, vol. 14, no. 3, pp. 453–463, 2013.

[40] M. H. Boyer, J. R. Shainoff, and O. D. Ratnoff, "Acceleration of fibrin polymerization by calcium ions," *Blood*, vol. 39, no. 3, pp. 382–387, 1972.

[41] T. Kawase, K. Okuda, L. F. Wolff, and H. Yoshie, "Platelet-rich plasma-derived fibrin clot formation stimulates collagen synthesis in periodontal ligament and osteoblastic cells in vitro," *Journal of Periodontology*, vol. 74, no. 6, pp. 858–864, 2003.

[42] P. A. M. Everts, A. van Zundert, J. P. A. M. Schönberger, R. J. J. Devilee, and J. T. A. Knape, "What do we use: platelet-rich plasma or platelet-leukocyte gel?" *Journal of Biomedical Materials Research—Part A*, vol. 85, no. 4, pp. 1135–1136, 2008.

[43] A. Cieslik-Bielecka, T. S. Gazdzik, T. M. Bielecki, and T. Cieslik, "Why the platelet-rich gel has antimicrobial activity?" *Oral Surgery, Oral Medicine, Oral Pathology, Oral Radiology, and Endodontology*, vol. 103, no. 3, pp. 303–305, 2007.

[44] D. J. F. Moojen, P. A. Everts, R. M. Schure et al., "Antimicrobial activity of platelet-leukocyte gel against *Staphylococcus aureus*," *Journal of Orthopaedic Research*, vol. 26, no. 3, pp. 404–410, 2008.

[45] H. El-Sharkawy, A. Kantarci, J. Deady et al., "Platelet-rich plasma: growth factors and pro- and anti-inflammatory properties," *Journal of Periodontology*, vol. 78, no. 4, pp. 661–669, 2007.

[46] K. Werther, I. J. Christensen, and H. J. Nielsen, "Determination of Vascular Endothelial Growth Factor (VEGF) in circulating blood: significance of VEGF in various leucocytes and platelets," *Scandinavian Journal of Clinical & Laboratory Investigation*, vol. 62, no. 5, pp. 343–350, 2002.

[47] E. Anitua, M. Sánchez, G. Orive, and I. Andía, "The potential impact of the preparation rich in growth factors (PRGF) in different medical fields," *Biomaterials*, vol. 28, no. 31, pp. 4551–4560, 2007.

[48] J. K. Kingston, W. M. Bayly, D. C. Sellon, K. M. Meyers, and K. J. Wardrop, "Effects of sodium citrate, low molecular weight heparin, and prostaglandin E_1 on aggregation, fibrinogen binding, and enumeration of equine platelets," *American Journal of Veterinary Research*, vol. 62, no. 4, pp. 547–554, 2001.

[49] A. G. Perez, J. F. S. Lana, A. A. Rodrigues, A. C. M. Luzo, W. D. Belangero, and M. H. A. Santana, "Relevant aspects of centrifugation step in the preparation of platelet-rich plasma," *ISRN Hematology*, vol. 2014, Article ID 176060, 8 pages, 2014.

Hindawi Publishing Corporation
International Journal of Dentistry
Volume 2015, Article ID 428286, 8 pages
http://dx.doi.org/10.1155/2015/428286

Research Article

Mechanical Properties of Elastomeric Impression Materials: An In Vitro Comparison

Dino Re,[1] Francesco De Angelis,[2] Gabriele Augusti,[1] Davide Augusti,[1] Sergio Caputi,[2] Maurizio D'Amario,[3] and Camillo D'Arcangelo[2]

[1]*Department of Oral Rehabilitation, Istituto Stomatologico Italiano, University of Milan, 20122 Milan, Italy*
[2]*Department of Medical, Oral and Biotechnological Sciences, University of Chieti, 66100 Chieti, Italy*
[3]*Department of Life, Health and Environmental Sciences, University of L'Aquila, 67100 L'Aquila, Italy*

Correspondence should be addressed to Gabriele Augusti; g.augusti@libero.it

Received 7 September 2015; Accepted 8 November 2015

Academic Editor: Vesna Miletic

Purpose. Although new elastomeric impression materials have been introduced into the market, there are still insufficient data about their mechanical features. The tensile properties of 17 hydrophilic impression materials with different consistencies were compared. *Materials and Methods.* 12 vinylpolysiloxane, 2 polyether, and 3 hybrid vinylpolyether silicone-based impression materials were tested. For each material, 10 dumbbell-shaped specimens were fabricated ($n = 10$), according to the ISO 37:2005 specifications, and loaded in tension until failure. Mean values for tensile strength, yield strength, strain at break, and strain at yield point were calculated. Data were statistically analyzed using one-way ANOVA and Tukey's tests ($\alpha = 0.05$). *Results.* Vinylpolysiloxanes consistently showed higher tensile strength values than polyethers. Heavy-body materials showed higher tensile strength than the light bodies from the same manufacturer. Among the light bodies, the highest yield strength was achieved by the hybrid vinylpolyether silicone (2.70 MPa). Polyethers showed the lowest tensile (1.44 MPa) and yield (0.94 MPa) strengths, regardless of the viscosity. *Conclusion.* The choice of an impression material should be based on the specific physical behavior of the elastomer. The light-body vinylpolyether silicone showed high tensile strength, yield strength, and adequate strain at yield/brake; those features might help to reduce tearing phenomena in the thin interproximal and crevicular areas.

1. Introduction

The success rate of prosthetic tasks relies on different factors. Adequate clinical protocols [1, 2] based on careful tooth preparations and standardized luting or cementation procedures [3, 4] proved to be crucial. Similarly, the dimensional accuracy and a reliable detailed reproduction of both impressions and corresponding models from which a restoration can be manufactured in the laboratory appear mandatory [5]. The ideal impression material should exhibit adequate mechanical properties to withstand stresses under various clinical scenarios. Elastomeric impression materials offer high elastic recovery and acceptable flexibility on removal of the impression from the mouth [6]. Recently, new elastomeric impression materials have been introduced, with the claim of very high elastic recovery and high tear and tensile strengths. Vinylpolysiloxanes (VPSs) (addition silicones) have a moderately low-molecular-weight silicone that contains silane groups. Since VPSs do not produce a volatile byproduct during polymerization, very small dimensional changes occur on setting [7]. VPS are intrinsically hydrophobic in nature, which can result in voids at the margin of the tooth preparation in the impression and bubbles in gypsum casts. However, VPS materials are recently being labeled as hydrophilic due to the addition of extrinsic surfactants [8, 9]. Polyethers (PE) are composed of a moderately low-molecular-weight polyether, a silica filler, and a plasticizer. Dimensional stability and wettability (resulting in minimal voids and detailed reproduction of intraoral structures) are the main features of PE materials [10, 11]. On the other hand, a difficulty of removing impressions made of polyether from the mouth, and also an increased risk of die breakage, could be associated

with the higher rigidity of these materials when compared to VPS [11]. Recently, vinylpolyether silicone (VPES) products were commercially introduced. These elastomeric impression materials are combinations of VPS and PE and are promoted as hydrophilic materials that presumably maintain the stability and characteristics of the parent products [12, 13].

Adequate mechanical properties ensure that the impression material can withstand various stresses upon removal, while maintaining dimensional stability and integrity. The tear of elastomeric materials is a mechanical rupture process initiated and propagated at a site of high stress concentration caused by cut, defect, or localized deformation. *Tear*, *tensile*, and *yield strengths* are important properties for impression materials; they have been investigated by several studies [6, 9, 14, 15]. Lu et al. have found a lower tensile strength of a soft polyether (Impregum, 3M ESPE) compared to two hydrophilic addition silicones (Imprint II, 3M ESPE and Flexitime, Heraeus); the authors also reported higher tear properties and tensile strength of heavy-body materials than light viscosities [9]. Chai et al.—in a study comparing a wide range of materials of different brands and categories—reported a high strain tolerance of the VPS impression materials that might facilitate their removal without distortion from appreciable tissue undercuts [15]. Moderate rigidity of polyether was also recognized [15]. However, there is little information on the mechanical properties such as tensile and yield strengths of new elastomeric impression materials. Knowledge of these clinically relevant mechanical properties facilitates the selection of impression materials in various clinical situations.

The purpose of this study was to compare tensile properties (tensile strength at break, yield strength, ultimate strain at break, and strain at yield point) of 17 hydrophilic elastomeric impression materials. Materials with different consistencies (heavy-, medium-, and light-body) were investigated. The tested null hypothesis was the fact that there would be no significant differences in mechanical properties among these impression materials.

2. Materials and Methods

Tensile strength at break (TSb), yield strength (YS), ultimate strain at break (USb), and strain at yield point (Sy) of seventeen commercially available elastomeric impression materials with heavy- (HB), medium- (MB), or light-body (LB) consistencies were evaluated in this study. The complete list of the materials employed is summarized in Table 1 and included 12 VPSs, 2 PEs, and 3 VPESs.

For each impression material, 10 dumbbell-shaped specimens were fabricated ($n = 10$), according to the design described as type 1 and type C, respectively, within the ISO 37:2005 and within the ASTM.D412 specifications (see Figure 1 and Table 2).

For this purpose, a stainless steel split mold made out of two perfectly fitting upper and lower plates was used (Figures 2(a) and 2(b)). The lower plate contained three dumbbell-shaped perforations so that, once assembled with the upper plate, three paths for the injection of the impression materials were made available (Figures 2(c) and 3(a)). This allowed for the production of up to three samples at the same time (Figure 3(b)).

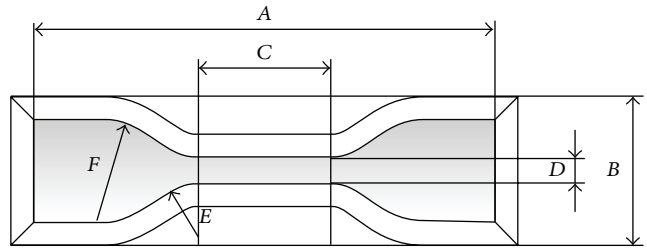

Figure 1: Shape of dumbbell test specimens produced according to type 1 of the ISO 37:2005 specifications and/or type C of ASTM.D412 specifications. The actual extent of the dimensions indicated by uppercase letters is specified in Table 2.

The specimens were prepared at standard laboratory conditions (23°C ± 1°C) by dispensing impression material from the cartridge into the already assembled steel mold, through lateral apertures specifically designed for placing the differently shaped cartridge tips. Before injection, a small amount of material was extruded and discarded to ensure proper mixing in the dispensing tip. A timer was started immediately after the impression material was first dispensed into the mold.

The upper and the lower plates of the split mold were kept assembled for the whole setting time recommended by each manufacturer and under a constant 5 Kg load. After complete setting and mold removal, any excess impression material residue was carefully trimmed away with a razor blade. Benchmarks were drawn on the specimen, 12.5 mm on either side of the center line, thus setting the test length of the dumbbell specimens at 25 mm, according to ISO 37:2005 and ASTM.D412 (Table 2). Specimen dimensions were recorded with a digital caliper (Mitutoyo, Tokyo, Japan) before testing. Three areas of each specimen narrow portion were measured and checked three times to accurately confirm their width and thickness, which were averaged to obtain a final measurement. Specimens that were not in accordance with the dimensions specified within the ISO 37:2005 (Table 2) were discarded; entirely new specimens were subsequently prepared.

Immediately following preparation (Figure 4), the specimens were secured into the Instron universal testing machine (Instron Corp., Canton, MA, USA), gripping them on both sides by pneumatic clamps at the location of the previously applied benchmarks. Before the test began, the jig was adjusted so that the specimen was neither in compression nor in tension. The specimens were loaded in tension until failure (Figure 5) with a crosshead speed of 250 mm/minute. The yield point was defined according to the 0.2% offset method, by estimating a 0.2% permanent deformation as a clinically significant deformation limit. The USb (mm) and the Sy (mm) were recorded.

Table 1: Information on the materials tested.

Group	Material (trade name)	Manufacturer	Viscosity	Composition	Setting time
Acqu-HB	Aquasil ULTRA DECA Heavy (dynamic mix)	Dentsply DeTrey GmbH, Konstanz, Germany	HB	Polyvinylsiloxane	Regular
Hydro-HB	Hydrorise Heavy (dynamic mix)	Zhermack SpA, Badia Polesine (RO), Italy	HB	Polyvinylsiloxane	Regular
Affi-HB	Affinis System Heavy Body 360 (dynamic mix)	Coltène/Whaledent AG, Altstätten, Switzerland	HB	Polyvinylsiloxane	Regular
Flexi-HB	Flexitime DYNAMIX Heavy Tray (dynamic mix)	Heraeus Kulzer GmbH, Hanau, Germany	HB	Polyvinylsiloxane	Regular
Impr-HB	Impregum PENTA Duosoft H (dynamic mix)	3M ESPE, Seefeld, Germany	HB	Polyether	Regular
Exa-HB	Exa'lence Regular Set Heavy (dynamic mix)	GC Corporation, Tokyo, Japan	HB	Vinylpolyether silicone	Regular
Acqu-MB	Aquasil ULTRA MONO (syringe automix)	Dentsply DeTrey GmbH, Konstanz, Germany	MB	Polyvinylsiloxane	Regular
Hydro-MB	Hydrorise Regular Body (syringe automix)	Zhermack SpA, Badia Polesine (RO), Italy	MB	Polyvinylsiloxane	Regular
Affi-MB	Affinis Regular Body (syringe automix)	Coltène/Whaledent AG, Altstätten, Switzerland	MB	Polyvinylsiloxane	Regular
Flexi-MB	Flexitime Medium Flow (syringe automix)	Heraeus Kulzer GmbH, Hanau, Germany	MB	Polyvinylsiloxane	Regular
Exa-MB	Exa'lence Medium Body (syringe automix)	GC Corporation, Tokyo, Japan	MB	Vinylpolyether silicone	Regular
Acqu-LB	Aquasil ULTRA LV (syringe automix)	Dentsply DeTrey GmbH, Konstanz, Germany	LB	Polyvinylsiloxane	Regular
Hydro-LB	Hydrorise Light Body (syringe automix)	Zhermack SpA, Badia Polesine (RO), Italy	LB	Polyvinylsiloxane	Regular
Affi-LB	Affinis Light Body (syringe automix)	Coltène/Whaledent AG, Altstätten, Switzerland	LB	Polyvinylsiloxane	Regular
Flexi-LB	Flexitime Light Flow (syringe automix)	Heraeus Kulzer GmbH, Hanau, Germany	LB	Polyvinylsiloxane	Regular
Impr-LB	Impregum Garant Duosoft L (syringe automix)	3M ESPE, Seefeld, Germany	LB	Polyether	Regular
Exa-LB	Exa'lence Light Body (syringe automix)	GC Corporation, Tokyo, Japan	LB	Vinylpolyether silicone	Regular

HB = heavy body; MB = medium body; and LB = light body.

Table 2: Dimensions for dumbbell test specimens according to type 1 of the ISO 37:2005 specifications and/or type C of ASTM.D412 specifications. Each uppercase letter relates to the corresponding dimension as indicated in Figure 1.

Dimension (mm)	
A: overall length (minimum)	115
B: width of ends	25.0 ± 1
C: length of narrow portion	33 ± 2
D: width of narrow portion	6 ± 0.4
E: transition radius outside	14 ± 1
F: transition radius inside	25 ± 2
G: thickness of narrow portion	2 ± 0.2
H: test length	25 ± 0.5

The TSb (MPa) was calculated using the equation

$$\mathrm{TSb} = \frac{\mathrm{Fb}}{W * t}, \quad (1)$$

while the YS (MPa) was obtained from the force recorded at the yield point using the equation

$$\mathrm{YS} = \frac{\mathrm{Fy}}{W * t}, \quad (2)$$

where Fb (N) is the force recorded at brake, Fy (N) is the force recorded at yield, W (mm) is the width of the narrow portion of the die, and t (mm) is the thickness of the test length.

Mean values and standard deviations for TSb, YS, USb, and Sy were calculated in each group. A normal distribution was verified for the analyzed variables before applying statistical tests. Data were subjected to a one-way analysis of variance (ANOVA) and Tukey's HSD test for multiple comparisons. The level of α was set at 0.05 in all tests.

3. Results

Mean values and standard deviations achieved for TSb, YS, USb, and Sy are shown in Table 3, which also summarizes the results of the one-way ANOVA and Tukey's tests.

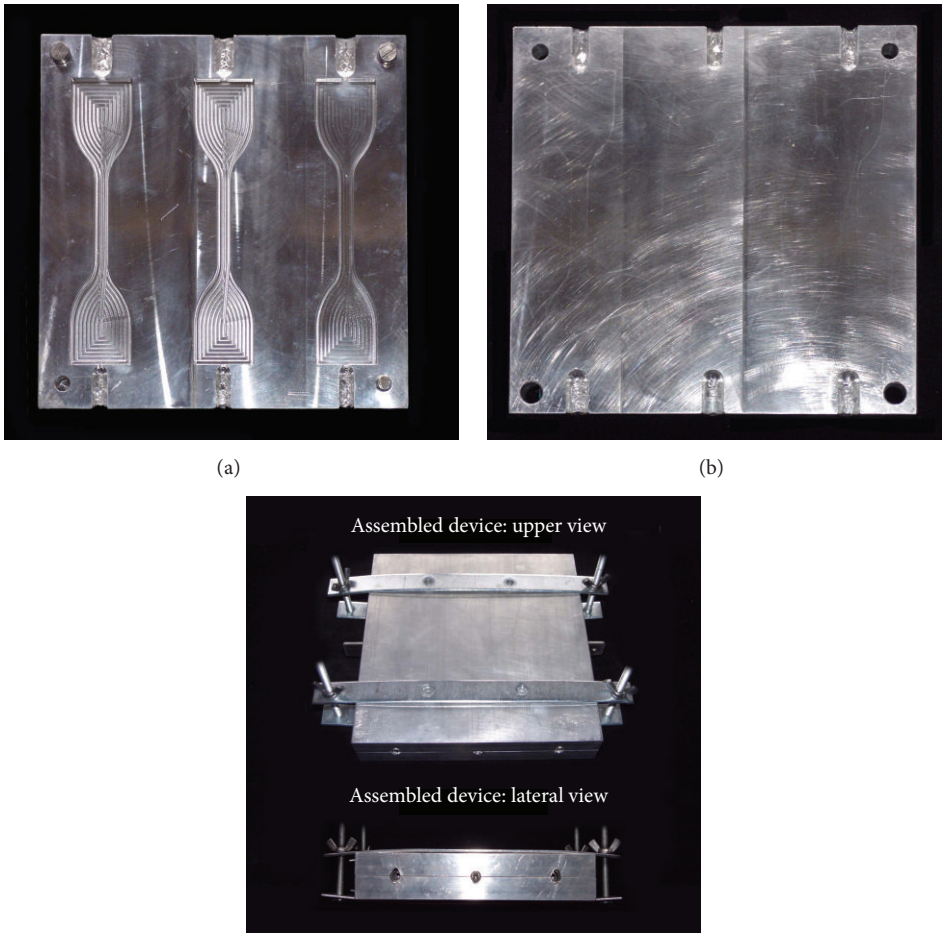

(a) (b)

(c)

Figure 2: Stainless steel split mold used to produce the dumbbell test specimens: lower (a) and upper (b) plates. Once the mold was assembled (c), paths for the injection of the impression materials through lateral apertures were made available.

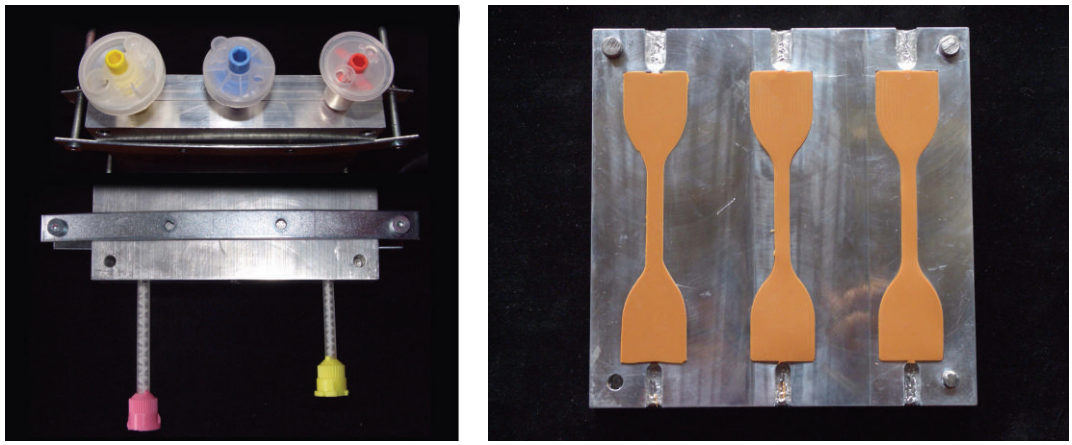

(a) (b)

Figure 3: Injection of the impression materials through dedicated, commercially available tips (a) allowed the production of up to three samples at the same time (b).

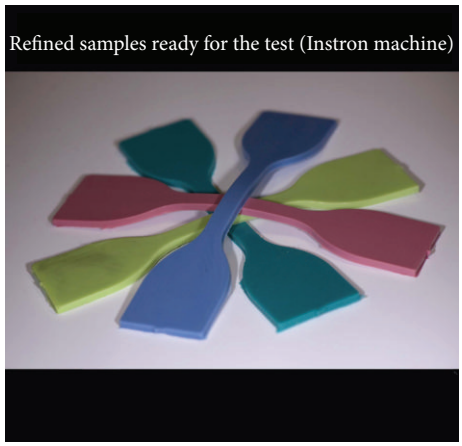

Figure 4: Refined dumbbell test specimens ready for the test (Instron machine).

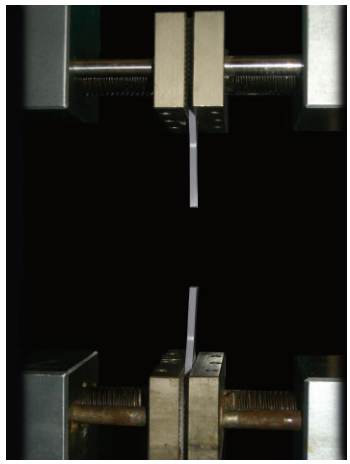

Figure 5: Example of a specimen loaded in tension until failure.

VPSs consistently showed higher tensile strength at brake (TSb) values than PEs. Among VPSs, Aquasil exhibited the highest TSb value (5.1 MPa) compared to all other materials tested, irrespective of the viscosity. Within the heavy bodies, Aquasil TSb was statistically comparable to Affinis (4.93 MPa) and Flexitime (4.91 MPa), while within the light bodies Aquasil (4.98 MPa) was comparable to Exa'lence (4.03 MPa) and Flexitime (3.02 MPa). Comparing the different viscosities of products from the same manufacturer, heavy-body materials showed higher tensile strength values than the light bodies; such a difference proved to be not statistically significant ($P > 0.05$) for Aquasil (HB: 5.1 MPa, LB: 4.98 MPa—$P = 1.000$) and Impregum (HB: 1.49 MPa, LB: 1.47 MPa—$P = 1.000$). A different behavior was recorded for the VPES material, whose medium and light viscosities (MB = 3.16 MPa; LB = 4.03 MPa) showed significantly increased TSb values ($P < 0.001$) compared to the HB viscosity (1.42 MPa).

As for the TSb, also regarding the yield strength (YS), the HB VPSs showed slightly increased mean values compared to the corresponding LB viscosities; however the differences in yield strength were statistically significant just for Affinis (HB: 2.85 MPa, LB: 1.12 MPa).

Concerning the ultimate strain at break (USb), statistical analysis showed that heavy-body VPSs had significantly reduced mean values compared to the corresponding light bodies, with the exception of Affinis (HB: 47.19 mm, LB: 47.55 mm) and Aquasil (HB: 34.53 mm, LB: 45.88 mm). On the contrary, for PE impression materials, the heavy-body

Table 3: Mean values (and standard deviations, SD) recorded for tensile strength at break (TSb), yield strength (YS), ultimate strain at break (USb), and strain at yield point (Sy) in the different experimental groups.

TSb (SD) (MPa)		YS (SD) (MPa)	
Acqu-HB*	5.10[a] (0.40)	Affi-HB*	2.85[a] (1.26)
Acqu-LB***	4.98[a,b] (0.39)	Acqu-MB**	2.70[a,b] (1.28)
Flexi-HB*	4.90[a,b] (0.99)	Exa-LB***	2.70[a,b] (0.91)
Affi-HB*	4.88[a,b] (0.52)	Acqu-HB*	2.36[a,b,c] (0.97)
Acqu-MB**	4.18[b,c] (0.59)	Flexi-HB*	2.12[a,b,c,d] (0.99)
Exa-LB***	4.03[c] (0.56)	Acqu-LB***	1.97[a,b,c,d] (0.81)
Hydro-HB*	3.19[d] (1.02)	Flexi-LB***	1.78[a,b,c,d] (1.01)
Exa-MB**	3.16[d] (0.52)	Affi-MB**	1.77[a,b,c,d] (0.64)
Flexi-LB***	2.93[d,e] (0.54)	Hydro-HB*	1.60[b,c,d] (0.98)
Affi-MB**	2.60[d,e,f] (0.37)	Flexi-MB**	1.47[b,c,d] (0.56)
Hydro-LB***	2.30[e,f,g] (0.31)	Hydro-MB**	1.38[c,d] (0.46)
Flexi-MB**	2.10[f,g,h] (0.34)	Hydro-LB***	1.35[c,d] (0.47)
Affi-LB***	2.03[f,g,h] (0.55)	Exa-MB**	1.35[c,d] (0.69)
Hydro-MB**	1.77[g,h] (0.31)	Affi-LB***	1.12[c,d] (0.51)
Impr-LB***	1.46[h] (0.19)	Impr-HB*	1.11[d] (0.46)
Impr-HB*	1.44[h] (0.42)	Exa-HB*	0.96[d] (0.32)
Exa-HB*	1.42[h] (0.29)	Impr-LB***	0.94[d] (0.26)
USb (SD) (mm)		**Sy (SD) (mm)**	
Hydro-LB***	101.26[a] (13.86)	Flexi-LB***	56.57[a] (27.60)
Flexi-LB***	90.39[a,b] (15.72)	Hydro-LB***	51.43[a,b] (19.46)
Hydro-MB**	81.59[a,b] (21.25)	Flexi-MB**	51.01[a,b] (17.23)
Flexi-MB**	77.61[b] (9.71)	Impr-HB*	48.23[a,b,c] (22.42)
Impr-HB*	77.17[b] (21.11)	Exa-LB***	45.74[a,b,c] (15.06)
Exa-LB***	71.69[b,c] (12.95)	Hydro-MB**	35.61[a,b,c,d] (29.68)
Exa-MB**	56.56[c,d] (11.17)	Affi-MB**	35.09[a,b,c,d] (13.29)
Affi-MB**	56.43[c,d] (12.52)	Aqua-MB**	28.32[b,c,d,e] (12.86)
Exa-HB*	54.21[c,d,e] (17.76)	Affi-LB***	27.23[b,c,d,e] (15.44)
Affi-LB***	47.55[b,c,d,e] (10.21)	Affi-HB*	26.24[c,d,e] (12.18)
Affi-HB*	47.19[d,e] (6.01)	Aqua-LB***	18.74[d,e] (5.67)
Aqua-MB**	46.09[d,e] (8.08)	Impr-LB***	18.56[d,e] (6.07)
Aqua-LB***	45.88[d,e,f] (5.07)	Exa-MB**	16.92[d,e] (13.27)
Impr-LB***	45.68[d,e,f] (10.81)	Aqua-HB*	15.64[d,e] (6.29)
Hydro-HB*	41.77[d,e,f] (14.53)	Exa-HB*	14.01[d,e] (10.37)
Aqua-HB*	34.53[e,f] (3.65)	Hydro-HB*	12.09[d,e] (8.42)
Flexi-HB*	26.23[f] (2.80)	Flexi-HB*	9.43[e] (4.29)

The same superscript letters indicate no statistically significant differences ($P > 0.05$).
*Heavy body.
**Medium body.
***Light body.

product showed higher USb values than the light-body product (HB: 77.17 mm, LB: 45.68 mm). The medium-body materials of some brands (Flexitime and Hydrorise) presented intermediate USb values, while for other brands the USb of the medium body was comparable to the corresponding LB (Aquasil) or HB (Exa'lence, Affinis). Comparing the different brands within the same viscosity, Heraeus Kulzer Flexitime and Zhermack Hydrorise showed the highest USb values both among the light bodies (101.25 mm and 90.39 mm, resp.) and among the medium bodies (81.59 mm and 77.61 mm, resp.). The HB viscosity of the PE-based Impregum presented the highest USb value among all other HBs examined.

Regarding the strain at yield point (Sy) the lowest values were generally recorded on HB viscosities. HB VPSs had steadily lower Sy values compared to LB viscosities. Only for PE impression materials the heavy body showed higher Sy values than the light body (HB: 48.23 mm, LB: 18.56 mm). Flexitime showed the highest Sy values among the LB products (56.57 mm) and the lowest values among the HB materials (9.43 mm).

4. Discussion

When an impression is removed from the mouth, the material must withstand the forces associated with separating the impression from the tooth and its surrounding tissues. The material located at or close to undercut areas could permanently deform on removal. Thus, elastic recovery is important in determining the accuracy of an impression material [9]. The clinical tear performance of a material also appears crucial [15, 16]: it involves complex interactions between polymer and fillers, flow to a particular film thickness, release properties from tooth and soft tissue, presence of internal and surface defects, and rate of impression withdrawal. Because of the complexities of integrating and measuring these properties, laboratory tests evaluating the propagation energy of a tear have been employed as common ways to evaluate elastic dental materials [9, 17]. New "hydrophilic" elastomeric impression materials have been recently introduced with the goals of reducing marginal voids and distortion in the impressions and improving the quality of gypsum dies, but there are still insufficient data on their mechanical properties.

Based on the results of the present study, the null hypothesis that there was no difference in the tensile properties among the different impression materials and consistencies tested was rejected.

Tensile strength at break is the maximum tensile stress applied in stretching a specimen to rupture [9]. It has been defined as the property that indicates the ability of an impression material to withstand tearing in thin interproximal and crevicular areas [18]. Statistical analysis showed significant differences in the tensile strengths of different products, supporting findings in the literature [9, 19]. VPSs consistently showed higher tensile strength values than PEs. Comparing the different viscosities of materials produced by the same manufacturer, heavy-body VPSs showed higher tensile strength values than the light bodies. It should however be considered that although heavy-body impression materials showed higher tensile resistance, the tensile properties of light bodies appear more clinically relevant, since the most likely torn portions of the impression are the thin interproximal and crevicular areas. This may highlight an advantageous peculiarity of the new VPES hybrid material, which showed very high tensile strength values for the light- and medium-body viscosities. The actual behavior of the MB viscosities proved to be quite unpredictable: despite what one could expect, only for Exa'lence and Affinis, the TSb of the medium body showed an intermediate TSb value between those of the corresponding HB and LB viscosities.

The yield strength determines the materials' ability to withstand stress without permanent deformation. The strain at yield point indicates the amount of undercut an impression material can overcome without permanent elastic deformation. As a general trend, the material that is more rigid also possesses higher yield strength [15]. Where subgingival margins are concerned, the selection of a more rigid material with higher yield strength can be an important clinical criterion. Walker at al. [20] recently suggested that high impression material rigidity and hardness are not predictors of impression removal difficulty. A performing material should display high yield strength and adequate elastic recovery and should require the expenditure of large amounts of energy to initiate and propagate tearing. The polymerized material have to maintain its elasticity under stresses created, for instance, when it flexes over tissue undercuts. The distortion of an impression material beyond its elastic range may cause permanent deformation and renders it inaccurate [15]. Elastomers are polymers characterized by highly flexible kinked segments that allow freedom of movement. Under stress (load/area), the segments will uncoil. Upon removal of the stress, an ideal elastomer will exhibit complete elastic recovery; the segments spring back to prestressed conformations and the piece returns to its original dimensions. Permanent deformation occurs upon elongation of the segments past the point where elastic recovery is possible. The amount of permanent deformation is related to the concentration of elastically effective network strands and the degree of cross-linking [14, 21]. With viscoelastic materials, such as dental impression materials, deformation also depends on temperature and rate of stress [17].

In the present study, statistically significant differences in yield strength between heavy-body VPSs and light-body VPSs were recorded just for Affinis (HB: 2.85 MPa, LB: 1.12 MPa). However, we found high coefficient of variations (standard deviation values) for both the yield strength and the strain at yield parameters; such wide variability might influence the statistical significance of results that should be interpreted with caution. An explanation for the recorded high standard deviations might be found in the testing apparatus: during tensile loading of samples, when testing tear energy, the tear could deviate from the central axis of the specimen and the observed elongation might not be accurate. Beside Affinis group, all the other tested VPSs showed slightly increased but statistically similar YS values when the HBs were compared with the corresponding LBs produced by the same manufacturer. This may probably suggest a weak influence of the different viscosities (HB, MB, and LB) on the YS of VPSs, in contrast with what had been observed for

the TSb. On the other hand, the new VPES hybrid material yielded the highest YS with the LB viscosity. PE impression materials showed the lowest yield strength, regardless of the viscosity. This appears in accordance with Lu et al.'s work [9] that demonstrated that the PE impression materials tested had significantly lower tensile strength and higher strain in compression compared to new addition silicone materials.

From the standpoint of clinical application, materials with high tensile strength are not necessarily considered to be superior to the materials with low tensile strength. Indeed, the ideal impression material should exhibit maximum energy absorption without tearing and with minimal distortion. Nevertheless, according to the authors, it is also desirable that the material tears rather than deforms on a critical point such as a margin, as in clinical practice it appears easier to properly judge and consequently discard a torn impression, rather than a deformed one. As a consequence, an impression material showing a TSb/YS ratio sufficiently close to 1 (i.e., yield strength value relatively close to the corresponding tensile strength at break) should probably be preferred, especially concerning the light bodies, which are generally employed in thin interproximal and crevicular areas. From the present results, the TSb/YS ratios ranged between 0.396 (Acqu-LB group) and 0.764 (Hydro-MB group).

Among the light bodies investigated in the present study, both Acqu-LB and Exa-LB showed relatively high mean values for both tensile and yield strength. While for Exa-LB the TSb/YS ratio was relatively high (0.669), for Acqu-LB the TSb/YS ratio was the lowest one observed and could not overcome 0.396. This can be probably seen as a further clinical advantage of the new VPES hybrid material.

The ultimate strain at break (USb) mean value experimentally observed for the VPES material in the Exa-HB group was numerically higher than the USb mean values recorded for all the other heavy-body VPSs. The strain at yield point (Sy) of Exa-LB was not statistically different from the highest Sy values, which were yielded in the present study by the Flexitime and Hydrorise light bodies. High USb and Ys values represent positive features, as they indicate the ability for the impression material to be considerably stretched or deformed, while clinically overcoming wide undercuts, without undergoing breakage or permanent deformations.

Many studies [9, 14, 15, 20, 22–24] on tear strength have been carried out so far; however, standardized test methods have not been established. As a result, comparison between different impression materials using the available literature data still appears quite difficult [15, 17].

The ANSI/ADA standard specifies that tear strength specimens of dental elastomeric impression materials should be tested 1 hour following polymerization [25]. Nevertheless, impressions are clinically subjected to tensile forces immediately after the manufacturer's setting time. A previous research revealed that there are significant differences between testing immediately after the setting time and 24 hours following the setting time [23]. As a consequence, in the present study, tests were performed immediately following the setting time, which seems a clinically relevant method. Among the limitations of our investigation there is its specific in vitro nature; moreover, the elastic recovery from compressive and tensile strains was not considered. In addition, the applied ANSI/ADA specification just takes into consideration a thickness of 2 mm for the fabrication of samples. Future researches are necessary to simulate the clinical oral behavior of impression materials.

5. Conclusions

The choice of an impression material for particular applications should be based on the specific property data rather than on the type and class of the elastomer. With regard to the mechanical properties tested, considering all different viscosities, VPSs and VPESs showed higher in vitro results for tensile strength at break (TSb) and yield strength (YS) than PE. Heavy-body VPSs generally showed higher TSb values than the light bodies from the same manufacturer. Within the light bodies (LB) that are typically employed in the interproximal/subgingival areas and thus appear more subject to clinical tearing, the best performances in terms of TSb and YS were observed in the Acqu-LB and Exa-LB groups, with Exa-LB conveniently showing a relatively high TSb/YS ratio.

Conflict of Interests

The authors of this paper certify that they have no proprietary, financial, or other personal interests of any nature or kind in any product, service, and/or company that is presented in this paper.

References

[1] C. D'Arcangelo, M. Zarow, F. De Angelis et al., "Five-year retrospective clinical study of indirect composite restorations luted with a light-cured composite in posterior teeth," *Clinical Oral Investigations*, vol. 18, no. 2, pp. 615–624, 2014.

[2] C. D'Arcangelo, F. De Angelis, M. Vadini, and M. D'Amario, "Clinical evaluation on porcelain laminate veneers bonded with light-cured composite: results up to 7 years," *Clinical Oral Investigations*, vol. 16, no. 4, pp. 1071–1079, 2012.

[3] R. W. Wassell, D. Barker, and J. G. Steele, "Crowns and other extra-coronal restorations: try-in and cementation of crowns," *British Dental Journal*, vol. 193, no. 1, pp. 17–28, 2002.

[4] C. D'Arcangelo, F. De Angelis, M. D'Amario, S. Zazzeroni, C. Ciampoli, and S. Caputi, "The influence of luting systems on the microtensile bond strength of dentin to indirect resin-based composite and ceramic restorations," *Operative Dentistry*, vol. 34, no. 3, pp. 328–336, 2009.

[5] M. J. German, T. E. Carrick, and J. F. McCabe, "Surface detail reproduction of elastomeric impression materials related to rheological properties," *Dental Materials*, vol. 24, no. 7, pp. 951–956, 2008.

[6] T. A. Hamalian, E. Nasr, and J. J. Chidiac, "Impression materials in fixed prosthodontics: influence of choice on clinical procedure," *Journal of Prosthodontics*, vol. 20, no. 2, pp. 153–160, 2011.

[7] M. Braden, "Dimensional stability of condensation silicone rubbers," *Biomaterials*, vol. 13, no. 5, pp. 333–336, 1992.

[8] R. S. Kess, E. C. Combe, and B. S. Sparks, "Effect of surface treatments on the wettability of vinyl polysiloxane impression materials," *Journal of Prosthetic Dentistry*, vol. 84, no. 1, pp. 98–102, 2000.

[9] H. Lu, B. Nguyen, and J. M. Powers, "Mechanical properties of 3 hydrophilic addition silicone and polyether elastomeric impression materials," *Journal of Prosthetic Dentistry*, vol. 92, no. 2, pp. 151–154, 2004.

[10] F. S. Gonçalves, D. A. Popoff, C. D. Castro, G. C. Silva, C. S. Magalhães, and A. N. Moreira, "Dimensional stability of elastomeric impression materials: a critical review of the literature," *The European Journal of Prosthodontics and Restororative Dentistry*, vol. 19, no. 4, pp. 163–166, 2011.

[11] G. Vivekananda Reddy, N. Simhachalam Reddy, J. Itttigi, and K. N. Jagadeesh, "A comparative study to determine the wettability and castability of different elastomeric impression materials," *Journal of Contemporary Dental Practice*, vol. 13, no. 3, pp. 356–363, 2012.

[12] A. Pandita, T. Jain, N. S. Yadav, S. M. A. Feroz, Pradeep, and A. Diwedi, "Evaluation and comparison of dimensional accuracy of newly introduced elastomeric impression material using 3D laser scanners: an in vitro study," *Journal of Contemporary Dental Practice*, vol. 14, no. 2, pp. 265–268, 2013.

[13] U. Nassar, A. Oko, S. Adeeb, M. El-Rich, and C. Flores-Mir, "An in vitro study on the dimensional stability of a vinyl polyether silicone impression material over a prolonged storage period," *Journal of Prosthetic Dentistry*, vol. 109, no. 3, pp. 172–178, 2013.

[14] S. O. Hondrum, "Tear and energy properties of three impression materials," *International Journal of Prosthodontics*, vol. 7, no. 6, pp. 517–521, 1994.

[15] J. Chai, Y. Takahashi, and E. P. Lautenschlager, "Clinically relevant mechanical properties of elastomeric impression materials," *International Journal of Prosthodontics*, vol. 11, no. 3, pp. 219–223, 1998.

[16] N. Perakis, U. C. Belser, and P. Magne, "Final impressions: a review of material properties and description of a current technique," *International Journal of Periodontics and Restorative Dentistry*, vol. 24, no. 2, pp. 109–117, 2004.

[17] N. S. Salem, E. C. Combe, and D. C. Watts, "Mechanical properties of elastomeric impression materials," *Journal of Oral Rehabilitation*, vol. 15, no. 2, pp. 125–132, 1988.

[18] J. Klooster, G. I. Logan, and A. H. L. Tjan, "Effects of strain rate on the behavior of elastomeric impression," *The Journal of Prosthetic Dentistry*, vol. 66, no. 3, pp. 292–298, 1991.

[19] R. G. Craig, N. J. Urquiola, and C. C. Liu, "Comparison of commercial elastomeric impression materials," *Operative Dentistry*, vol. 15, no. 3, pp. 94–104, 1990.

[20] M. P. Walker, N. Alderman, C. S. Petrie, J. Melander, and J. Mcguire, "Correlation of impression removal force with elastomeric impression material rigidity and hardness," *Journal of Prosthodontics*, vol. 22, no. 5, pp. 362–366, 2013.

[21] W. D. Cook, F. Liem, P. Russo, M. Scheiner, G. Simkiss, and P. Woodruff, "Tear and rupture of elastomeric dental impression materials," *Biomaterials*, vol. 5, no. 5, pp. 275–280, 1984.

[22] W. D. Sneed, R. Miller, and J. Olson, "Tear strength of ten elastomeric impression materials," *Journal of Prosthetic Dentistry*, vol. 49, no. 4, pp. 511–513, 1983.

[23] L. Brauchli, M. Zeller, and A. Wichelhaus, "Shear bond strengths of seven self-etching primers after thermo-cycling," *Journal of Orofacial Orthopedics*, vol. 72, no. 5, pp. 371–380, 2011.

[24] N. C. Lawson, J. O. Burgess, and M. Litaker, "Tear strength of five elastomeric impression materials at two setting times and two tearing rates," *Journal of Esthetic and Restorative Dentistry*, vol. 20, no. 3, pp. 186–193, 2008.

[25] ADA, "Specification no. 19 for dental elastomeric impression material. Revised ANSI/ADA Specification no. 18—2004," Council on Dental Materials, Instruments, and Equipment.

Hindawi Publishing Corporation
International Journal of Dentistry
Volume 2015, Article ID 357653, 9 pages
http://dx.doi.org/10.1155/2015/357653

Research Article

Titanium Oxide: A Bioactive Factor in Osteoblast Differentiation

P. Santiago-Medina,[1] P. A. Sundaram,[2] and N. Diffoot-Carlo[1]

[1]*Department of Biology, University of Puerto Rico, Mayaguez, PR 00680, USA*
[2]*Department of Mechanical Engineering, University of Puerto Rico, Mayaguez, PR 00680, USA*

Correspondence should be addressed to P. A. Sundaram; paul.sundaram@upr.edu

Received 12 August 2015; Revised 19 October 2015; Accepted 27 October 2015

Academic Editor: Tihana Divnic-Resnik

Titanium and titanium alloys are currently accepted as the gold standard in dental applications. Their excellent biocompatibility has been attributed to the inert titanium surface through the formation of a thin native oxide which has been correlated to the excellent corrosion resistance of this material in body fluids. Whether this titanium oxide layer is essential to the outstanding biocompatibility of titanium surfaces in orthopedic biomaterial applications is still a moot point. To study this critical aspect further, human fetal osteoblasts were cultured on thermally oxidized and microarc oxidized (MAO) surfaces and cell differentiation, a key indicator in bone tissue growth, was quantified by measuring the expression of alkaline phosphatase (ALP) using a commercial assay kit. Cell attachment was similar on all the oxidized surfaces although ALP expression was highest on the oxidized titanium alloy surfaces. Untreated titanium alloy surfaces showed a distinctly lower degree of ALP activity. This indicates that titanium oxide clearly upregulates ALP expression in human fetal osteoblasts and may be a key bioactive factor that causes the excellent biocompatibility of titanium alloys. This result may make it imperative to incorporate titanium oxide in all hard tissue applications involving titanium and other alloys.

1. Introduction

Titanium alloys have become the most popular metallic biomaterials in dental applications because of their excellent biocompatibility [1]. This is attributed to the inert nature of the titanium surface due to the formation of a thin native titanium oxide layer [2] which also provides excellent corrosion resistance. Although titanium alloys have virtually replaced other metallic biomaterials in dental implant applications, currently there is little insight into the reasons for this excellent biocompatibility of titanium surfaces. A number of studies have pointed out various factors that contribute to the biocompatibility of titanium or of modified titanium surfaces [3–6]. While these studies have investigated both proliferation and differentiation of osteoblast cell lines evidenced in many instances by gene expression to corroborate biocompatibility, the emphasis has been on physical factors such as roughness, texture, wettability, or substrate microstructural features. Some importance has been paid to the substrate composition, whether Ti or Ti alloy, and the makeup of the surface modified layer. In recent work [3], the plausible role of titanium oxide in contributing to this outstanding biocompatibility was observed. In studying titanium alloys, it was noticed that ALP activity was higher on oxidized titanium alloys compared to corresponding untreated materials [7, 8]. Despite having a good understanding of the signaling pathways in osteoblast differentiation [4], the effect of titanium oxide on osteoblast differentiation has not been fully researched even though the fact that a thin native titanium oxide layer forms on all titanium alloys is well known and a large amount of research has been conducted on these popular biomaterials.

It is still unclear at the present time whether osteoblast differentiation is affected by titanium oxide or by the oxygen released from the titanium oxide. A recent report suggests that oxygen tension, in and of itself, has a strong effect on osteoblast differentiation and may in fact regulate this process [5], and hypoxic cell cultures demonstrated a lower level of mineralization resulting in a more chondrogenic tissue in comparison to higher levels of oxygen in cell cultures [6]. Healing of fractures has also been reported much earlier to be delayed in the absence of oxygen [9]. In contrast, reactive

oxygen species (ROS) has been reported to suppress bone formation and stimulate bone resorption [10]. Osteoblast differentiation involves a complex molecular pathway consisting of various transcription factors and it is well known that many transitional stages comprise the pathway for this process and that several signaling molecules play key roles in overall skeletal development [4]. It is currently unknown if titanium oxide plays a critical role in any step of the signaling cascade. Understanding the manner in which titanium oxide affects osteoblast differentiation may be critical in titanium implantology in terms of reducing hospitalization time and formulating efficient therapeutic procedures.

In this study, hFOB cells were cultured for 10 days on the oxide formed on the surface of two titanium-based alloys from two different methods of oxidation and the degree of osteoblast differentiation was measured through quantification of ALP activity using a commercial assay kit to compare with unoxidized titanium alloy surfaces in an effort to determine if titanium oxide indeed played a role in the differentiation process.

2. Materials and Methods

2.1. Preparation of Titanium Disks. Various samples of the two titanium-based alloys, gamma-TiAl (γ-TiAl [Ti-48Al-2Cr-2Nb (at.%)]) and Ti-6Al-4V (wt.%), were machined in the form of 7 mm diameter cylindrical rods. From these, disks with an approximate thickness of 1 mm were obtained using a slow-speed diamond saw (Buehler). Both surfaces of the disks were ground using 240, 320, 600, and 1200 grit silicon carbide paper in an Ecomet 3 (Buehler). These metal disks were then sonicated in 0.8% Alconox (Fisher, Pittsburgh, Pennsylvania) and 70% ethanol for 10 minutes each, rinsed with deionized water, and dried with a hot-air blow-dryer.

2.2. Thermal Oxidation. Both γ-TiAl and Ti-6Al-4V disks were oxidized in a laboratory furnace (CM Furnaces Inc.) in air at 500°C or 800°C for 1 h and later placed in 48-well cell culture plates (Corning). The nomenclature followed in this paper is as follows: γ-TiAl and Ti-6Al-4V disks oxidized at 500°C and 800°C are hereafter referred to as GTi5, GTi8, TiV5, and TiV8, respectively, while untreated disks are designated as GTi and TiV. Atomic force microscopy (AFM) was used to obtain average surface roughness values of the oxidized surfaces. These are given in Table 1.

2.3. Micro Arc Oxidation. Other γ-TiAl and Ti-6Al-4V disk samples were processed using micro arc oxidation (MAO). For the MAO process, a stainless steel beaker was used as the cathode, while the titanium disk (either γ-TiAl or Ti-6Al-4V) was used as the anode. Each sample was mounted in a titanium holder specially designed to allow complete exposure of the sample to the electrolyte [11]. A *Hoefer PS300-B* high voltage power supply (300 V; 500 mA) was operated in galvanostatic mode in order to form the titanium oxide film on the sample surface using the MAO process. Process conditions of sample current of 200 mA and 225 mA for durations of 3 and 4 minutes for each case were utilized based on an earlier study [11]. After treatment, the samples were rinsed with distilled water and then dried with a blow dryer. The micro arc oxidized samples will be henceforth referred to as MAOGTi for the γ-TiAl samples and the MAOTiV for the Ti-6Al-4V samples, respectively. The oxides formed on both γ-TiAl and Ti-6Al-4V as a result of the MAO treatment for the applied process conditions are mainly rutile and anatase as reported earlier [11, 12]. For thermal oxidation, alumina is the dominant oxide formed on γ-TiAl at 500°C, while rutile is dominant at 800°C [13–16]. For Ti-6Al-4V, thermal oxidation at 500°C produces a combination of an oxide diffused Ti(O) and rutile where the latter phase appears to grow at high temperatures between 650°C and 800°C [17]. The average roughness values of these surfaces were extracted from topography analysis using AFM and presented in Table 1.

Table 1: Average roughness values (in μm) measured on Ti alloy sample surfaces for various treatments using AFM.

Treatment	Ti-6Al-4V	γ-TiAl
None	51.74	49.30
Oxidation at 500°C	102.40	31.34
Oxidation at 800°C	318.80	65.88
MAO 200 mA, 3 min	246.30	174.50
MAO 200 mA, 4 min	247.60	185.90
MAO 225 mA, 3 min	213.30	137.50
MAO 225 mA, 4 min	301.70	189.80

2.4. Human Fetal Osteoblast Cell Line. Human osteoblast cells, cell line hFOB 1.19 (ATCC, Manassas, Virginia), were cultured in 90% Dulbecco's Modified Eagle's Medium Nutrient Mixture F-12 Ham (DMEM) (Sigma-Aldrich, St. Louis, Missouri) with 2.5 mM L-Glutamine and 15 mM Hepes, without phenol red, supplemented with 0.3 mg/mL G-418 (Calbiochem, San Diego, California) and 10% Fetal Bovine Serum (FBS) (Hyclone, Logan, Utah). Cells were grown in 25 cm^2 plastic culture flasks (Corning, Corning, New York) and incubated at 33.5°C until confluence. At approximately 100% confluence, cells were washed three times with Phosphate Buffer Saline (PBS) solution (137 mM NaCl, 2.7 mM KCl, 4.3 mM Na_2HPO_4, and 1.4 mM KH_2HPO_4) and harvested using 0.25% trypsin-0.53 mM EDTA (Gibco, Gaithersburg, Maryland) at 37°C for 5 min. Cells were then pelleted by low speed centrifugation (3,300 rpm) for 5 minutes and subcultured at a 1 : 3 ratio.

2.5. Alkaline Phosphatase Assay. Cells were seeded in 48-well plates (Becton, Dickinson, Lincoln Park, NJ) at a density of 5×10^4 cells/cm^2 on TiV, TiV5, TiV8, GTi, GTi5, GTi8, MAOTiV, and MAOGTi disks (7 mm in diameter), using the commercial Alkaline Phosphatase Colorimetric Assay Kit (ab83369, Abcam) in order to evaluate osteoblast differentiation quantitatively on thermally oxidized, micro arc oxidized, and untreated γ-TiAl and Ti-6Al-4V disks. Samples were incubated for 3 days at 33.5°C and then for 7 days at 39.5°C to allow osteoblast differentiation. hFOB cells grown on coverslips were used as controls. Modifications to the suggested protocol were made to achieve a more

efficient cell lysis, including washing the samples carefully three times with PBS and homogenizing in 60 μL of the Assay Buffer. Also, Triton X-100 (80 μL) was utilized to lyse the cells for an efficient measurement of intracellular ALP. Stop solution (20 μL) was added to terminate ALP activity in the sample. The solution in each well was transferred to a 96-well plate (Becton, Dickinson, Lincoln Park, NJ). *p*NPP solution (50 μL) was added to each well containing the test samples and background controls. The reaction was incubated for 60 minutes at 25°C, protected from light.

A standard curve was generated to determine the concentration of ALP activity in the sample for which 40 μL of the 5 mM *p*NPP solution was diluted with 160 μL Assay Buffer to generate a 1 mM *p*NPP standard. 0, 4, 8, 12, 16, and 20 μL were added to 96-well plate in duplicate to generate 0, 4, 8, 12, 16, and 20 nmol/well *p*NPP standard. The final volume was brought to 120 μL with Assay Buffer. ALP enzyme solution (10 μL) was added to each well containing the *p*NPP standard. The reaction was incubated for 60 minutes at 25°C, protected from light. All reactions were stopped by adding 20 μL Stop Solution to each standard and sample reaction except the sample background control reaction (since 20 μL Stop Solution had been added to the background control when prepared previously). The optical density was measured at 405 nm in a microplate reader. The background was corrected by subtracting the value derived from the zero (0) standards from all standards, samples, and sample background control. The *p*NPP standard curve was plotted and the sample readings were applied to the standard curve to get the amount of *p*NPP generated. ALP activity of the test samples was calculated using the equation, ALP activity (U/mL) = $A/V/T$, where A is amount of *p*NPP generated by samples (in μmol), V is volume of sample added to the assay well (in mL), and T is reaction time (in minutes).

2.6. Statistical Analysis. Three independent experiments were performed for each ALP assay, and since each experiment had three replicates, a total of nine replicates per surface were evaluated (MAO γ-TiAl, thermally oxidized γ-TiAl, untreated γ-TiAl, MAO Ti-6Al-4V, thermally oxidized Ti-6Al-4V, untreated Ti-6Al-4V, and control glass coverslips) for a 10-day period of culture. The data from the ALP assay is presented as the mean ± standard deviation (SD) of the optical density of differentiated cells on the different surfaces corresponding to the amount of alkaline phosphatase detected. Each value represents the mean of three measurements of cell differentiation performed on a specific surface as mentioned above. A factorial analysis of variance (ANOVA) was used to assess the significant interactions between type of metal (γ-TiAl or Ti-6Al-4V) and type of surface treatment (micro arc oxidization at 200 mA, 3 min, 200 mA, 4 min, 225 mA, 3 min, and 225 mA, 4 min; thermal oxidization at 500°C and 800°C). All significant interactions were graphically analyzed and, in addition, a randomized block design was performed to reduce the variance in the data. Furthermore, a contrast test was performed to compare the type of metal (γ-TiAl and Ti-6Al-4V) with the surface treatments. Significant differences in cell differentiation on the type of metal and surfaces tested were confirmed using the LSD Fisher test. All analyses were performed using Infostat (Infostat Inc.). p values < 0.05 were considered to be statistically significant.

3. Results

SEM images of glass coverslips, untreated Ti-6Al-4V and γ-TiAl surfaces (TiV and GTi), micro arc oxidized Ti-6Al-4V and γ-TiAl surfaces (MAOTiV and MAOGTi), and thermally oxidized Ti-6Al-4V and γ-TiAl surfaces (TiV5, TiV8, GTi5, and GTi8), are shown in Figure 1. GTi and TiV (Figures 1(a) and 1(b)) exhibit a smoother surface of the passive oxide layer formed instantaneously on Ti alloys. In contrast, rounded surface structures were visible in TiV5, suggesting clusters of oxide granules. GTi8 and TiV8, on the other hand, exhibited a rougher surface in comparison to the other samples (Figures 1(e) and 1(f)). Larger oxide granules were present on TiV8 (Figure 1(e)) compared to those on GTi8 (Figure 1(f)), conferring an irregular appearance to this surface and suggesting that TiV8 oxide layer could possibly be thicker. The MAO surfaces for Ti-6Al-4V (MAOTiV) (Figure 1(g)) demonstrated a number of large pores on the oxide surface typical of similar treatments on Ti alloys [18, 19]. Although pores were also clearly visible on the surface of MAOGTi, these were smaller and on the average in the submicron range.

SEM images shown in Figure 2 indicate that hFOB 1.19 cells grew normally on the surfaces of untreated γ-TiAl and Ti-6Al-4V disks. Cell attachment and proliferation were similar on both metal surfaces, suggesting normal growth, cell confluence, and attachment under *in vitro* conditions. The osteoblast cells were spread and flattened on the glass coverslips exhibiting such close contact with each other, that detection of cellular boundaries was difficult. Fibrous networks corresponding to fibrillar collagen, the main component of bone ECM, which aid in the adhesion of cells and important for the proper assembly of the extracellular matrix, are visible lending further testimony to the normal growth of osteoblasts on these surfaces. The ECM, which serves as a calcium phosphate reservoir, provides support for the cells, offers protection, and is very important in homeostasis, appears to be forming copiously [20]. Included are nodules of mineralization with a sponge-like morphology and intimately associated with the fibrillar network and scattered throughout the samples [21]. The maturation of the ECM is evidenced by the presence of fibrous networks associated with cells and an increase in nodules of mineralization. On the thermally oxidized Ti-6Al-4V and γ-TiAl alloys at 500°C, cellular attachment and proliferation were similarly observed. A cell multilayer, constituted by elongated and polygonal cells with some round shaped cells (Figure 2), along with the presence of a few small rounded structures which may correspond to mineral nodules, was observed. At higher magnification (Figure 3), the mineral nodules appeared to be in close contact with cells and had a sponge-like appearance. On the thermally oxidized Ti-6Al-4V alloys at 800°C, only irregular structures were observed. There was cell debris indicative of cytotoxicity of the oxide (Figure 3) in agreement with an earlier report [20]. However, on thermally oxidized γ-TiAl alloys, fibrous networks and mineralized nodules

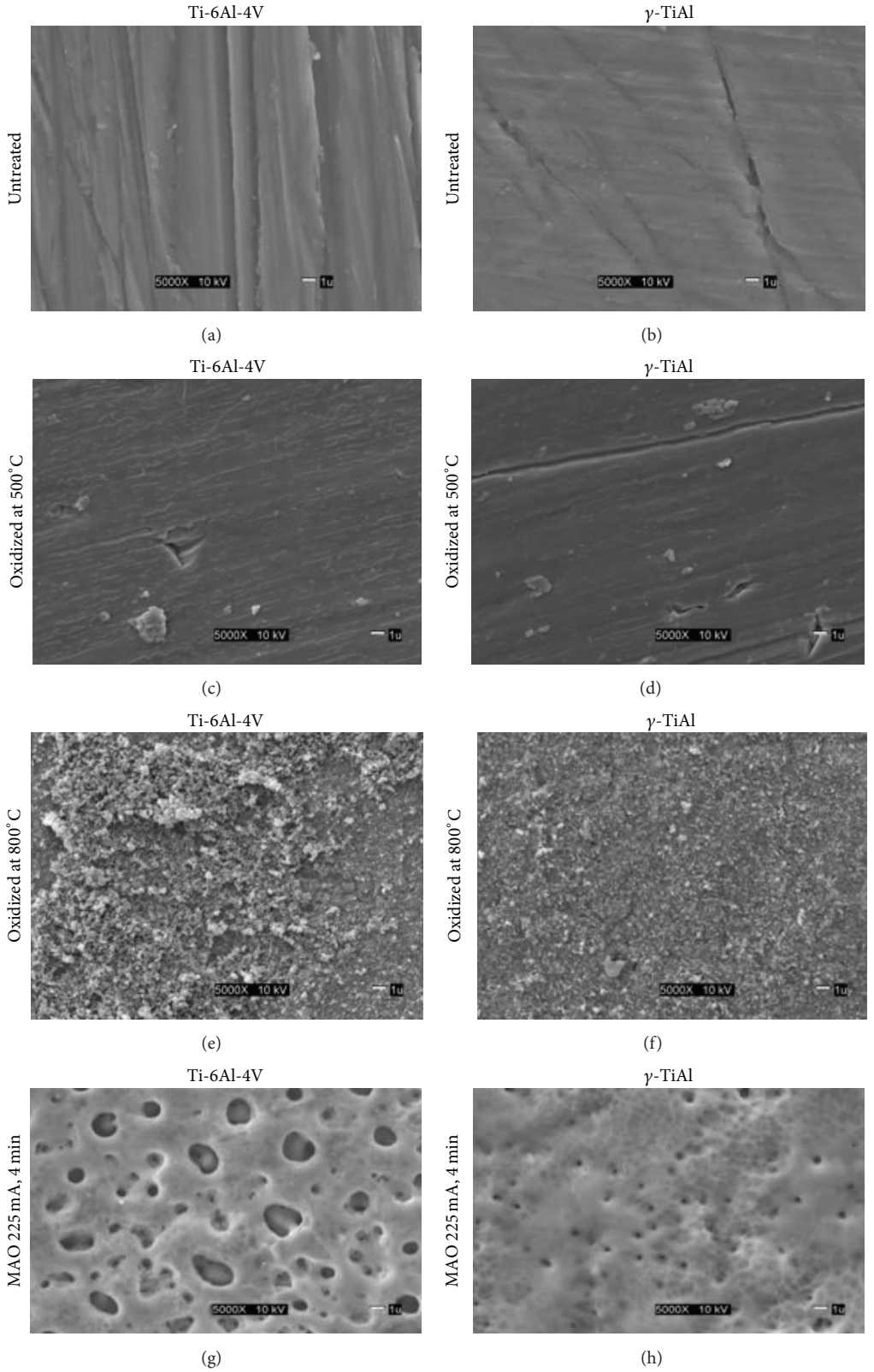

Figure 1: SEM images of Ti-6Al-4V and γ-TiAl alloys. (a), (b): untreated, (c), (d): oxidized at 500°C, (e), (f): oxidized at 800°C, and (g), (h): MAO at 225 mA, 4 mins.

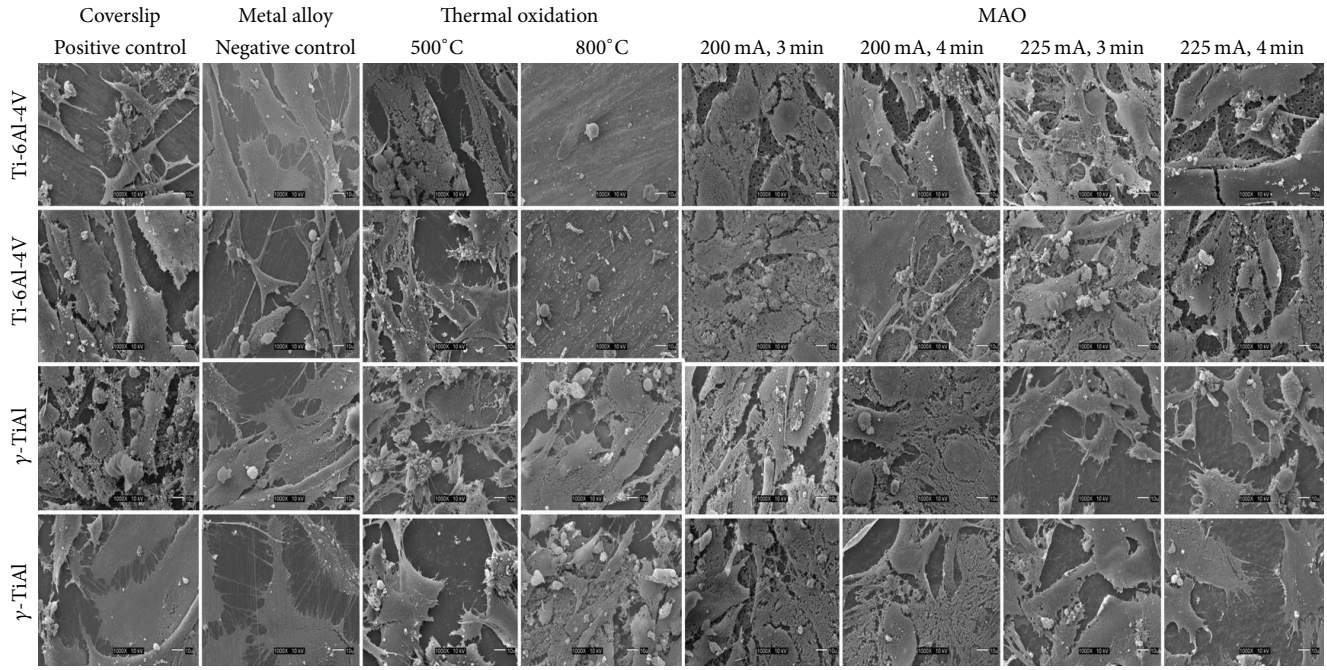

Figure 2: SEM micrographs of hFOB 1.19 cells on a glass coverslip (positive control), GTi and TiV (untreated alloys), thermally oxidized TiV5 and GTi5 (500°C), TiV8 and GTi8 (800°C), micro arc oxidized (MAO) TiV (200 mA and 225 mA at 3 min and 4 min), and MAOGTi (200 mA and 225 mA at 3 min and 4 min) disks. Magnification 1000x.

were observed on elongated cells (see Figure 3). Slender cytoplasmic projections (filopodia) extended from the cells in all directions on all micro arc oxidized Ti-6Al-4V and γ-TiAl disks, confirming the biocompatibility of the substrate materials [12]. In addition, sheet-like cytoplasmic protrusions extending from the cell body in all directions suggest the ability of cellular movement, spreading of the cells on the substrate, and/or the fact that cellular division (mitosis) may be occurring. The presence of mineralized nodules again suggests the maturation of the ECM and the formation of bone-like tissue indicating osteoblast differentiation evidenced by a high degree of ALP activity. Taken together, normal cell attachment and proliferation on all the surfaces with the exception of TiV8 indicate the excellent biocompatibility of control, untreated, and treated titanium alloy surfaces.

Standard calibration curves were used to extrapolate the values of alkaline phosphatase (ALP) activity on experimental disks 10 days after seeding based on the alkaline phosphatase assay. The ALP activity, measured as described in Section 2, is plotted in Figure 4 for the various sample surfaces that were utilized in the experiment to measure osteoblast differentiation. It is clear that little ALP activity is observed on the untreated Ti alloy samples while the positive controls (glass coverslips) indicate reasonable ALP activity corresponding to osteoblast differentiation. For the surface treatments of thermal oxidation and MAO, the Ti samples clearly showed relatively higher ALP activity. The highest ALP activity is observed for the Ti alloys subjected to the MAO treatment. As an exception, it must be noted that the ALP activity on Ti-6Al-4V oxidized at 800°C is rather low compared to the other treated samples. ANOVA revealed significant interactions between the factors tested (type of metal and treatment) and ALP activity. The interaction between the type of metal (γ-TiAl or Ti-6Al-4V) and surface treatment (micro arc oxidation at 200 mA, 3 min, 200 mA, 4 min, 225 mA, 3 min, and 225 mA, 4 min; thermal oxidation at 500°C or 800°C) was significant ($p < 0.05$). There were also significant differences in the amount of alkaline phosphatase detected among these six surfaces studied after 10 days of incubation at 33.5°C and 39.5°C, respectively. Additionally, alkaline phosphatase activity was lower on the positive control (glass coverslips) and even much lower on untreated titanium alloy surfaces in comparison with the micro arc and thermally oxidized alloys. Furthermore, ALP activity increased in γ-TiAl and Ti-6Al-4V alloys and in the MAO treatments where the samples were exposed for longer process times to current density. Although qualitatively there were no significant differences in the number of osteoblast cells attached on the micro arc oxidized or thermally oxidized surfaces collectively, ALP activity was significantly higher on the cell cultures that grew on the micro arc oxidized surfaces in comparison to the thermally oxidized substrates (see Figure 4). Surface roughness of the oxidized surfaces does not appear to show a correlation with ALP activity.

4. Discussion

hFOB adherence is clearly excellent on all surfaces with the exception of TiV8 which may possibly be due to the cellular response to toxic compounds or harmful ions such as vanadium in the oxide layer as a result of thermal oxidation [22]. As such, titanium oxide alone does not pose problems of cytotoxicity since cells did attach and proliferate on surfaces of both alloys subject to oxidation at 500°C and also γ-TiAl

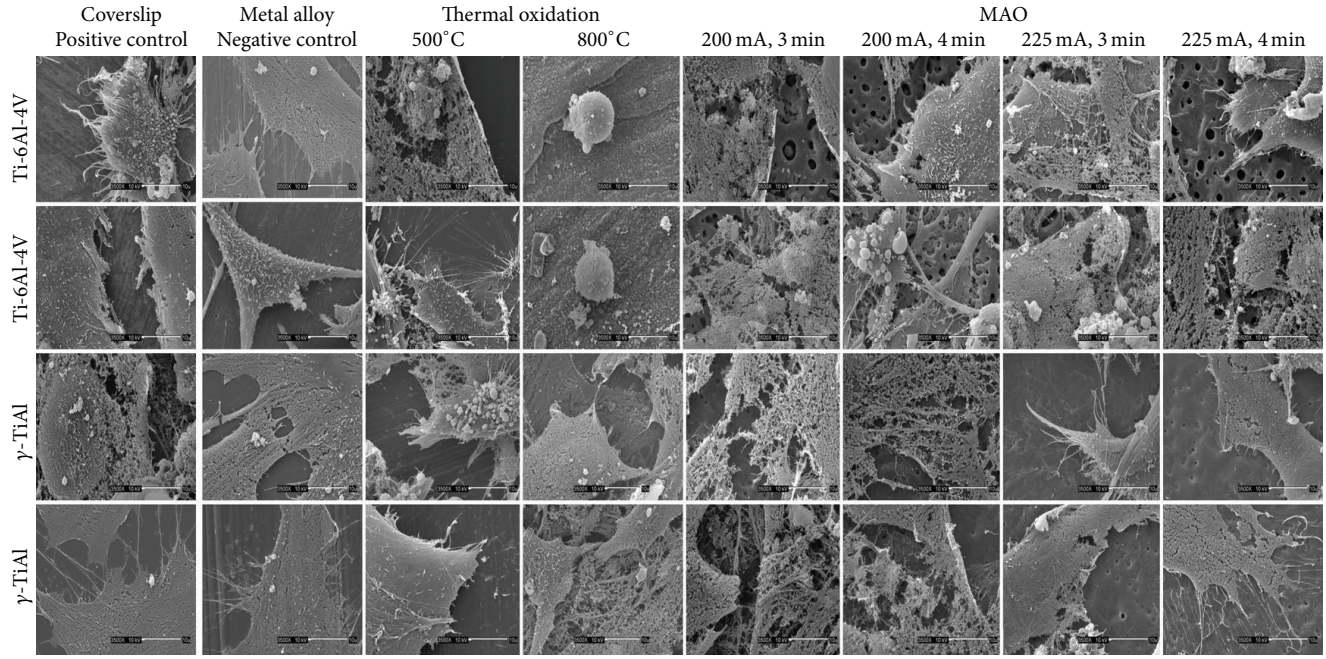

Figure 3: SEM micrographs of hFOB 1.19 cells seeded on a glass coverslip (positive control), GTi and TiV (untreated alloys), TiV5 and GTi5 (500°C), TiV8 and GTi8 (800°C), MAOTiV (200 mA and 225 mA at 3 min and 4 min), and MAOGTi (200 mA and 225 mA at 3 min and 4 min) disks and incubated for 10 days (3 days at 33.5°C and subsequently 7 days at 39.5°C). Magnification 3500x.

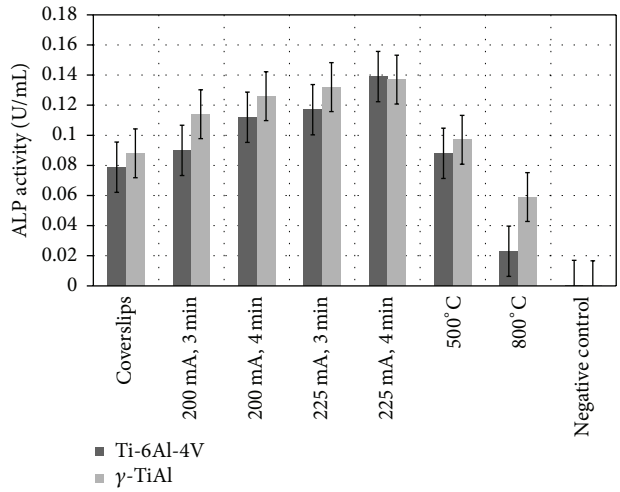

Figure 4: Alkaline phosphatase activity on thermally oxidized and MAO treated Ti-6Al-4V and γ-TiAl alloys. ALP activity on positive control (glass coverslips) and untreated Ti alloys is also shown.

oxidized at 800°C where the oxide formed is predominantly composed of titanium oxide in the form of rutile or anatase [23]. An earlier study showed normal cell attachment on TiV8 2 days after seeding but cell debris as a result of subsequent cell death for longer periods of incubation [20].

Osteoblast differentiation, on the other hand, occurred to different extents on all the substrates as measured by ALP activity. Osteoblast differentiation is a well-coordinated physiological process occurring in three stages which include cell proliferation, ECM production and maturation, and matrix mineralization [24]. Correspondingly, proliferative osteoprogenitors such as *Msx2* and *RP59* are expressed in the first stage, followed by *Runx2*, *Osx*, and OC (osteocalcin) during the later stages in this process of differentiation. During proliferation, Col 1 and ALP are detected earlier on followed by the secretion of RGD containing proteins such as bone sialoproteins (BSP) and osteopontin (OP) and culminating in the synthesis of OC in the last stage of differentiation. Bone morphogenetic proteins (BMPs) and various members of TGF-β family are secreted by the osteoblast cells and, once sequestered in the extracellular matrix (ECM), these have also been reported to be critical for osteoblast differentiation [25]. Interaction between Type I collagen and $\alpha 2\beta 1$ integrin activates a mitogen-activated protein kinase (MAPK) pathway which results in the phosphorylation and activation of *Cbfa1*, in turn stimulating the differentiation of osteoblasts. The ECM which contains BMPs can then induce ALP activity in preosteoblasts [26]. During osteogenesis, the lack of expression of *Runx2* and *Osx* may result in the formation of demineralized bone, although data suggests that these transcriptional factors act independently of each other [27]. Expression of *Runx2* along with *Cbf*β and alkaline phosphatase has been found to be critical in the early stage of differentiation while *Osx* becomes very important in the later stage of osteoblast differentiation. While, in the present study, cell attachment and proliferation occur normally on all the substrates, except for TiV8, alkaline phosphatase activity measurements indicate that osteoblast differentiation varies depending on the nature of the substrate. The presence of mineral nodules in the ECM on the titanium sample surfaces provides physical evidence to corroborate the activity of osteoblasts in one of their functional stages after maturation

as observed in osteoblast cultures at longer periods of incubation [28]. Ti-6Al-4V and γ-TiAl thermally oxidized disks at 500°C showed both irregular and rounded mineralized structures on the surface. Similar cell morphology and function were observed for the MAO surfaces for both alloys, suggesting the ability of these surfaces to also promulgate differentiation.

The fact that ALP activity was significantly lower on the untreated alloys (TiV, GTi) suggests that the titanium oxide formed on the surface of these alloys may be strongly correlated with the differentiation of the osteoblasts. It was demonstrated in an earlier study that the oxide layer on MAO treated alloys consists of titanium oxide with peaks for both anatase and rutile phases in all the coating conditions applied in this study [11]. Both anatase and rutile have been shown to be beneficial in enhancing nucleation and subsequent hydroxyapatite (HA) precipitation, thereby increasing bioactivity of the titanium surface [29]. The results from the present study also suggest that the incorporation of calcium (Ca) and phosphorus (P) into the titanium oxide may be favorable for cell differentiation. While Ca and P are important in the observation of increased ALP activity on MAO treated surfaces, the Ti alloys samples which were thermally oxidized at 500°C (devoid of Ca and P) also show a reasonably high ALP activity compared to control glass coverslips. A recent study has shown higher elemental oxygen concentration and higher water wettability on TiO_2 surfaces when compared to bare titanium surfaces resulting in a twofold increase in ALP activity and mineralized nodule area [30]. It also appears that the topography of bioengineered titanium surfaces affects gene expression and phenotypic response of osteoprogenitor cells [31]. Higher ALP activity on surfaces containing titanium oxide may possibly be correlated with the surface topography of the substrate which may affect cell proliferation and differentiation [31, 32]. Thus it may be argued that the osteoblast differentiation does not depend solely on Ca and P ions but more so on the presence of titanium oxide. In contrast, another research suggests cell cytotoxicity due to TiO_2 resulting from the interaction between TiO_2 nanoparticles and the lysosomal compartment, independently of the known apoptotic signaling pathways [33]. However, this has not been fully studied. In addition, TiO_2 has been reported to possess antibacterial characteristics in stark contrast to its positive biocompatibility [34].

Although it is clear from this study that titanium oxide increases the ALP activity in osteoblasts, the mechanism associated with this process is still unknown. It was proposed that BMP-2 controls alkaline phosphatase expression and osteoblast mineralization by a Wnt autocrine loop in mesenchymal stem cells (MSCs) [35]. Among the factors that regulate MSC growth and differentiation are soluble factors and cell-substrate interactions, although little is known about the molecular mechanisms by which soluble and substrate signals regulate MSC function. These authors showed that the commitment of human MSCs to the osteogenic and adipogenic lineages *in vitro* involves signaling by mitogen-activated protein kinase (MAPK) pathways. In particular, it was found that dexamethasone, ascorbic acid, and β-glycerophosphate induce MSC differentiation by regulating the extracellular signal-regulated kinase (ERK1/2) cascade. Furthermore, blocking the ERK1/2 pathway inhibits osteogenic differentiation of MSCs and leads to adipogenesis. Thus MAPK pathways, which are generally activated by growth factors/cytokines and integrin-mediated cell adhesion, play a critical role in directing MSC commitment. MAPK pathways are also activated by physical stimuli to regulate the function of a variety of cell types, including bone cells. In bone, it has been proposed that mature cells such as osteocytes and osteoblasts are responsible for sensing and responding to mechanical stimuli [36]. It is unknown whether the progenitors that give rise to these cells are responsive to mechanical signals. Various signaling pathways, including BMP, Wnt, and notch, regulate bone homeostasis. It is difficult at the present time to determine which of these is affected by titanium oxide to the extent of upregulating ALP activity. While it is clearly demonstrated that hypoxia suppresses osteoblast differentiation and as a consequence bone formation, the mode by which TiO_2 increases ALP activity is not clear cut. One may speculate that a chemical reaction between TiO_2 and the culture medium may somehow result in the release of oxygen and this normoxia has a positive impact on osteoblast differentiation. However, it is clear that TiO_2 is a bioactive factor which indeed upregulates ALP activity, although the manner in which the oxide indeed participates in the biochemical signaling cascade which occurs during differentiation does require further study. This information may be vital in the future of implantology in accelerating fracture healing and other tissue regenerative processes in dental and orthopedic applications. If titanium oxide indeed upregulates osteoblast differentiation, the manufacturers of titanium-based implants would find it advantageous to incorporate titanium oxide as a coating on every surface layer in contact with the tissue side of the implant. Clearly, further research is needed to interrogate the empirical ability of titanium oxide to preferentially favor osteoblast differentiation or at least ALP activity.

5. Conclusions

(1) ALP activity is much higher on oxidized surfaces of both titanium alloys compared to untreated surfaces most probably due to the presence of titanium oxide.

(2) The higher ALP activity on micro arc oxidized surfaces is attributed to the Ca and P content which are not present in the thermally oxidized titanium alloys.

(3) The mechanism for the upregulation of ALP due to titanium oxide needs further study although it is clear that TiO_2 is a bioactive factor in osteoblast differentiation.

Conflict of Interests

There is no financial conflict of interests regarding the data or content of this study.

Acknowledgments

This study was supported by the NIH Grant SO6GM-08103 through the MBRS-SCORE Program at the University of Puerto Rico, Mayaguez Campus. The authors thank Jose Almodovar from the University of Puerto Rico, Mayaguez Campus, who assisted in the acquisition of the immunofluorescence images.

References

[1] H. J. Rack and J. I. Qazi, "Titanium alloys for biomedical applications," *Materials Science and Engineering C*, vol. 26, no. 8, pp. 1269–1277, 2006.

[2] I. Milošev, M. Metikoš-Huković, and H.-H. Strehblow, "Passive film on orthopaedic TiAlV alloy formed in physiological solution investigated by X-ray photoelectron spectroscopy," *Biomaterials*, vol. 21, no. 20, pp. 2103–2113, 2000.

[3] P. Santiago-Medina, P. A. Sundaram, and N. Diffoot-Carlo, "The effects of micro arc oxidation of gamma titanium aluminide surfaces on osteoblast adhesion and differentiation," *Journal of Materials Science: Materials in Medicine*, vol. 25, no. 6, pp. 1577–1587, 2014.

[4] G. L. Lin and K. D. Hankenson, "Integration of BMP, Wnt, and notch signaling pathways in osteoblast differentiation," *Journal of Cellular Biochemistry*, vol. 112, no. 12, pp. 3491–3501, 2011.

[5] C. Nicolaije, M. Koedam, and J. P. T. M. van Leeuwen, "Decreased oxygen tension lowers reactive oxygen species and apoptosis and inhibits osteoblast matrix mineralization through changes in early osteoblast differentiation," *Journal of Cellular Physiology*, vol. 227, no. 4, pp. 1309–1318, 2012.

[6] A. Salim, R. P. Nacamuli, E. F. Morgan, A. J. Giaccia, and M. T. Longaker, "Transient changes in oxygen tension inhibit osteogenic differentiation and Runx2 expression in osteoblasts," *Journal of Biological Chemistry*, vol. 279, no. 38, pp. 40007–40016, 2004.

[7] B. Feng, J. Weng, B. C. Yang, S. X. Qu, and X. D. Zhang, "Characterization of surface oxide films on titanium and adhesion of osteoblast," *Biomaterials*, vol. 24, no. 25, pp. 4663–4670, 2003.

[8] G. Zhao, Z. Schwartz, M. Wieland et al., "High surface energy enhances cell response to titanium substrate microstructure," *Journal of Biomedical Materials Research A*, vol. 74, no. 1, pp. 49–58, 2005.

[9] R. B. Heppenstall, C. W. Goodwin, and C. T. Brighton, "Fracture healing in the presence of chronic hypoxia," *The Journal of Bone and Joint Surgery—American Volume*, vol. 58, no. 8, pp. 1153–1156, 1976.

[10] X.-C. Bai, D. Lu, A.-L. Liu et al., "Reactive oxygen species stimulates receptor activator of NF-κB ligand expression in osteoblast," *Journal of Biological Chemistry*, vol. 280, no. 17, pp. 17497–17506, 2005.

[11] L. Lara Rodriguez, P. A. Sundaram, E. Rosim-Fachini, A. M. Padovani, and N. Diffoot-Carlo, "Plasma electrolytic oxidation coatings on γtiAl alloy for potential biomedical applications," *Journal of Biomedical Materials Research B: Applied Biomaterials*, vol. 102, no. 5, pp. 988–1001, 2014.

[12] L.-H. Li, Y.-M. Kong, H.-W. Kim et al., "Improved biological performance of Ti implants due to surface modification by micro-arc oxidation," *Biomaterials*, vol. 25, no. 14, pp. 2867–2875, 2004.

[13] S. Becker, A. Rahmel, M. Schorr, and M. Schütze, "Mechanism of isothermal oxidation of the intel-metallic TiAl and of TiAl alloys," *Oxidation of Metals*, vol. 38, no. 5-6, pp. 425–464, 1992.

[14] A. Gil, H. Hoven, E. Wallura, and W. J. Quadakkers, "The effect of microstructure on the oxidation behaviour of TiAl-based intermetallics," *Corrosion Science*, vol. 34, no. 4, pp. 615–630, 1993.

[15] N. Zheng, W. Fischer, H. Grübmeier, V. Shemet, and W. J. Quadakkers, "The significance of sub-surface depletion layer composition for the oxidation behaviour of γ-titanium aluminides," *Scripta Metallurgica et Materiala*, vol. 33, no. 1, pp. 47–53, 1995.

[16] J. W. Fergus, "Review of the effect of alloy composition on the growth rates of scales formed during oxidation of gamma titanium aluminide alloys," *Materials Science and Engineering A*, vol. 338, no. 1-2, pp. 108–125, 2002.

[17] S. Kumar, T. S. N. Sankara Narayanan, S. Ganesh Sundara Raman, and S. K. Seshadri, "Thermal oxidation of Ti6Al4V alloy: microstructural and electrochemical characterization," *Materials Chemistry and Physics*, vol. 119, no. 1-2, pp. 337–346, 2010.

[18] P. Whiteside, E. Matykina, J. E. Gough, P. Skeldon, and G. E. Thompson, "In vitro evaluation of cell proliferation and collagen synthesis on titanium following plasma electrolytic oxidation," *Journal of Biomedical Materials Research Part A*, vol. 94, no. 1, pp. 38–46, 2010.

[19] M. Dicu, A. Matei, M. Abrudeanu, and C. Ducu, "Synthesis and properties of the porous titania coatings formed on titanium by plasma electrolytic oxidation for biomedical application," *Journal of Optoelectronics and Advanced Materials*, vol. 13, no. 3, pp. 324–331, 2011.

[20] S. A. Bello, I. de Jesús-Maldonado, E. Rosim-Fachini, P. A. Sundaram, and N. Diffoot-Carlo, "In vitro evaluation of human osteoblast adhesion to a thermally oxidized γ-TiAl intermetallic alloy of composition Ti-48Al-2Cr-2Nb (at.%)," *Journal of Materials Science: Materials in Medicine*, vol. 21, no. 5, pp. 1739–1750, 2010.

[21] M. C. Advincula, F. G. Rahemtulla, R. C. Advincula, E. T. Ada, J. E. Lemons, and S. L. Bellis, "Osteoblast adhesion and matrix mineralization on sol-gel-derived titanium oxide," *Biomaterials*, vol. 27, no. 10, pp. 2201–2212, 2006.

[22] D. R. Haynes, S. D. Rogers, S. Hay, M. J. Pearcy, and D. W. Howie, "The differences in toxicity and release of bone-resorbing mediators induced by titanium and cobalt-chromium-alloy wear particles," *The Journal of Bone & Joint Surgery—American Volume*, vol. 75, no. 6, pp. 825–834, 1993.

[23] C. Delgado-Alvarado and P. A. Sundaram, "Corrosion evaluation of Ti-48Al-2Cr-2Nb (at.%) in Ringer's solution," *Acta Biomaterialia*, vol. 2, no. 6, pp. 701–708, 2006.

[24] T. A. Owen, M. Aronow, V. Shalhoub et al., "Progressive development of the rat osteoblast phenotype in vitro: reciprocal relationships in expression of genes associated with osteoblast proliferation and differentiation during formation of the bone extracellular matrix," *Journal of Cellular Physiology*, vol. 143, no. 3, pp. 420–430, 1990.

[25] G. Xiao, R. Gopalakrishnan, D. Jiang, E. Reith, M. D. Benson, and R. T. Franceschi, "Bone morphogenetic proteins, extracellular matrix, and mitogen-activated protein kinase signaling pathways are required for osteoblast-specific gene expression and differentiation in MC3T3-E1 cells," *Journal of Bone and Mineral Research*, vol. 17, no. 1, pp. 101–110, 2002.

[26] Y. Takeuchi, K. Nakayama, and T. Matsumoto, "Differentiation and cell surface expression of transforming growth factor-β receptors are regulated by interaction with matrix collagen in murine osteoblastic cells," *Journal of Biological Chemistry*, vol. 271, no. 7, pp. 3938–3944, 1996.

[27] K. Nakashima and B. de Crombrugghe, "Transcriptional mechanisms in osteoblast differentiation and bone formation," *Trends in Genetics*, vol. 19, no. 8, pp. 458–466, 2003.

[28] U. Müller, T. Imwinkelried, M. Horst, M. Sievers, and U. Graf-Hausner, "Do human osteoblasts grow into open-porous titanium?" *European Cells and Materials*, vol. 11, pp. 8–15, 2006.

[29] J.-M. Wu, S. Hayakawa, K. Tsuru, and A. Osaka, "Low-temperature preparation of anatase and rutile layers on titanium substrates and their ability to induce in vitro apatite deposition," *Journal of the American Ceramic Society*, vol. 87, no. 9, pp. 1635–1642, 2004.

[30] N. Tsukimura, N. Kojima, K. Kubo et al., "The effect of superficial chemistry of titanium on osteoblastic function," *Journal of Biomedical Materials Research Part A*, vol. 84, no. 1, pp. 108–116, 2008.

[31] J. Isaac, A. Galtayries, T. Kizuki, T. Kokubo, A. Berdal, and J.-M. Sautier, "Bioengineered titanium surfaces affect the gene expression and phenotypic response of osteoprogenitor cells derived from mouse calvarial bones," *European Cells and Materials*, vol. 20, pp. 178–196, 2010.

[32] Z. Huang, R. H. Daniels, R.-J. Enzerink, V. Hardev, V. Sahi, and S. B. Goodman, "Effect of nanofiber-coated surfaces on the proliferation and differentiation of osteoprogenitors *in vitro*," *Tissue Engineering A*, vol. 14, no. 11, pp. 1853–1859, 2008.

[33] Y. Zhu, J. W. Eaton, and C. Li, "Titanium dioxide (TiO_2) nanoparticles preferentially induce cell death in transformed cells in Bak/Bax-independent fashion," *PLoS ONE*, vol. 7, no. 11, Article ID e50607, 2012.

[34] H. Lin, Z. Xu, X. Wang et al., "Photocatalytic and antibacterial properties of medical-grade PVC material coated with TiO_2 film," *Journal of Biomedical Materials Research Part B: Applied Biomaterials*, vol. 87, no. 2, pp. 425–431, 2008.

[35] G. Rawadi, B. Vayssière, F. Dunn, R. Baron, and S. Roman-Roman, "BMP-2 controls alkaline phosphatase expression and osteoblast mineralization by a Wnt autocrine loop," *Journal of Bone and Mineral Research*, vol. 18, no. 10, pp. 1842–1853, 2003.

[36] P. G. Robey and J. D. Termine, "Human bone cells in vitro," *Calcified Tissue International*, vol. 37, no. 5, pp. 453–460, 1985.

Hindawi Publishing Corporation
International Journal of Dentistry
Volume 2015, Article ID 141890, 7 pages
http://dx.doi.org/10.1155/2015/141890

Research Article

Effect of EDTA Conditioning and Carbodiimide Pretreatment on the Bonding Performance of All-in-One Self-Etch Adhesives

Shipra Singh,[1] Rajni Nagpal,[1] Shashi Prabha Tyagi,[1] and Naveen Manuja[2]

[1]*Department of Conservative Dentistry and Endodontics, Kothiwal Dental College and Research Centre, Moradabad 244001, India*
[2]*Department of Pediatric Dentistry, Kothiwal Dental College and Research Centre, Moradabad 244001, India*

Correspondence should be addressed to Rajni Nagpal; rajni_hisar@yahoo.co.in

Received 21 July 2015; Revised 26 September 2015; Accepted 29 September 2015

Academic Editor: Paulo H. P. D'Alpino

Objective. This study evaluated the effect of ethylenediaminetetraacetic acid (EDTA) conditioning and carbodiimide (EDC) pretreatment on the shear bond strength of two all-in-one self-etch adhesives to dentin. *Methods*. Flat coronal dentin surfaces were prepared on one hundred and sixty extracted human molars. Teeth were randomly divided into eight groups according to two different self-etch adhesives used [G-Bond and OptiBond-All-In-One] and four different surface pretreatments: (a) adhesive applied following manufacturer's instructions; (b) dentin conditioning with 24% EDTA gel prior to application of adhesive; (c) EDC pretreatment followed by application of adhesive; (d) application of EDC on EDTA conditioned dentin surface followed by application of adhesive. Composite restorations were placed in all the samples. Ten samples from each group were subjected to immediate and delayed (6-month storage in artificial saliva) shear bond strength evaluation. Data collected was subjected to statistical analysis using three-way ANOVA and post hoc Tukey's test at a significance level of $p < 0.05$. *Results and Conclusion*. EDTA preconditioning as well as EDC pretreatment alone had no significant effect on the immediate and delayed bond strengths of either of the adhesives. However, EDC pretreatment on EDTA conditioned dentin surface resulted in preservation of resin-dentin bond strength of both adhesives with no significant fall over six months.

1. Introduction

Adhesion to dentin may be achieved either following an "etch-and-rinse" or a "self-etch" approach. Self-etch approach has been claimed to be user-friendlier and less technique-sensitive. Another important clinical benefit of self-etch adhesives is the absence of, or at least lower incidence of postoperative sensitivity [1]. This has been attributed to their less aggressive and more superficial interaction with dentin leaving tubules largely obstructed by smear [2]. However, some studies have shown a potential disadvantage in incorporating the smear layer into the hybrid layer [3–5]. Although the smear layer is reinforced by impregnated resin, bonding defects may be produced [6]. Since such defects may decrease the resistance and stability of the hybridized smear layer, its removal by incorporating a separate etching step may be necessary to obtain reliable, strong resin-dentin bonds [7–9]. Therefore, a conditioning system capable of changing the tooth surface by removing the smear layer and partially removing the surface layer of hydroxyapatite while simultaneously not destroying the organic portion of the dentin may be beneficial as pretreatment for mild self-etch adhesives. Some studies have demonstrated that separate phosphoric acid etching of dentin could decrease the bond strength and durability of self-etch adhesives [10, 11]. Therefore, conditioning with a mild etchant like EDTA may prove to be beneficial for bonding of mild self-etch adhesives to dentin.

Whereas phosphoric acid etching of dentin leads to dissolving both the extra and the intrafibrillar minerals resulting in recession and collapse of the collagen matrix, only partial removal of the smear layer with the maintenance of about 30% of the smear plugs and no morphological alterations of the dentin surface is observed following application of 17% EDTA on dentin for 60 seconds [12]. Phosphoric acid-etching of dentin causes collagen fibrils to become slightly denatured and swollen compared to EDTA-treatment [13].

Jacques and Hebling reported that pretreatment with a mild etchant such as 0.5 M EDTA improved the bond

strength of the Clearfil SE bond [14]. Torii et al. also reported that EDTA conditioning was effective in improving dentin bonding for all-in-one adhesives [15]. Therefore, it may be anticipated that EDTA conditioning may improve the bonding efficacy of mild all-in-one self-etch adhesives to dentin [16]. Moreover EDTA has been shown to have a MMP inhibitory effect which may help in improving the durability of resin-dentin bond [17].

Degradation of the resin-dentin bonds, due to hydrolysis of the collagen fibrils, involves the participation of endogenous matrix metalloproteinases (MMPs) which become entrapped within the dentin substrate during tooth development [18, 19]. Therefore, the use of MMP inhibitors and collagen cross-linkers have been suggested as a valid alternative in an attempt to prolong the resin-dentin bond stability by overcoming this self-degradation process [20]. Chlorhexidine (CHX), Galardin (GL), CMT, SB-3 CT, proanthocyanidins (PA), 1-ethyl-3-(3-dimethylaminopropyl) carbodiimide (EDC), tetracycline, and quaternary ammonium methacrylates or benzalkonium chloride have been employed in various studies to improve the durability of resin-dentin bond [21–25].

The potential of cross-linkers is related to the possibility to improve the mechanical strength of the collagen network, improve the resistance to enzymatic degradation, and inactivate exposed MMPs bound to matrix collagen. When acid-etched dentin containing activated matrix-bound MMPs is treated with cross-linking agents, they inactivate the catalytic site of proteases [26]. Carbodiimide [EDC, 1-ethyl-3-(3-dimethylaminopropyl)] has been described as a collagen cross-linker with MMP inhibitory properties. EDC have been used as alternative cross-linking agents to glutaraldehyde, since they contain no potentially cytotoxic aldehyde residuals [27, 28]. EDC effectively improves the durability of resin-dentin bonds by increasing the mechanical properties of the collagen matrix [29]. Most of the research regarding the effect of EDC on dental adhesion has been done using etch-and-rinse adhesives; however the effect of EDC on bonding of contemporary self-etch adhesives needs to be evaluated. Moreover the effect of prior EDTA conditioning on the bonding of specific all-in-one adhesive systems still needs to be determined. Hence, the aim of this study was to investigate the effect of (i) EDTA conditioning, (ii) EDC pretreatment, or (iii) combined effect of EDTA preconditioning and EDC application on the immediate and long-term bonding efficacy of two different all-in-one self-etch adhesives. The null hypothesis tested was that there is no effect of EDTA or EDC pretreatment on the immediate and delayed bond strength of two different all-in-one self-etch adhesives to dentin.

2. Materials and Method

The study was performed in one hundred and sixty freshly extracted noncarious, human molars. The teeth were examined under stereomicroscope (Olympus, Tokyo, Japan) and teeth free of caries, cracks, or any developmental defects were included. Teeth were cleaned of debris. Calculus was removed using ultrasonic scaler and then the teeth were stored in 0.5% Chloramine T Trihydrate (Sigma Aldrich, Bangalore, India) for no more than 3 months. Tooth crowns were flattened using a low-speed diamond saw (Isomet, Buehler Ltd., Lake Bluff, IL, USA) under water irrigation unless superficial dentin was visible and a standardized smear layer was created with 600-grit silicon-carbide (SiC) paper. The samples were embedded in an autopolymerizing resin at the level of cementoenamel junction with long axis perpendicular to the acrylic resin surface. Teeth were randomly divided into eight groups according to two different self-etch adhesives used (G-Bond (GC Corp., Tokyo, Japan) and OptiBond-All-In-One (KERR, Orange, CA, USA)) (Table 2) and four different surface pretreatments. Each group was further divided into two subgroups for immediate (a) and delayed (b) bond strength evaluation.

Group 1 (GB). G-Bond was applied following manufacturer's instructions.

Group 2 (GB-EDTA). Dentin conditioning with 24% EDTA gel for 1 minute (Trisodium EDTA Gel, Pyrex Pharmaceuticals, Roorkee), followed by rinsing with distilled water, blot dried prior to application of G-bond.

Group 3 (GB-EDC). Application of EDC (0.3 M for 1 minute) on smear covered dentin surface and blot dried before application of G-Bond.

Group 4 (GB-EDTA + EDC). Dentin was conditioned with 24% EDTA gel for 1 minute, rinsed with distilled water, and blot dried. This was followed by application of EDC (0.3 M) for 1 minute and then blot dried, followed by application G-Bond adhesive.

Group 5 (OB). OptiBond-All-In-One was applied following manufacturer's instructions.

Group 6 (OB-EDTA). Dentin conditioning with EDTA (24% gel for 1 minute) followed by rinsing with water blot dried prior to application of OptiBond-All-In-One.

Group 7 (OB-EDC). Application of EDC (0.3 M for 1 minute) on smear covered dentin surface and blot dried before application of OptiBond-All-In-One.

Group 8 (OB-EDTA + EDC). Dentin was conditioned with 24% EDTA gel for 1 minute, rinsed with distilled water, and blot dried. This was followed by application of EDC (0.3 M) for 1 minute and then blot dried, followed by application OptiBond-All-In-One adhesive.

Transparent plastic tubes 54-HL (TYGON Medical tubing, Saint Gobain, Akron, OH, USA) of internal diameter 3 mm and 2 mm height with thickness 0.5 mm were precut and placed perpendicular to the prepared surface. A hybrid resin composite (Filtek Z350 XT, Body Shade A1, Nanohybrid, 3 M ESPE) was filled into the precut tubes. Each bonded specimen was light-cured for 20 seconds using Spectrum 800 (Dentsply, Caulk, Milford, USA) at light intensity of 600 mW/cm^2. The plastic tubes were gently cut and carefully removed with a number 11 surgical blade after polymerization.

Table 1: Mean shear bond strength values both immediate and delayed for G-Bond and OptiBond-All-In-One adhesives.

Immediate Testing			Delayed Testing			p value
Groups	Mean	SD	Groups	Mean	SD	
1a (GB)	33.30^{abc}	5.54	1b	23.10^{c}	5.53	0.022*
2a (GB-EDTA)	38.40^{ab}	9.23	2b	27.90^{ab}	8.97	0.018*
3a (GB-EDC)	37.70^{abc}	7.72	3b	32.70^{ab}	8.11	0.429
4a (GB-EDTA + EDC)	40.80^{a}	7.58	4b	34.90^{a}	5.49	0.286
5a (OB)	29.00^{c}	6.99	5b	20.30^{c}	5.83	0.020*
6a (OB-EDTA)	32.30^{abc}	4.79	6b	22.30^{c}	7.45	0.006*
7a (OB-EDC)	30.20^{bc}	5.29	7b	25.60^{bc}	5.52	0.344
8a (OB-EDTA + EDC)	31.90^{abc}	6.44	8b	27.60^{abc}	6.96	0.403

Groups with the same superscripts are not statistically different ($p > 0.05$); * denotes statistically significant groups.

Table 2: Composition and manufacturer's instructions of adhesive systems used in the study.

Adhesive	Composition	Manufacture	Technique
G-Bond	4-MET, phosphate ester monomer, UDMA, acetone, water, microfiller, and photoinitiator	GC Corp.; Tokyo, Japan	(i) Shake the bottle thoroughly prior to dispensing (ii) Immediately apply to the prepared enamel and dentin surfaces using the disposing applicator (iii) Leave undisturbed for 5–10 seconds (iv) Dry thoroughly for 5 seconds with oil free air under maximum air pressure. The final results should be a thin, rough, adhesive film with the appearance of frosted glass and which doesn't visibly move under further air pressure (v) Light cure for 10 seconds
OptiBond-All-In-One	GPDM, GDM, HEMA, Bis-GMA, water, ethanol, acetone, silica, CQ, and sodium hexafluorosilicate	OP; Kerr; Orange, CA, USA	(i) Shake adhesive bottle briefly. (vigorously for 10 seconds) (ii) Using the disposable applicator brush, apply a generous amount of OptiBond-All-In-One adhesive to enamel/dentin surface. Scrub the surface with a brushing motion for 20 seconds (iii) Apply a second application of OptiBond-All-In-One All-In-One adhesive with a brushing motion for 20 seconds (iv) Dry the adhesive with gentle air first and then medium air for at least 5 seconds with oil-free air (v) Light cure for 10 seconds

3. Determination of Dentin Shear Bond Strength

Half of the specimens (1a–8a) were then stored in distilled water at 37°C for 24 hours for immediate testing. The remaining half samples from each group (1b–8b) were stored in artificial saliva (ICPA, Wet Mouth) for 6 months before shear bond strength evaluation [30, 31]. Shear bond strength was determined using a universal testing machine (Instron, ADMET, Enkay Enterprises, New Delhi) using the corresponding computer software. The specimens were placed and stabilized by the jig, while a straight knife-edge rod (2.0 mm) was applied at the tooth restoration interface at a crosshead speed of 1 mm/minute. Load was applied until restoration failure. The mode of failure was determined by observation under a stereomicroscope (Olympus, Tokyo, Japan) at 10x magnification and classified into adhesive (A), mixed (M), and cohesive (C) failures in either dentin or resin. The statistical analysis was done using three-way ANOVA and post hoc Tukey's test SPSS 16.0 version (Statistical Package, SPSS Inc., Chicago, IL, USA) at a significance level of $p < 0.05$.

4. Results

Mean shear bond strength values and standard deviation of all the groups are presented in Table 1. There was no significant difference in bond strengths between the two adhesives when used according to manufacturer's instructions (Table 2). EDTA pre-conditioning had no significant effect on the immediate bond strength of either of the adhesives (Groups 1a and 2a; $p = 0.707$; Groups 5a and 6a; $p = 0.959$). EDC pretreatment alone also had no significant effect on the immediate bond strength of G-Bond (Groups 1a and 3a; $p = 0.836$) and OptiBond-All-In-One (Groups 5a and 7a; $p = 0.999$). Mixed fractures were the most common failure mode in all the groups (Figure 1). There was no significant difference in the mode of failure between the two tested adhesives.

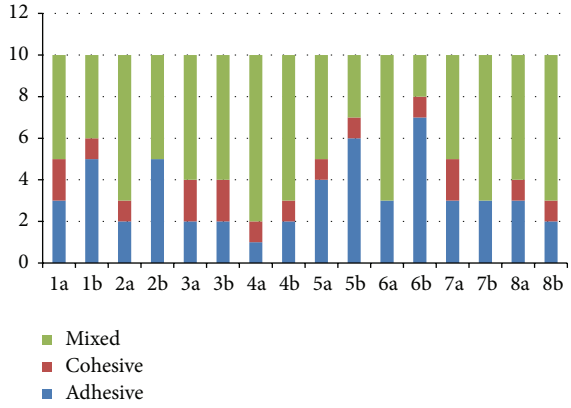

Figure 1: Failure modes in different experimental groups.

There was a significant reduction in bond strength for both adhesives G-Bond and OptiBond All-In-One after six months storage (Groups 1a and 1b; $p = 0.022$; Groups 5a and 5b; $p = 0.020$). EDTA preconditioning could not prevent the fall in bond strength over a six-month storage period (Groups 2a and 2b; $p = 0.018$; Groups 6a and 6b; $p = 0.006$). However, EDC pretreatment alone (Groups 3a and 3b; $p = 0.429$; Groups 7a and 7b; $p = 0.344$) or EDC application on EDTA conditioned dentin surface (Groups 4a and 4b; $p = 0.286$; Groups 8a and 8b; $p = 0.403$) resulted in preservation of resin-dentin bond strength of both the adhesives with no significant fall over six months. Failure mode analysis revealed mixed fractures to be the most common in Groups 3b : 4b; 7b and 8b. An increase in adhesive fractures was observed in Groups 1b : 2b; 5b : 6b (Figure 1).

5. Discussion

In the present study, no significant difference was observed between the immediate shear bond strength values of G-Bond and OptiBond-All-In-One adhesives and mixed fractures were the most common failure mode. Bond strength of polymerized adhesives depends upon various factors such as the type of cross-linking monomers, presence and type of filler particles, degree of conversion, and the amount of residual organic solvents. The carboxylic group of 4-MET (4-methacryloyloxyethyl trimellitic acid) renders G-Bond monomers hydrophilic, but less reactive than UDMA (urethane dimethacrylate) in hydrogen bonding with water and it functions as a proton donor that bonds ionically with calcium in hydroxyapatite crystalites [32, 33]. Thus, an extremely thin interface nanointeraction zone (300 nm) is formed as opposed to the traditional hybrid layer appellation that provides resistance to acute debonding stresses and better bond durability and survival of adhesion, minimizing voids. Strong air blowing of the primed surface as suggested in G-Bond accelerates the evaporation of solvent-acetone and the resultant water droplets formed due to phase separation. The excess of nonpolymerizable hydrophilic components (water, acetone, and glutaraldehyde) may give rise to hydration forces that repel water at film boundaries and hence less water sorption [32]. Aromatic rings present in G-Bond are more stable [34].

OptiBond-All-In-One contains 35 to 45% acetone and 4–9% ethanol. The solvent evaporation from adhesives is influenced by the vapor pressure [35]. As the vapor pressure of acetone is high, it volatilizes rapidly and may dehydrate the dentin. The presence of water in self-etch adhesives is necessary to ensure the ionization of the acidic monomers, but it is not as efficient as acetone or ethanol as a solvent because of its lower vapor pressure [36]. The presence of acetone and ethanol in OptiBond-All-In-One might balance the solvent evaporation without dehydrating dentin, because ethanol ensures the wetness of the substrate, and its vapor pressure is intermediate between acetone and water. Another explanation for the good performance of OptiBond-All-In-One could be the content of glycerol phosphate dimethacrylate monomer in its formulation, a surfactant monomer that may have facilitated the penetration of hydrophobic components into dentin, reducing the phase separation [37, 38]. G-Bond is HEMA (2-hydroxyethyl methacrylate) free adhesive whereas OptiBond-All-In-One is HEMA containing adhesive [33, 39–41]. The hydrophilic monomer, HEMA, in various concentrations is frequently added to one-step self-etch adhesives because of its positive influence on adhesion to dentin, the miscibility of hydrophilic and hydrophobic components in the adhesive blend, and prevention of phase separation. The hydrophilic monomer of HEMA tends to cluster together before polymerization, leading to creation of hydrophilic domains. Moreover, HEMA attracts water even after polymerization. When HEMA is cured in the presence of water, polymerization is incomplete and a porous hydrogel is formed that allows water to permeate through the adhesive layer, compromising bonding effectiveness. It was reported that the amount of water sorption of adhesive polymers increased proportionally to their HEMA concentrations [39]. Some studies have shown that the removal of HEMA from self-etch adhesives would minimize water sorption, while others have observed that the 10% HEMA content would be beneficial for the adhesive system performance [39]. There is still a controversy about the role of HEMA in the bonding performance of adhesives. In the study by Felizardo et al. [39] it was concluded that the influence of HEMA on bond strength to dentin was material dependent.

As there are numerous factors involved in bond degradation, several methods have been proposed (i.e., load cycling, thermal cycling, prolonged water, and artificial saliva incubation) for reproducing clinical situations and simulating the oral environment to test the durability of dentin bonding [42]. In our study, after storage in artificial saliva for six months, both G-Bond and OptiBond-All-In-One depicted significant reduction in the bond strength when used without any pretreatment. Several studies have provided morphological evidence of resin elution and/or hydrolytic degradation of collagen matrices after long-term storage [43]. Accordingly, more adhesive failures were observed after 6-month period.

EDTA is a molecule containing four carboxylic acid groups that can chelate calcium. It has been widely used to dissolve the mineral phase of dentine without altering dentin proteins, thereby avoiding major alterations of the native

fibrillar structure of dentin collagen. Further, EDTA has an inhibitory effect on the matrix-bound MMPs of demineralized dentin [17]. In the current study, EDTA preconditioning had no significant effect on the immediate bond strength of the tested self-etch adhesives. Kasraei et al. reported that EDTA application before one-step self-etch adhesive significantly improved the bond strength [44]. However, they used liquid EDTA at 0.5 M concentration for 30 seconds and the adhesives evaluated were also different from our study. Soares et al. also depicted increased bond strength of self-etch adhesive systems used with EDTA preconditioning [45]. However, they conducted the study on bovine incisors using two-step self-etch adhesives whereas, in our study, one-step all-in-one adhesives were used. It has been reported that the efficiency of EDTA depends on many factors: penetration depth of the material, hardness of the dentin, duration of application, pH, form (liquid or gel), and concentration of material [42]. Although EDTA is an excellent MMP inhibitor, it is also water soluble; hence it might be rinsed off EDTA-treated dentin [17]. This might not be able to sustain MMP inhibition for much longer duration. Therefore, in the current study no improvement in durability could be observed after EDTA pretreatment with significant reduction in bond strength after six months, along with an increase in the number of adhesive failures. Another important aspect that must be considered is EDTA delivery form. Even at a higher concentration, a 24% EDTA gel might not be able to etch dentin in the same manner as EDTA in aqueous solution due to its lower wetting capacity. Stape et al. evaluated the effect of 24% EDTA on bond strength of resin cements to dentin and concluded that the effect varied with the different resin cements [46]. Parihar and Pilania also concluded that the effect of EDTA preconditioning on bonding of self-adhesive resin cement was product dependent [47].

EDC, a cross-linking agent with very low cytotoxicity, has shown promising results in eliminating dentin collagen degradation and preserving dentin bond strength with clinically acceptable procedure time [48]. It is the most stable cyanamide isomer, which is able to assemble amino acids into peptides. They are examples of zero length cross-linking agents. However, application of EDC alone in this study, on the dentin surface, without prior EDTA conditioning had no significant effect on the immediate bond strength of both self-etch adhesives. Probably as there was no exposed collagen, EDC was not able to strengthen the collagen matrix by increased cross-linking, whereas most of the studies, which report improved bonding effectiveness with EDC, have been performed using etch and rinse adhesives where EDC is applied to dentin previously demineralized by phosphoric acid which exposes the collagen fibrils.

EDTA removes the smear layer and mildly demineralizes the dentin. Because EDTA does not denature collagen in comparison to phosphoric acid, it creates thinner hybrid layers that are more easily infiltrated with resin [49–52]. Conditioning with 24% EDTA for 1 minute has been shown to demineralize the dentin and expose the collagen fibrils. Subsequent application of EDC promotes cross-linking amongst exposed collagen fibrils. Thus, in the present study, dentin pretreatment with EDC (with and without EDTA) resulted in bond strength preservation after 6 months of storage in artificial saliva for both adhesives used. All EDC treated groups at 6 months revealed mixed fracture patterns to be the most common failure mode. A previous in vitro study also reported that EDC application for 1 minute was effective in inactivating soluble rhMMP-9 and matrix-bound dentin proteinases [53].

Our results are supported by the study of Mazzoni et al., who reported preservation of resin-dentin bond with 1 minute EDC pretreatment and by the study of Bedran-Russo et al. who also reported increased durability of resin-dentin bonds in EDC pretreated group [54, 55]. EDC is capable of cross-linking proteins through covalent peptide bonds by activating the free carboxyl group of glutamic and aspartic acids present in protein molecules to form O-acylisourea intermediate that reacts with the epsilon amino group of lysine or hydroxylysine in an adjacent polypeptide chain to form a stable amide cross-link [56, 57]. Cross-linking increases the mechanical properties of dentin collagen and makes the fibrils more resistant to degradation [55]. Furthermore EDC shows no transdentinal cytotoxicity on odontoblast-like cells and is able to increase the mechanical properties of the collagen matrix [25, 58]. Further studies are required to evaluate the effect of different concentration, time, pH, and form of application of EDTA and EDC on the long-term bonding efficacy of different contemporary adhesive systems to dentin. Effect of incorporation of EDC in the adhesive composition on the resin polymerization also needs to be investigated.

6. Conclusion

Carbodiimide pretreatment of dentin surface resulted in significant preservation of resin-dentin bond over six-month storage period for both all-in-one self-etch adhesives tested. EDTA pretreatment of dentin surface before application of self-etch adhesives had no effect on the durability of resin-dentin bond.

Conflict of Interests

The authors declare that there is no conflict of interests regarding the publication of this paper.

References

[1] M. Unemori, Y. Matsuya, A. Akashi, Y. Goto, and A. Akamine, "Self-etching adhesives and postoperative sensitivity," *American Journal of Dentistry*, vol. 17, no. 3, pp. 191–195, 2004.

[2] J. Perdigão, S. Geraldeli, and J. S. Hodges, "Total-etch versus self-etch adhesive: effect on postoperative sensitivity," *Journal of the American Dental Association*, vol. 134, no. 12, pp. 1621–1629, 2003.

[3] F. R. Tay, R. Carvalho, H. Sano, and D. H. Pashley, "Effect of smear layers on the bonding of a self-etching primer to dentin," *Journal of Adhesive Dentistry*, vol. 2, no. 2, pp. 99–116, 2000.

[4] F. R. Tay, N. M. King, K.-M. Chan, and D. H. Pashley, "How can nanoleakage occur in self-etching adhesive systems that

demineralize and infiltrate simultaneously?" *Journal of Adhesive Dentistry*, vol. 4, no. 4, pp. 255–269, 2002.

[5] H. Koibuchi, N. Yasuda, and N. Nakabayashi, "Bonding to dentin with a self-etching primer: the effect of smear layers," *Dental Materials*, vol. 17, no. 2, pp. 122–126, 2001.

[6] K. Miyasaka and N. Nakabayashi, "Effect of Phenyl-P/HEMA acetone primer on wet bonding to EDTA-conditioned dentin," *Dental Materials*, vol. 17, no. 6, pp. 499–503, 2001.

[7] T. Toida and N. Nakabayashi, "Adhesion of shrunken demineralized dentin—effects of methacrylates with hydrophilic and hydrophobic groups dissolved in primers on recovery of shrunken demineralized dentin," *The Journal of the Japanese Society for Dental Materials and Devices*, vol. 16, no. 3, pp. 232–238, 1997.

[8] B. Van Meerbeek, J. De Munck, Y. Yoshida et al., "Buonocore Memorial Lecture. Adhesion to enamel and dentin: current status and future challenges," *Operative Dentistry*, vol. 28, no. 3, pp. 215–235, 2003.

[9] N. Manuja, R. Nagpal, and S. Chaudhary, "Bonding efficacy of 1-step self-etch adhesives: effect of additional enamel etching and hydrophobic layer application," *Journal of Dentistry for Children*, vol. 79, no. 1, pp. 3–8, 2012.

[10] G. Kato and N. Nakabayashi, "The durability of adhesion to phosphoric acid etched, wet dentin substrates," *Dental Materials*, vol. 14, no. 5, pp. 347–352, 1998.

[11] Y. Torii, K. Itou, Y. Nishitani, K. Ishikawa, and K. Suzuki, "Effect of phosphoric acid etching prior to self-etching primer application on adhesion of resin composite to enamel and dentin," *American Journal of Dentistry*, vol. 15, no. 5, pp. 305–308, 2002.

[12] Z. C. Çehreli and N. Altay, "Etching effect of 17% EDTa and a non-rinse conditioner (NRC) on primary enamel and dentin," *American Journal of Dentistry*, vol. 13, no. 2, pp. 64–68, 2000.

[13] Y. Wang and P. Spencer, "Analysis of acid-treated dentin smear debris and smear layers using confocal Raman microspectroscopy," *Journal of Biomedical Materials Research*, vol. 60, no. 2, pp. 300–308, 2002.

[14] P. Jacques and J. Hebling, "Effect of dentin conditioners on the microtensile bond strength of a conventional and a self-etching primer adhesive system," *Dental Materials*, vol. 21, no. 2, pp. 103–109, 2005.

[15] Y. Torii, R. Hikasa, S. Iwate, F. Oyama, K. Itou, and M. Yoshiyama, "Effect of EDTA conditioning on bond strength to bovine dentin promoted by four current adhesives," *American Journal of Dentistry*, vol. 16, no. 6, pp. 395–400, 2003.

[16] A. Cederlund, B. Jonsson, and J. Blomlöf, "Shear strength after ethylenediaminetetraacetic acid conditioning of dentin," *Acta Odontologica Scandinavica*, vol. 59, no. 6, pp. 418–422, 2001.

[17] J. M. Thompson, K. Agee, S. J. Sidow et al., "Inhibition of endogenous dentin matrix metalloproteinases by ethylenediaminetetraacetic acid," *Journal of Endodontics*, vol. 38, no. 1, pp. 62–65, 2012.

[18] A. J. V. Strijp, D. C. Jansen, J. DeGroot, J. M. Ten Cate, and V. Everts, "Host-derived proteinases and degradation of dentine collagen in situ," *Caries Research*, vol. 37, no. 1, pp. 58–65, 2003.

[19] A. Mazzoni, F. Mannello, F. R. Tay et al., "Zymographic analysis and characterization of MMP-2 and -9 forms in human sound dentin," *Journal of Dental Research*, vol. 86, no. 5, pp. 436–440, 2007.

[20] J. De Munck, P. E. Van Den Steen, A. Mine et al., "Inhibition of enzymatic degradation of adhesive-dentin interfaces," *Journal of Dental Research*, vol. 88, no. 12, pp. 1101–1106, 2009.

[21] J. Hebling, D. H. Pashley, L. Tjäderhane, and F. R. Tay, "Chlorhexidine arrests subclinical degradation of dentin hybrid layers in vivo," *Journal of Dental Research*, vol. 84, no. 8, pp. 741–746, 2005.

[22] R. Nagpal, N. Manuja, and I. K. Pandit, "Effect of proanthocyanidin treatment on the bonding effectiveness of adhesive restorations in pulp chamber," *Journal of Clinical Pediatric Dentistry*, vol. 38, no. 1, pp. 49–53, 2013.

[23] L. Breschi, A. Mazzoni, A. Ruggeri, M. Cadenaro, R. Di Lenarda, and E. D. S. Dorigo, "Dental adhesion review: aging and stability of the bonded interface," *Dental Materials*, vol. 24, no. 1, pp. 90–101, 2008.

[24] D. Scheffel, C. Delgado, D. G. Soares et al., "Increased durability of resin-dentin bonds following cross-linking treatment," *Operative Dentistry*, vol. 40, no. 5, pp. 533–539, 2015.

[25] D. L. S. Scheffel, J. Hebling, R. H. Scheffel et al., "Inactivation of matrix-bound Matrix metalloproteinases by cross-linking agents in acid-etched dentin," *Operative Dentistry*, vol. 39, no. 2, pp. 152–158, 2014.

[26] Y. Liu, L. Tjäderhane, L. Breschi et al., "Limitations in bonding to dentin and experimental strategies to prevent bond degradation," *Journal of Dental Research*, vol. 90, no. 8, pp. 953–968, 2011.

[27] L. L. H. Huang-Lee, D. T. Cheung, and M. E. Nimni, "Biochemical changes and cytotoxicity associated with the degradation of polymeric glutaraldehyde derived cross-links," *Journal of Biomedical Materials Research*, vol. 24, no. 9, pp. 1185–1201, 1990.

[28] H. Petite, J.-L. Dukval, V. Frei, N. Abdul-Malak, M.-F. Sigot-Luizard, and D. Herbage, "Cytocompatibility of calf pericardium treated by glutaraldehyde and by the acyl azide methods in an organotypic culture model," *Biomaterials*, vol. 16, no. 13, pp. 1003–1008, 1995.

[29] D. L. S. Scheffel, L. Bianchi, D. G. Soares et al., "Transdentinal cytotoxicity of carbodiimide (EDC) and glutaraldehyde on odontoblast-like cells," *Operative Dentistry*, vol. 40, no. 1, pp. 44–54, 2015.

[30] A. Panigrahi, K. T. Srilatha, R. G. Panigrahi, S. Mohanty, S. Kbhuyan, and D. Bardhan, "Microtensile bond strength of embrace wetbond hydrophilic sealant in different moisture contamination: an in-vitro study," *Journal of Clinical and Diagnostic Research*, vol. 9, no. 7, pp. ZC23–ZC25, 2015.

[31] R. Subramonian, V. Mathai, J. M. C. Angelo, and J. Ravi, "Effect of three different antioxidants on the shear bond strength of composite resin to bleached enamel: an in vitro study," *Journal of Conservative Dentistry*, vol. 18, no. 2, pp. 144–148, 2015.

[32] B. Poptani, K. S. Gohil, J. Ganjiwale, and M. Shukla, "Microtensile dentin bond strength of fifth with five seventh-generation dentin bonding agents after thermocycling: an in vitro study," *Contemporary Clinical Dentistry*, vol. 3, no. 6, pp. 167–171, 2012.

[33] S. Sauro, D. H. Pashley, F. Mannocci et al., "Micropermeability of current self-etching and etch-and-rinse adhesives bonded to deep dentine: a comparison study using a double-staining/confocal microscopy technique," *European Journal of Oral Sciences*, vol. 116, no. 2, pp. 184–193, 2008.

[34] S. Bouillaguet, P. Gysi, J. C. Wataha et al., "Bond strength of composite to dentin using conventional, one-step, and self-etching adhesive systems," *Journal of Dentistry*, vol. 29, no. 1, pp. 55–61, 2001.

[35] T. Ikeda, J. De Munck, K. Shirai et al., "Effect of air-drying and solvent evaporation on the strength of HEMA-rich versus HEMA-free one-step adhesives," *Dental Materials*, vol. 24, no. 10, pp. 1316–1323, 2008.

[36] K. L. Van Landuyt, J. Snauwaert, J. De Munck et al., "Systematic review of the chemical composition of contemporary dental adhesives," *Biomaterials*, vol. 28, no. 26, pp. 3757–3785, 2007.

[37] X. Guo, P. Spencer, Y. Wang, Q. Ye, X. Yao, and K. Williams, "Effects of a solubility enhancer on penetration of hydrophobic component in model adhesives into wet demineralized dentin," *Dental Materials*, vol. 23, no. 12, pp. 1473–1481, 2007.

[38] C. H. Zanchi, E. A. Münchow, F. A. Ogliari et al., "Development of experimental HEMA-free three-step adhesive system," *Journal of Dentistry*, vol. 38, no. 6, pp. 503–508, 2010.

[39] K. R. Felizardo, L. V. F. M. Lemos, R. V. de Carvalho, A. Gonini Junior, M. B. Lopes, and S. K. Moura, "Bond strength of HEMA-containing versus HEMA-free self-etch adhesive systems to dentin," *Brazilian Dental Journal*, vol. 22, no. 6, pp. 468–472, 2011.

[40] M. Takahashi, M. Nakajima, K. Hosaka, M. Ikeda, R. M. Foxton, and J. Tagami, "Long-term evaluation of water sorption and ultimate tensile strength of HEMA-containing/-free one-step self-etch adhesives," *Journal of Dentistry*, vol. 39, no. 7, pp. 506–512, 2011.

[41] K. L. V. Landuyt, A. Mine, J. D. Munck et al., "Are one-step adhesives easier to use and better performing? Multifactorial assessment of contemporary one-step self-etching adhesives," *The Journal of Adhesive Dentistry*, vol. 11, no. 3, pp. 175–190, 2009.

[42] S. Sauro, F. Mannocci, M. Toledano, R. Osorio, D. H. Pashley, and T. F. Watson, "EDTA or H_3PO_4/NaOCl dentine treatments may increase hybrid layers' resistance to degradation: a microtensile bond strength and confocal-micropermeability study," *Journal of Dentistry*, vol. 37, no. 4, pp. 279–288, 2009.

[43] L. Breschi, A. Mazzoni, A. Ruggeri, M. Cadenaro, R. D. Lenarda, and E. S. S. Dorigo, "Dental adhesion review: aging and stability of the bonded interface," *Dental Materials*, vol. 24, no. 1, pp. 90–101, 2008.

[44] S. Kasraei, M. Azarsina, and Z. Khamverdi, "Effect of Ethylene diamine tetra acetic acid and sodium hypochlorite solution conditioning on microtensile bond strength of one-step self-etch adhesives," *Journal of Conservative Dentistry*, vol. 16, no. 3, pp. 243–246, 2013.

[45] C. J. Soares, C. G. Castro, P. C. F. Santos Filho, and A. S. Da Mota, "Effect of previous treatments on bond strength of two self-etching adhesive systems to dental substrate," *Journal of Adhesive Dentistry*, vol. 9, no. 3, pp. 291–296, 2007.

[46] T. H. S. Stape, M. S. Menezes, B. C. F. Barreto, F. H. B. Aguiar, L. R. Martins, and P. S. Quagliatto, "Influence of matrix metalloproteinase synthetic inhibitors on dentin microtensile bond strength of resin cements," *Operative Dentistry*, vol. 37, no. 4, pp. 386–396, 2012.

[47] N. Parihar and M. Pilania, "SEM evaluation of effect of 37% phosphoric acid gel, 24% EDTA gel and 10% maleic acid gel on the enamel and dentin for 15 and 60 seconds: an in−vitro study," *International Dental Journal of Students' Research*, vol. 1, no. 2, pp. 29–41, 2012.

[48] D. Scheffel, L. Bianchi, D. Soares et al., "Transdentinal cytotoxicity of carbodiimide (EDC) and glutaraldehyde on odontoblast-like cells," *Operative Dentistry*, vol. 40, no. 1, pp. 44–54, 2015.

[49] S. Habelitz, M. Balooch, S. J. Marshall, G. Balooch, and G. W. J. Marshall Jr., "In situ atomic force microscopy of partially demineralized human dentin collagen fibrils," *Journal of Structural Biology*, vol. 138, no. 3, pp. 227–236, 2002.

[50] J. P. S. Blomlöf, L. B. Blomlöf, A. L. Cederlund, K. R. Hultenby, and S. F. Lindskog, "A new concept for etching in restorative dentistry," *International Journal of Periodontics & Restorative Dentistry*, vol. 19, no. 1, pp. 31–35, 1999.

[51] S. Sauro, M. Toledano, F. S. Aguilera et al., "Resin-dentin bonds to EDTA-treated vs. acid-etched dentin using ethanol wet-bonding," *Dental Materials*, vol. 26, no. 4, pp. 368–379, 2010.

[52] S. Sauro, M. Toledano, F. S. Aguilera et al., "Resin–dentin bonds to EDTA-treated vs. acid-etched dentin using ethanol wet-bonding. Part II: effects of mechanical cycling load on microtensile bond strengths," *Dental Materials*, vol. 27, no. 6, pp. 563–572, 2011.

[53] A. Tezvergil-Mutluay, M. M. Mutluay, K. A. Agee et al., "Carbodiimide cross-linking inactivates soluble and matrix-bound MMPs, *in vitro*," *Journal of Dental Research*, vol. 91, no. 2, pp. 192–196, 2012.

[54] A. Mazzoni, V. Angeloni, F. M. Apolonio et al., "Effect of carbodiimide (EDC) on the bond stability of etch-and-rinse adhesive systems," *Dental Materials*, vol. 29, no. 10, pp. 1040–1047, 2013.

[55] A. K. B. Bedran-Russo, C. M. P. Vidal, P. H. Dos Santos, and C. S. Castellan, "Long-term effect of carbodiimide on dentin matrix and resin-dentin bonds," *Journal of Biomedical Materials Research Part B: Applied Biomaterials*, vol. 94, no. 1, pp. 250–255, 2010.

[56] R. Timkovich, "Detection of the stable addition of carbodiimide to proteins," *Analytical Biochemistry*, vol. 79, no. 1-2, pp. 135–143, 1977.

[57] R. Zeeman, P. J. Dijkstra, P. B. Van Wachem et al., "Successive epoxy and carbodiimide cross-linking of dermal sheep collagen," *Biomaterials*, vol. 20, no. 10, pp. 921–931, 1999.

[58] D. L. S. Scheffel, J. Hebling, R. H. Scheffel et al., "Stabilization of dentin matrix after cross-linking treatments, in vitro," *Dental Materials*, vol. 30, no. 2, pp. 227–233, 2014.